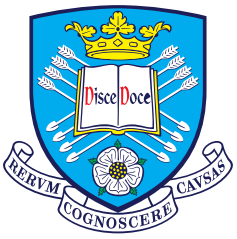

The University Of Sheffield.

Optimising the cost-benefit balance of induced resistance by chemical agents in tomato and lettuce using hyperspectral imaging

Mustafa Yassin

A thesis submitted in partial fulfilment of the requirements for the degree of Doctor of Philosophy

School of Biosciences
Faculty of Science
The University of Sheffield

Submitted: 25th March 2022

Acknowledgements

I would like to express my deepest gratitude to my primary supervisors, Jurriaan Ton, Adrian Newton and Stephen Rolfe, who provided me with guidance and immense support throughout my PhD. To the other members of my supervisory team, Matthew Cromey, Nicola Holden and Tracy Valentine, I am also very grateful for their support and encouragement. I wish to extend my special thanks to Joost Stassen, who provided me with essential computer scripts and taught me valuable computational skills. I would like to express my gratitude for the continues support and friendship given to me by all the members of the Ton Lab. Finally, I would like to thank the Royal Horticultural Society, the Mylnefield trust (James Hutton Institute) and ENZA Zaden for generously funding my PhD.

Thesis Abstract

Induced resistance (IR) agents are molecules of varied origins that can sensitise the plant immune system for a faster and/or stronger deployment of inducible defences upon pathogen exposure. These agents provide durable broad-spectrum protection, because they act on multiple defence genes and pathway, and generally lack direct biocidal activity making them less damaging for the environment. Accordingly, disease protection by IR agents holds promise as an alternative to traditional pesticides. However, owing to variable protection efficacy and detrimental side effects on growth and yield, the adoption of IR agents in crop protection schemes remains low. While the efficacy of IR agents can be improved by increased dosage, this often also increases their detrimental effects on plant growth and yield. This PhD thesis presents a research project that aimed to optimise the cost-benefit balance of chemical IR in two pathosystems, tomato-*Botrytis cinerea* and lettuce-*Bremia lactucae,* using three separate IR agents, β-aminobutyric acid (BABA), R-beta-homoserine (RBH) and chitosan (ChP). By exploiting hyperspectral imaging to track disease and chemical stresses non-destructively, I first developed a method to specifically quantify the chemical stress responses associated with relatively high doses of the IR agents. Following that, I developed hyperspectral markers that specifically quantify the IR responses against both plant diseases. From these two approaches, I used these hyperspectral markers to test a set of combined low-concentration doses of IR agents in the lettuce-*B. lactucae* interaction to optimise the IR response, while minimising the associated stress response. This approach revealed that combinations of low concentrations of BABA and RBH can deliver synergistic levels of protection against *B. lactucae* without detrimental costs on plant growth.

Contribution statement

This work contains previously published material. Chapter 1 and Chapter 6 of this thesis contain sections first published in the review paper:

Yassin, M., Ton, J., Rolfe, S.A., Valentine, T.A., Cromey, M., Holden, N. and Newton, A.C. (2021), **The rise, fall and resurrection of chemical-induced resistance agents**. *Pest Manag Sci*, 77: 3900-3909. https://doi.org/10.1002/ps.6370

The concepts and theme of the paper were conceived together by Ton, J, Newton, A.C and Yassin, M. The paper was researched and written by Yassin, M. The other listed authors made contributions in the form of comments, suggestions and editing of the final manuscript.

Wiley the publisher of *Pest management Science* gives permission for the use of this work in my thesis. All co-authors have also given their permission for the inclusion of the work in my thesis.

Contents

List of Figures

List of Tables

Chapter 1
General introduction

1.1 The impact of plant diseases on food security

Food security is one of the most complex challenges of the 21st century, and plant health is a vital part of achieving it. In the short-term, after a steady decline from the beginning of the century, the number undernourished people in the world sharply increased as result of the COVID-19 pandemic, with more than 700 million people facing hunger in 2021 (FAO, 2021b). The continuing impact of the pandemic on incomes and supply chains is worsening food insecurity in many countries (World Bank, 2022). Increasing energy prices (IEA, 2021) growing violent conflicts (ICG, 2021),and a fracturing global order (Tisdall, 2022), suggest food production and distribution systems will continue to deteriorate. In the longer-term, the prediction is that a 60% increase in food production is required to feed a population of 10 billion in 2050 while also navigating the effects of a changing climate (Hunter *et al.*, 2017). Plants have a key role in this complex challenge, they provide over 80% of the food humans consume (FAO, 2021a) and nearly all livestock feed (Mottet *et al.*, 2017). Consequently, plant pests and diseases have a large impact on food security. Estimates for food crop losses due to plant diseases range from 10.1 to 28.1% (Ristaino *et al.*, 2021). Thus, plant protection measures are a cornerstone of current and future global food security strategy.

1.2 The need to diversify plant protection methods

The use of biocidal chemicals to combat plant pests and diseases has made it possible to increase crop yields. However, there is increasing interest in diversifying from these protection methods to mitigate some of their inherent shortcomings (Barzman *et al.*, 2015; Lechenet *et al.*, 2017; Pertot *et al.*, 2017). In recent decades, the philosophy behind the control of these pests and pathogens has been driven by a 'zero tolerance' approach, where elimination of the causal agents is the unstated aim. This has rarely, if ever, been achieved. Instead the extreme selection pressures

exerted on the surviving pest and pathogen populations has often rendered genetic resistance ineffective (Mundt, 2014; Crété *et al*., 2020) or has resulted in populations acquiring resistance to biocidal chemical agents (Ishii, 2006; Deising, Reimann and Pascholati, 2008; Lucas, Hawkins and Fraaije, 2015). Though the use of these biocidal agents has enabled substantial increases in agricultural productivity, they are associated with a plethora of proven or perceived negative health and environmental effects and there is a widespread desire to reduce their use (Aktar, Sengupta and Chowdhury, 2009; Nicolopoulou-Stamati *et al*., 2016; Zubrod *et al*., 2019). An alternative approach with potential is to take advantage of recent advances in our understanding of plant-microbe interactions and use control strategies that leverage the plant immune system in a systems context, namely Integrated Pest (/crop) management.

1.3 The plant immune system

Plants possess a sophisticated innate immune system that provides the first line of defence against attackers. This is controlled by a complex network of interconnected signalling pathways that are directly activated upon recognition of Microbe-Associated Molecular Patterns (PAMPs) and/or Damage-Associated Molecular Patterns (DAMPs). The model of plant–pathogen interactions by Jones and Dangl, (2006), also referred to as the 'zig-zag' model (Fig 1.1), is perhaps the most popular model of the plant innate immune system which distinguishes three forms of disease resistance. Effector-triggered immunity (ETI) – commonly known as race-specific or vertical resistance – is a qualitative form of disease resistance that relies on the presence of single resistance genes (R). The associated R proteins enable direct or indirect recognition of susceptibility-inducing pathogen effectors and activate a rapid immune response, which is typically associated with hypersensitive cell death. Accordingly, ETI provides high levels of protection against biotrophic pathogens (Cui, Tsuda and Parker, 2015). However, because of its monogenic nature, ETI has a narrow range of taxonomic effectiveness and limited durability due to the evolutionary pressures on pathogens to evolve alternative effectors, thereby avoiding recognition by R proteins (García-Arenal and McDonald, 2003; Mundt, 2014). Pattern Triggered Immunity (PTI) is a quantitative form of disease resistance, which provides high-level resistance against a broad range of attackers. PTI is triggered by a multitude of conserved molecular patterns that are produced during infestation or infection by pests and diseases respectively, which activate a range of different pathways and defence mechanisms that become active at different stages of the interaction. However, PTI is not sufficiently effective against virulent pathogens (Jones and Dangl, 2006; Couto and Zipfel, 2016), which employ effector molecules that subvert PTI-controlling pathways, a process commonly referred to as Effector-Triggered Susceptibility (ETS) (Jones and Dangl, 2006; Pel and Pieterse, 2013). In addition to PTI-suppressing effectors, ETS by biotrophic pathogens also involves 2nd level effectors that suppress ETI-related signalling and hypersensitive cell death-related (Jones and Dangl, 2006; Rajamuthiah and Mylonakis, 2014; Thordal-Christensen, 2020). Within

the framework of the zig-zag model by Jones and Dangl (2006) the residual level of resistance after ETS-mediated repression of PTI and ETI is referred to as basal resistance (BR). Since its inception, the zig-zag model has been interpreted as a co-evolutionary arm's race, during which pathogens evolved ETS to suppress PRR-dependent PTI and plants counter-evolved R-proteins to recognise effector activity and activate ETI.

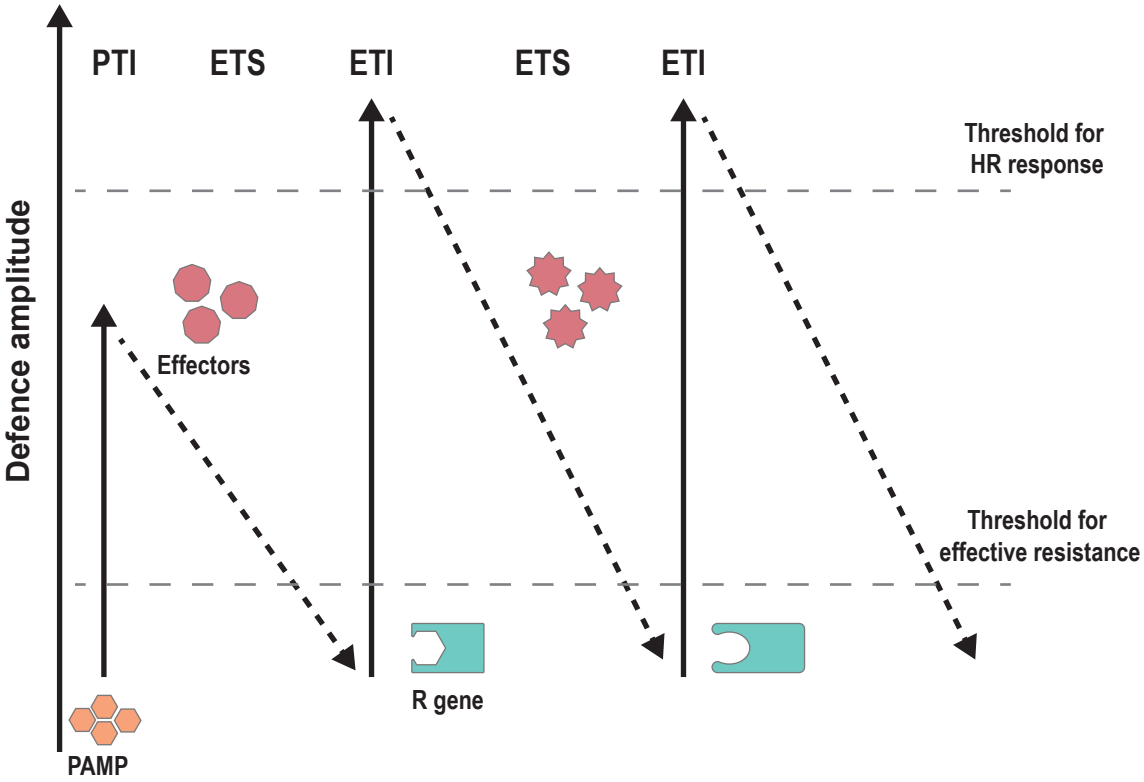

Fig 1.1 | The 'zig zag model'. A scheme showing the co-evolution between plants and biotrophic pathogens in successive steps. Recognition of PAMPs by plant PRRs lead to PAMP-triggered immunity (PTI). Under subsequent selection pressure, pathogen develops effectors that disable PAMP recognition and effector- triggered susceptibility (ETS) ensues. Some plants acquire R genes that encode proteins that recognise effectors which leads to effector triggered immunity (ETI). Pathogens develops effectors to circumvent ETI leading to ETS and the evolutionary arms race continues. Reproduced from Jones and Dangl (2006).

Although proven exceedingly useful for the conceptual interpretation of plant innate immunity and evolution, the zig-zag model is not without limitations (Pritchard and Birch, 2014). Foremost among them is that the model only represents plant innate immunity against biotrophic pathogens. Furthermore, while it is acceptable to portray ETI, PTI and BR as different types of resistance within an evolutionary context, they are remarkably similar from a mechanistic point. All three types of resistance share similar signalling pathways and defence mechanisms that become active during different stages of the interaction with avirulent, non-host and virulent

pathogens, respectively (Tsuda and Katagiri, 2010; Naveed *et al.*, 2020). These pathways and mechanisms include relatively early-acting local defences, such as the accumulation of reactive oxygen species and cell wall reinforcements (Luna *et al.*, 2011; Qi *et al.*, 2017; Bacete *et al.*, 2018; Kuźniak and Kopczewski, 2020). Also, there are later-acting defences that are controlled by de novo produced defence hormones, such as salicylic acid (SA), jasmonic acid (JA), ethylene (ET) and abscisic acid (ABA) (Ton, Flors and Mauch-Mani, 2009; Pieterse *et al.*, 2012), which all interact with each other to prioritise and fine tune an appropriate immune response (Koornneef and Pieterse, 2008; Vos *et al.*, 2015). Hence, from a mechanistic point of view, there is no clear partition between ETI, PTI and BR.

Although the plant innate immune system protects against the majority of potentially hostile microbes, it cannot prevent infection and damage by virulent pathogens. To minimise damage by these attackers, plants have evolved the ability to augment the level of innate immunity by forming a memory of previous pathogen encounters, resulting in a faster and/or stronger deployment of inducible plant defence mechanisms upon subsequent encounters. This so called defence priming results in induced resistance (IR), which is a form of phenotypic plasticity and can thus be regarded as plant acquired immunity (Wilkinson *et al.*, 2019). IR is often systemically expressed and has the benefits of being durable with broad-spectrum effectiveness, while also providing protection that is stronger than BR (Walters *et al.*, 2005).

1.4 The rise of chemical IR agents

Given the ability to augment plant resistance, many natural and synthetic IR-eliciting agents have been identified and characterised in detail. Initially, it was hoped these IR agents might provide benign means of protecting crops. Six decades ago, Ross, (1961) observed that localised infection of tobacco plants with tobacco mosaic virus (TMV) leads to immunity in distal non-infected leaves. This so called systemic acquired resistance (SAR) is a form of IR and is dependent on the plant defence hormone salicylic acid (SA) and the defence regulatory protein NPR1 (Sticher, Mauch-Mani and Métraux, 1997). Activation of this pathway results in direct activation and priming of a wide range of different basal defence mechanisms, including the production Pathogenesis Related (PR) proteins. The priming associated with SAR can provide long-lasting protection against a broad spectrum of (hemi-)biotrophic pathogens (Ross, 1961; Sticher, Mauch-Mani and Métraux, 1997; Spoel and Dong, 2012; Wilkinson *et al.*, 2019). In subsequent studies, it became clear that there are additional IR responses, which are controlled by partially different signalling pathways. For instance, induced systemic resistance (ISR), which is triggered by root colonization with beneficial soil microorganisms, such as plant growth-promoting rhizobacteria (PGPR), endophytic plant growth-promoting fungi (PGPF) and arbuscular mycorrhizal fungi (AMF), is under control by a signalling pathway partially different from SAR. In Arabidopsis,

ISR is dependent on the defence regulatory protein NPR1 but operates independently of SA (Pieterse *et al.*, 1996) .Instead, ISR is typically based on a priming of JA- and ET-dependent signalling pathways (Pieterse *et al.*, 1998, 2014). Based on prior discovery of JA as a wound-responsive defence hormone in plants (Farmer and Ryan, 1992), JA and its methylated derivative methyl-jasmonic acid (MeJA) have often been used as chemical IR agents against herbivores and necrotrophic pathogens (Délano-Frier *et al.*, 2004; Mageroy *et al.*, 2020). Moreover, while SAR is predominantly effective against biotrophic pathogens, ISR is more effective against necrotrophic pathogens (Ton *et al.*, 2002; Van Wees, Van der Ent and Pieterse, 2008). Further evidence, for the existence of alternative forms of IR came from the characterisation of β-aminobutyric acid-induced resistance (BABA-IR). BABA is a non-protein amino acid that is produced in low concentrations by stressed plant tissues (Thevenet *et al.*, 2017). Perception of BABA is dependent on the IBI1 receptor gene, which encodes an aspartyl-tRNA synthetase and controls BABA-IR against downy mildew and necrotrophic fungi (Luna, van Hulten, *et al.*, 2014). Furthermore, the underlying signalling pathways of BABA-IR vary according to the challenging pathogen and can either be SA-dependent or SA-independent (Zimmerli *et al.*, 2000; Ton *et al.*, 2005), providing broad-range protection against biotrophic and necrotrophic pathogens (Cohen, Vaknin and Mauch-Mani, 2016). The three classic examples of SAR, ISR and BABA-IR illustrate IR is controlled by a variety of different defence signalling pathways, depending on the eliciting agent, plant species and challenging pathogen. Despite this diversity, all IR responses share the common characteristic that they augment the effectiveness of BR through either a direct up-regulation or a priming of basal defence mechanisms (Wilkinson *et al.*, 2019).

To maximise the benefits of SAR, White, (1979) showed that injections of SA, aspirin and benzoic acid, each elicited SAR against tobacco mosaic virus (TMV) in tobacco. This pioneering experiment showed that SAR can be triggered without having to infect plants with pathogens and heralded an era of research into chemical IR agents. Research throughout the 1980s and 1990s led to the development of several functional SA analogues that act as potent SAR inducers, of which the best known are 2,6-dichloroisonicotinic acid (INA) and its derivative Acibenzolar-S-methyl (ASM). INA was shown to provide high level of protection in different crops including barley, cucumber and rice (Kogel *et al.*, 1994; Hijwegen and Verhaar, 1995; Schweizer, Buchala and Métraux, 1997). Similarly, ASM showed high resistance-inducing efficacy in a range of different crop pathosystems (Görlach *et al.*, 1996; Benhamou and Bélanger, 1998a, 1998b; Godard *et al.*, 1999). Based on these results, Syngenta launched Actigard®/Bion® as the first commercial IR agent, which includes ASM as the active ingredient. Other IR agents, such as BABA (Cohen, Vaknin and Mauch-Mani, 2016; Thevenet *et al.*, 2017) and Chitosan, a polymeric derivative of chitin (Trotel-Aziz *et al.*, 2006), yielded similarly high levels of crop protection against economically devastating plant diseases. Accordingly, IR agents emerged as potential alternative to fungicides, since they show little or no direct toxicity towards the pathogen or environment, while providing

broad-spectrum protection through augmentation of durable BR (Alexandersson *et al.*, 2016).

1.5 The fall of chemical IR agents

The initial ambition to employ chemical IR agents as main-stream crop protection products never materialised, which was largely due to undesirable non-target effects on plant growth and seed and variable efficacy against diseases. This was first highlighted by Heil *et al.*, (2000), who showed that wheat plants treated with ASM had lower biomass, developed fewer shoots and produced fewer seeds compared with untreated plants and this was particularly pronounced in plants grown with a limited nitrogen supply. Although a direct up-regulation of basal defence mechanisms could achieve high levels of protection, the associated costs made these agents less attractive for commercial exploitation as crop protection products. It was argued that the deployment of IR agents is only beneficial under conditions of high disease pressure, where the associated costs are outweighed by the benefits of disease protection (Heil *et al.*, 2000; Heil and Baldwin, 2002; Walters and Heil, 2007; Walters and Fountaine, 2009). Besides being metabolically costly, IR activators could also be phytotoxic. INA and its derivatives were deemed too toxic for agricultural use (Bektas and Eulgem, 2014). Similarly, BABA was found to cause toxicity via inhibition of AspRS enzyme activity (Luna, van Hulten, *et al.*, 2014). A third obstacle associated with chemical IR agents is that their efficacy can be highly variable between plant genotypes. In both cucumber (Hijwegen and Verhaar, 1995), and soybean (Dann *et al.*, 1998) INA efficacy varied by genotype. Efficacy may also be affected by the pathogen strain. In tomato, disease protection by BABA not only varied by host genotype but also by Phytophthora infestans isolate (Sharma, Butz and Finckh, 2010). Additionally, there is compelling evidence that environmental conditions affect the outcome of chemically induced IR (Dietrich, Ploss and Heil, 2005; Walters, 2010). Furthermore, chemically induced IR is generally transient lasting at most weeks (Knoth *et al.*, 2009; Luna, López, *et al.*, 2014; Sós-Hegedűs *et al.*, 2014; Rodriguez-Salus *et al.*, 2016) which necessitates multiple applications. This complex interplay of variables affecting IR efficacy has impeded wide-spread adoption of chemical IR agents in agriculture and horticulture.

1.6 The resurrection of chemical IR agents

Despite these complications, IR agents could still have potential as effective crop protection products and researchers continued to explore methods of improving their efficacy. One of the biggest drawbacks to IR agent utilisation was that they often exerted a high metabolic cost on plants. However, it was found that the costs associated with prolonged expression of defences, has resulted in the evolution of priming as a more cost-efficient strategy for IR, which allows plants to mount a faster and/or stronger BR response against attackers (Conrath *et al.*, 2006; Martinez-Medina *et al.*, 2016). Although priming typically manifests itself as a long-term consequence

of transient defence induction to biotic stress, chemical IR agents can serve as suitable priming stimuli when applied in relatively low doses (Walters and Heil, 2007). In some instances, plants receiving such treatments have been shown to display minimal defence induction before pathogen encounter, although their effectiveness tends to be lower than chemically induced IR mediated by direct up-regulation of defences (van Hulten *et al.*, 2006; Wang *et al.*, 2015). Furthermore, IR via priming is still associated with a reduction in plant growth and seed set, albeit minor, which can make it unfavourable in stress-free conditions (Martinez-Medina *et al.*, 2016; Douma *et al.*, 2017; Wilkinson *et al.*, 2019). However, these costs are outweighed by the benefits of protection under stressful conditions (van Hulten *et al.*, 2006; Walters and Fountaine, 2009; Martinez-Medina *et al.*, 2016). Given the significance of priming for plants in their natural environment, it has strong potential to be developed into an energetically (and environmentally) benign plant protection strategy. To this end, it is necessary to ascertain how a given IR chemical behaves - for instance, at what concentrations do IR agents switch from priming activity to a more costly direct induction of basal defences? Regardless of the nature of the priming stimuli, Martinez-Medina *et al.* (2016) proposed a set of sequential criteria that must be satisfied, namely 1) a memory of the priming stimulus with a low fitness cost, and 2) a stress trigger that induces a faster and/or stronger defence response resulting in improved disease protection. Indeed, since the potential of priming was highlighted by Conrath *et al.* (2006), the capacities of priming chemicals, both natural and synthetic, have been documented in a variety of plant pathosystems (Walters, Newton and Lyon, 2014). Although priming with IR agents can be less energetically costly, it often produced limited efficacy and variable performance. Nevertheless, strategies to optimise their performance have been explored and in particular, combined treatments strategies have shown encouraging results.

Several studies have shown that chemical IR agents and biological control agent (BCAs) in combination results in improved disease control. BCAs are naturally occurring communities antagonistic to specific plant pests and pathogens that have minimal non-target effects (Cook, 2000). In bread wheat plants (Triticum aestivum L.) receiving combined Methyl jasmonate (MeJA) and Trichoderma harzianum UBSTH-501, spot blotch (Bipolaris sorokiniana) symptoms were reduced significantly in comparison to plants receiving either treatment alone (Singh *et al.*, 2019). In another study, MeJA, SA and T. harzianum treatments individually gave a similar level of protection against Fusarium oxysporum wilt disease in tomato. However, their combination resulted in a synergistic induction of tomato antioxidant defences against F. oxysporum (Zehra *et al.*, 2017). Similarly, combining T. harzianum and ASM was significantly better at controlling Botrytis fabae disease severity in faba bean plants than either treatment alone (Abd El-Rahman and Mohamed, 2014). Other BCAs have also shown to complement chemical IR agents. For instance, the saprophytic yeast-like fungus Aureobasidium pullulans CG163 in combination with ASM showed significantly reduced leaf spot incidence compared to untreated plants. The CG163+ASM combination treatment was more effective than either treatment

alone (de Jong *et al.*, 2019). BCA-chemical IR agent combinations, in addition to improving protective efficacy, have also been shown to improve growth. In bread wheat plants, combined MeJA and T. harzianum treatment resulted in significantly higher biomass, both in the presence and absence of B. sorokiniana infection (Singh *et al.*, 2019). In tomato, combining MeJA or SA with T. harzianum improved the protection against F. oxysporum disease incidence more than treatment with SA or MeJA alone. Furthermore, due the improved protection, biomass was also significantly higher in plants receiving the combined treatment (Zehra *et al.*, 2017).

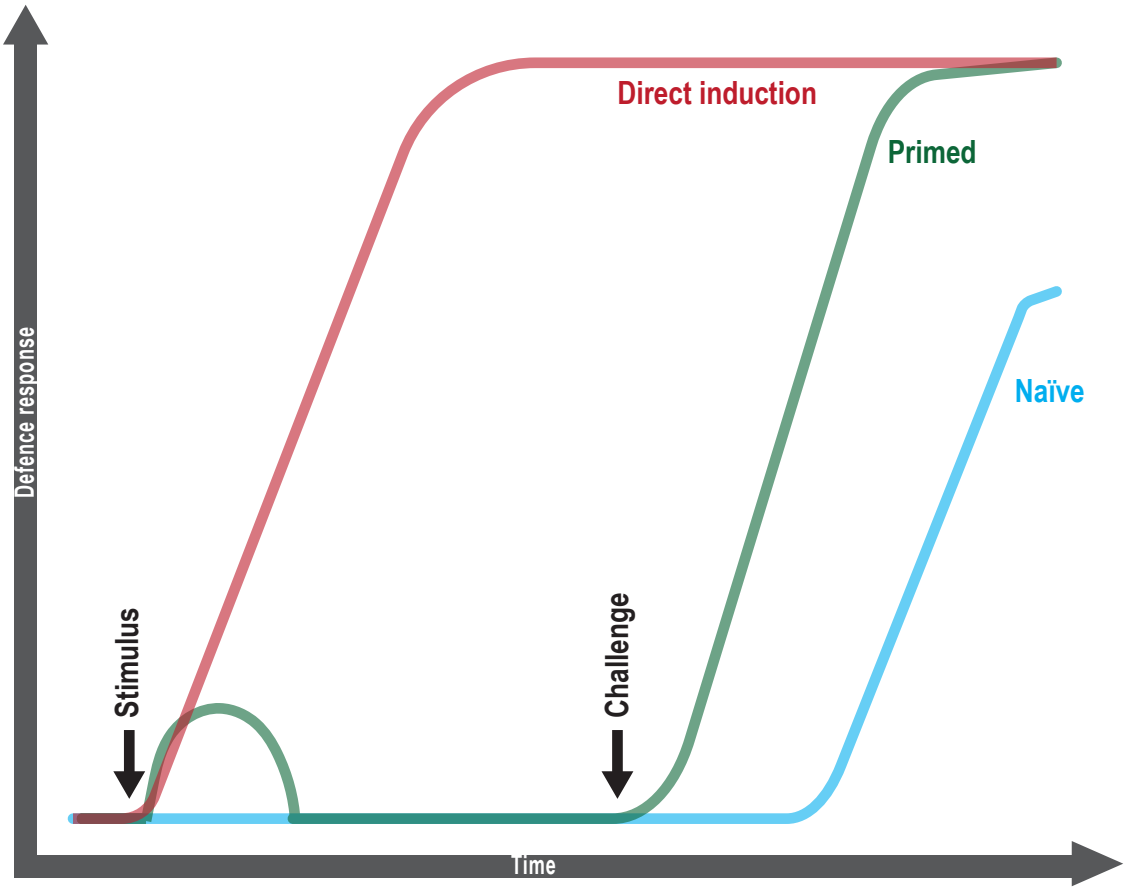

Fig 1.2 | Plant defence priming. A representation of the effects defence inducing stimuli on the amplitude of plant defence. Treatment with a stimulus (e.g. large dose) leads to direct induction of defences (red line). This direct induction is metabolically costly. An appropriate stimulus leads to defence priming (green line). The primed plant responds faster/stronger to a challenge. An untreated naïve plant (blue line) does not react until after a challenge. Adapted from Heil and Ton (2008).

Similarly, results from chemical IR agent – biocide combinations show a complementary potential in which the deleterious effects of both protection products can be reduced. An application of a mixture of BABA and the fungicide mancozeb was significantly more effective at controlling potato late blight (Phytophthora infestans) as well as tomato and cucumber mildew (Pseudoperonospora cubensis) than either BABA or mancozeb alone. The inclusion of BABA in the mancozeb fungicide synergistically increased its efficacy in plants with 5:1 BABA: mancozeb showing the highest synergy factor. Application of the BABA and mancozeb mixture did not have a synergistic interaction in controlling the pathogens in vitro, thus demonstrating BABA-induced resistance enhanced mancozeb fungicide efficacy with lower doses required to control disease (Baider and Cohen, 2003). In potato, a combination of BABA and the fungicide Fluazinam resulted in a synergistic action against late blight. Furthermore, full Fluazinam activity was achieved with a 20–25% lower dose under field conditions (Liljeroth *et al.*, 2010). Likewise, ASM efficacy improved in combination with mancozeb. In chickpea plants, repeated ASM application protected against chickpea blight (Didymella rabiei) but also resulted in yield penalties. Instead, using a ASM – mancozeb mix, with reduced application frequency, grain yields were better than those achieved with ASM or mancozeb applications alone (Sharma *et al.*, 2011).

Another approach has been the combining of different chemical IR agents. This strategy has shown promise under field conditions. In barley, Walters, Havis, Sablou, *et al.*, (2011) found improved control of powdery mildew using ASM, BABA and JA combined treatments. Given the growth costs associated with higher and more protective doses in many chemical IR agents, using low doses of multiple agents for additive or synergistic IR effects with minimal growth costs is a potential means of improving their efficacy. In one study, Reuveni, Zahavi and Cohen, (2001) established that BABA – ASM mix applied at half the recommended dose had an additive effect, effectively controlling Plasmopara viticola in grapevines. Despite the possibility to explore the effects of multiple IR agents that prime separate defence pathways that could result in positive interactions and the promise from these early studies, the strategy of combined chemical IR agents has received little further attention. This research has endeavoured to explore this possibility further and systematically evaluate the effects of mixed IR agent treatments in selected pathosystems using non-invasive image phenotyping.

1.7 IR agents selected for combination treatments

β-Aminobutyric acid (BABA) is a small four-carbon non-protein amino acid (Fig 1.3), in which the amino group is attached to the third carbon (β position). The β-carbon is chiral and so BABA comes in R and S enantiomers (Cohen, Vaknin and Mauch-Mani, 2016), and of these only the R enantiomer is associated with IR activity (Cohen, 1994; Cohen, Rubin and Vaknin,

2011). BABA-IR is the result of the stereospecific binding of R-BABA to the Impaired in BABA-induced Immunity 1 (IBI1) receptor (Schwarzenbacher, Luna and Ton, 2014). Treatment with BABA has been extensively reported to lead to IR in a wide range of pathosystems (Justyna and Ewa, 2013; Cohen, Vaknin and Mauch-Mani, 2016). However, BABA is also associated with phytotoxic side effects in many plant species (Wu *et al.*, 2010; Cohen, Vaknin and Mauch-Mani, 2016; Buswell *et al.*, 2018).

β-homoserine is another four-carbon non-protein β-amino acid (Fig 1.3). Relative to BABA it is a newer IR agent. In a screen for resistance-inducing, BABA structural analogues with less phytotoxicity, the R enantiomer of β-homoserine (RBH) was identified as a good candidate. Initial studies of RBH found positive IR activity and no significant phytotoxicity in Arabidopsis and tomato cv. Micro-Tom (Buswell *et al.*, 2018).

Chitosan is a co-polysaccharide composed of D-glucose amine and N-acetyl-D-glucose (Fig 1.3), and is produced by the deacetylation of chitin sourced from the exoskeleton of crustaceans (Elieh-Ali-Komi, Hamblin and Daniel, 2016). This naturally occurring polysaccharide generally lacks toxicity in plants and is some cases has been associated with plant growth promotion (De Vega *et al.*, 2021). Chitosan has also been reported to induce resistance in many pathosystems (Hadrami *et al.*, 2010; Malerba and Cerana, 2016).

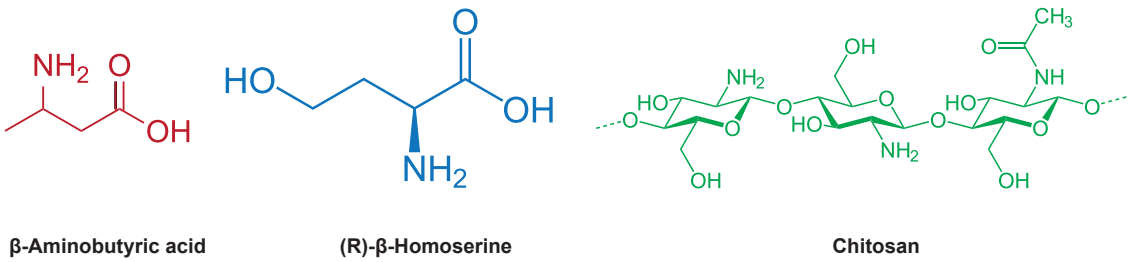

Fig 1.3 | Selected chemical IR agents. The chemical structures of the IR agents: β-Aminobutyric acid, (R)-β-Homoserine and Chitosan.

1.8 Pathosystems for testing IR agent combination treatments

1.8.1 Tomato-Botrytis cinerea

Botrytis cinerea is a necrotrophic fungal pathogen that is the causal agent of grey mould disease (Williamson *et al.*, 2007). This pathogen has a broad host range of more than 200 plant species including almost all fruit and vegetable crops (Williamson *et al.*, 2007; Weiberg *et al.*, 2013). B. cinerea triggers both pre-harvest and post-harvest disease (Williamson *et al.*, 2007), and causes global annual economic losses exceeding USD 10 billion (Weiberg *et al.*, 2013). The

fungus can exist in different forms including mycelia, sclerotia and conidia and these can serve as sources of new infection. The sclerotia are compact and hardened mycelium that contain food reserves, which develop inside decaying plant tissue and serve as a long-term survival mechanisms (Williamson *et al.*, 2007; Petrasch *et al.*, 2019). In the sclerotia, under appropriate conditions, UV light stimulates conidia development and these serve as vectors of infection (Williamson *et al.*, 2007). Following infection, sometimes a quiescent symptomless phase, where B. cinerea growth is arrested can occur, but normally, B. cinerea will initiate a necrotrophic phase that results in mycelium growth and rapid disease spread (Holz, Coertze and Williamson, 2007). Tomato (Solanum lycopersicum) is one of the crops most impacted by grey mould disease. Currently there are no, commercial tomato cultivars with genetic resistance to B. cinerea, and fungicides are the primary means of protection (Smith *et al.*, 2014).

1.8.2 Lettuce-Bremia Lactucae

Bremia lactucae is an obligate biotrophic oomycete that causes downy mildew in lettuce (Lactuca sativa). B. lactucae causes severe outbreaks of downy mildew disease worldwide, and is considered the biggest threat to lettuce production (Nordskog *et al.*, 2007; Fletcher *et al.*, 2019). In the infection cycle of B. lactucae, conidia from a previous infection land on the leaves of a susceptible host. These conidia germinate and colonise host leaf cells. Following germination, new conidia are released into the surrounding environment. These conidia when deposited on a new host and in the presence of water on leaf surfaces germinate to start a new infection. After the initial conidia deposit on leaves, downy mildew symptoms become visible 7 to 14 days later (Fall *et al.*, 2015; Fall, Van Der Heyden and Carisse, 2016). In agricultural fields, downy mildew outbreaks in lettuce tend to be sporadic, and are triggered by specific environmental conditions (Nordskog *et al.*, 2007). Generally, disease risk and severity is dependent on the quantity of B. lactucae conidia in the fields (Fall *et al.*, 2015). Resistance genes against B. lactucae regularly breakdown (Simko *et al.*, 2013; Fletcher *et al.*, 2019) and fungicides are also increasingly failing (Crute and Harrison, 1988; Brown *et al.*, 2007; Fletcher *et al.*, 2019).

1.9 Using hyperspectral imaging to evaluate combined IR agent treatments

Advancements in genome and transcriptome sequencing has enabled an increasing understanding of the effects of IR agents on the interaction between plants and pathogens. These methods continue to enable the development and characterisation of many IR agent treatments. Nevertheless, the ability to phenotype the effects of these IR agents in different pathosystems can be a bottleneck in the process of introducing effective IR agent treatments into agricultural practices. In the evaluation of the effects of plant disease status, destructive methods like measuring

gene expression and microscopy analysis (Fang and Ramasamy, 2015), or non-destructive visual scoring that categorises disease severity (Bock, Chiang and Del Ponte, 2022) are commonly used. These methods have disadvantages, the former tend to be resource and time intensive, while the later suffer from substantial variation in the observed scores between and within individual scorers (Fang and Ramasamy, 2015; Bock, Chiang and Del Ponte, 2022). Accordingly, interest in optical sensor technologies that enable high-throughput plant phenotyping has grown (Walter, Liebisch and Hund, 2015; Mahlein, 2016). Different optical sensor technologies that address the phenotyping bottleneck problem have been developed. Chlorophyll fluorescence sensors have been used to measure patterns of chlorophyll fluorescence emission in response to biotic and abiotic stresses (Baker, 2008). Infrared thermal imaging (thermography) has the capability to detect temperature changes in plants in response to diseases (Prashar and Jones, 2014). Red, green, and blue (RGB) cameras, which capture light at these eponymous bands, have been utilised to detect and measure visible disease symptoms in plants (Humplík *et al.*, 2015). While hyperspectral imaging (HSI) sensors are capable of tracking both visible and pre-symptomatic disease effects in plants through the detection of physiochemical changes in plants by measuring their interaction with the different regions of the electromagnetic spectrum (Mahlein *et al.*, 2018). Although less precise than destructive gold standard methods like plant defence gene expression analysis and microscopy, optical sensors are non-destructive and can measure the same individuals over time to give a broader picture. In contrast to visual scoring methods, optical sensors are typically more sensitive and consistent (Mutka and Bart, 2015).

Among these image phenotyping methods, HSI is the most versatile (Mutka and Bart, 2015; Mahlein *et al.*, 2018) and was the method of choice in this research. HSI sensors can capture electromagnetic radiation in the ultraviolet (UV; 350-400 nm), the visible (VIS; 400-700 nm), the near infrared (NIR; 700-1000 nm) and shortwave infrared (SWIR) ranges. In addition to capturing wide range of bands, HSI sensors can also have narrow spectral resolution – typically ≤ 1 nm –, which makes them a powerful phenotyping tool (Mahlein *et al.*, 2018). Such HSI sensors can be deployed in the field, mounted on ground vehicles or in the sky on drone, fixed-wing planes and satellites for remote sensing. However, they are more efficient in laboratory settings where they can be deployed at higher spatiotemporal resolutions (Dhondt, Wuyts and Inzé, 2013). Typically, in a laboratory setting, HSI systems consist of a mounting platform to hold/move the system, a broadband light source to illuminate the sample, a hyperspectral sensor to capture reflected light (Fig 1.4A), and a computer for control and data storage (Mahlein *et al.*, 2018). The HSI system captures spatio-spectral images in the form of hyperspectral data cubes (Fig 1.4B) that consist of two spatial and one spectral dimensions (Sarić *et al.*, 2022).

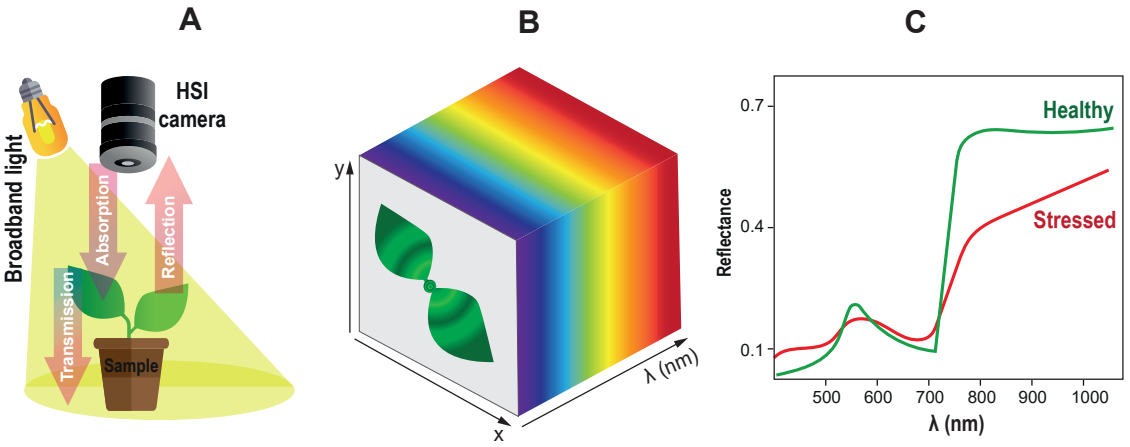

Fig 1.4 | Hyperspectral phenotyping. (A) Different light bands reflected from leaf surfaces are captured by a HSI sensor. (B) This produces a spatio-spectral hyperspectral reflectance data cube. (C) Spectral signatures plotted from the reflectance data can be used to assess a plants health status.

Based on the behaviour of light when it interacts with vegetation, hyperspectral data can be used to make inferences about the physiochemical states of plants. When plant leaves are illuminated, the light can be transmitted through the tissue, absorbed by chemicals in the tissue or reflected from the surface and the interior tissues. These interactions between light and plants, although complex, have been extensively characterised (Lowe, Harrison and French, 2017; Mahlein *et al.*, 2018). HSI data of this interaction is used to plot spectral reflectance signatures, which represent absorption/reflection intensities across the measured bands. Shape, position and intensity features in the spectral signature are unique fingerprints representing the condition of the imaged plant (Fig 1.4C) (Lowe, Harrison and French, 2017). Characteristically, in vegetation spectral signatures, the VIS region shows relatively high absorption due to pigments in leaves. Chlorophyll a and b selectively absorb in blue (400-500 nm) and red (600-700 nm) bands. A dip in the (500-600 nm) bands is due to less absorption of green light and the reason for the green appearance of plants. Other plant pigments also absorb VIS bands. Carotenoids strongly absorb blue light (400-500 nm), while anthocyanins absorb in the green region (500-600 nm) (Gay et al., 2008; Mahlein *et al.*, 2018). After the VIS region, there is a sharp increase in reflectance known as the red edge. After the red edge comes, a high reflectance plateau in the NIR region due to the pigments and cellulose in plant leaves transmitting most of the NIR light (Lowe, Harrison and French, 2017). Absorption and reflectance in the NIR region in plants is mostly the result leaf cellular structure. Beyond the NIR region reflectance decreases in the SWIR region and is dominated by absorption due to leave water content (Mahlein *et al.*, 2018).

Hyperspectral reflectance patterns in plants are affected by abiotic and biotic stresses and consequently can be used to assess plant health (Mishra *et al.*, 2017). Nevertheless, these spectral signatures are complex, they contain combined information from many plant processes and the information is spread across the measured spectrum (Mahlein *et al.*, 2018). One method of extracting specific information of interest from the complex spectral signatures has been the use of spectral vegetation indices (SVIs). These SVIs are ratios of bands which have been experimentally shown to correlate with specific plant properties (Xue and Su, 2017). For example the SVIs: ARI2 (Gitelson, Merzlyak and Chivkunova, 2001)., CRI2 (Gitelson *et al.*, 2002) and MCARI2 (Haboudane *et al.*, 2004), have been shown to track leaf anthocyanin, carotenoid and chlorophyll content respectively. Hyperspectral reflectance data and their derived SVIs have been extensively utilised to study a wide range of biotic stressors like pathogenic bacteria, fungi and oomycetes (Terentev *et al.*, 2022). Similarly, the effects of abiotic stressors on plants, including heavy metals, salt and drought have all been studied using HSI (Sytar *et al.*, 2017; Asaari *et al.*, 2019; Lassalle *et al.*, 2021). Given this versatility of HSI, it is an appropriate method for studying the effects of both chemical IR agents and microbial diseases in plants.

The use of such HSI data to phenotype plants can be computationally demanding. The hundreds spectral bands typically contained in HSI data and the many available SVIs that can be derived [See Table 2.1], often result in large and highly dimensional data. To reduce the required computational power, often spatially summarised data used (Manjunath *et al.*, 2013; Shrestha *et al.*, 2016). Furthermore, to handle the large number of variables contained in typical HSI data, various multivariable statistics, and machine learning approaches have been adapted and these enable the efficient and robust interpretation of experimentally derived HSI data (Paulus and Mahlein, 2020).

1.10 Scope of PhD thesis

The external application of IR agents enables plants to augment the efficacy of their innate immune response to subsequent pathogen encounters. Many such agents, both natural and synthetic, have been identified and characterised. These IR agents could offer a less damaging alternative to biocidal chemicals in the control of crop diseases. However, their adoption as mainstream crop protection products has been hampered because they are often associated with growth retardation at higher doses, and their protection can be incomplete and variable. Preliminary studies have suggested that combining IR agents has the potential to improve IR efficacy through synergistic interactions between the underpinning defence pathways. To date, however, this approach has not been adequately explored. The research described in this PhD thesis aimed to systematically characterise the potential of chemical IR agents in the tomato-*B. cinerea* and lettuce-*B. lactucae* pathosystems, using non-destructive hyperspectral imaging (HSI)

to separate the beneficial IR effects from the undesirable phytotoxicity effects. IR efficacy and phytotoxicity of concentration ranges of the three IR agents β-Aminobutyric acid (BABA), R-β-Homoserine (RBH) and Chitosan (ChP) were tested in these pathosystems before addressing the performance of combinations of these agents in the lettuce lettuce-*B. lactucae* pathosystem.

Chapter 2 presents an overview the common materials and methods used in the experiments described in this PhD thesis. The first experimental chapter, Chapter 3, describes the optimisation and selection of a non-invasive HSI method to quantify plant growth and phytotoxicity in tomato and lettuce by IR agents. The selected methods were then used to evaluate dose-dependent phytotoxic activities of BABA, RBH and ChP in these plant species. To separate IR effects from phytotoxicity effects, Chapter 4 describes the development of a non-destructive HSI method that selectively quantifies disease severity by pathogen infection, but that is unaffected by the phytotoxicity response to high doses of the IR agents. Using this method, the dose-dependent efficacies of the three IR agents were characterized in both the tomato-*B. cinerea* and lettuce-*B. lactucae* pathosystems. Chapter 5 presents the effects of combining low doses of IR agents with minimal phytotoxicity and limited IR effects on lettuce growth and IR efficacy against *B. lactucae*. Using various statistical models, the performance of pairwise combinations of the IR agents were evaluated, resulting in the identification of a mixed treatment that yielded synergistic levels of disease protection with no side-effects on plant growth. Finally, in chapter 6, the benefits of combining chemical IR agents are discussed in a wider context of integrated pest and disease management (IPM), placing particular emphasis on the practical considerations of commercial deployment of IR agents.

Chapter 2

Materials and general methods

This chapter contains the details of the materials used in the studies reported in this thesis. In addition, the details of shared general methods are presented here. Chapter specific methods are reported in the relevant sections.

2.1 Growth chamber conditions

All experimental stages involving plant germination, growth, chemical application, inoculation and imaging, was carried out in the same growth chamber (Fig 2.1). The day conditions in the chamber were set to 10 hours of light at an intensity of 200 μmol s^{-1} m^{-2} and a temperature 21°C. Night conditions were set to 14 hr dark at 19°C. Humidity was kept constant at 70%.

2.2 Seed germination and plant growth

To grow Moneymaker tomato (*Solanum lycopersicum*), seeds were sterilised by washing in 80% ethanol for 30 s, then in 4.5% bleach for 4 min and finally in distilled water (dH_2O) for 30 s four times. The sterilised seeds were germinated in Petri dishes containing 1.2 $mg.mL^{-1}$ agar gel (No. 2 Bacteriological, Neogen, USA) in the growth chamber. After six days, the newly germinated seedlings were transplanted into 70 mL pots containing 4:1 M3 soil (Levington, UK) and sand, and then watered every third day.

To grow Kavir lettuce (*Lactuca sativa*), seeds were germinated by sprinkling on top 70 mL pots containing 3:1 M3 soil and sand mix. After four days, the newly germinated seedlings were transplanted into 70 mL pots containing 3:1 M3 soil and sand mix, and then watered every fourth day.

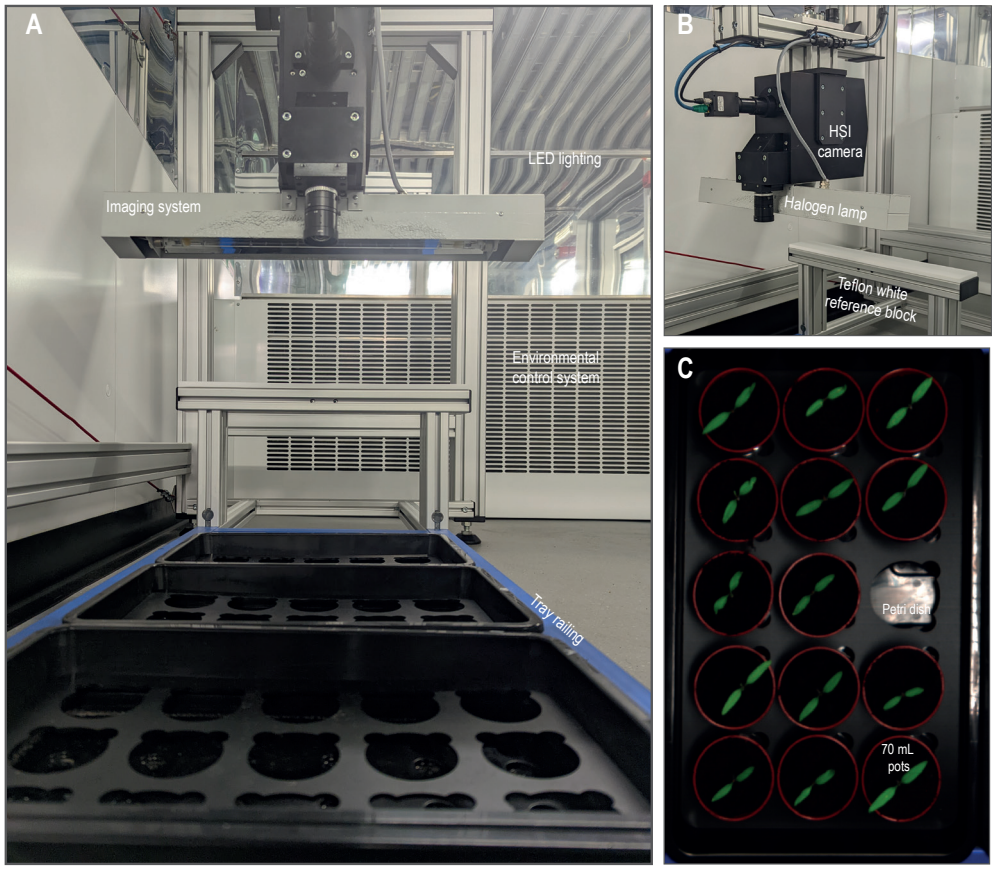

Fig 2.1 | Plant growth and phenotyping room. (A) The growth chamber with controlled temperature, humidity and lighting, a railing system for plant trays and an imaging system. (B) The hyperspectral-imaging camera with halogen lamp and Teflon white reference. (C) Tray for growing plants during treatment and imaging.

2.3 Chemical treatment preparation and application

Enantiopure, R-β-aminobutyric acid (BABA) and R-β-Homoserine (RBH) were synthesised and provided by the lab of Beining Chen (Department of Chemistry, The University of Sheffield, UK). ChitoPlant®, a water-soluble formulation of chitosan, was kindly provided by ChiPro (ChiPro GmbH; Bremen, Germany). Stock solutions of BABA and RBH in dH_2O were prepared freshly for each experiment. Then treatment solutions at concentrations x10 the desired treatment concentrations were prepared from the stock solutions. ChitoPlant® (ChP) stock solution was prepared by dissolving the powder in 0.02% v/v Silwet solution by magnetic stirring for 30 min. ChP treatment solutions were prepared by appropriate dilutions of the stock in 0.02% v/v Silwet. One day after transplanting into soil, seedlings were treated with the chemicals. BABA and RBH were applied by soil drenching. In the pots, 7 mL (10% of the pot volume) of the appropriate dose solution was placed on top of the soil using a syringe, and controls were treated with dH_2O. A Petri dish was placed under each pot to catch the

run-through solution for re-uptake. ChP was applied by spraying individual seedlings with 3 mL of appropriate dose solutions controls were sprayed with a similar amount of 0.02% v/v Silwet. In all experiments, for each chemical, 5 seedling replicates received each dose. However, since statistical power increases with the number of controls (Hong and Park, 2012), the number of replicates per chemical for the controls was set to 15.

2.4 Pathogen cultivations and inoculations

Botrytis cinerea strain B05.10 (van Kan *et al.*, 1997) inoculum solution was prepared by cultivating a plug of the fungus in Malt Extract Agar (MEA) plate in the dark, at room temperature for four days. Then to promote sporulation, the plate was placed under UV light (360 nm) for 12 hr and returned to the dark for four days. Conidia from the plate were harvested in dH_2O, the suspension was filtered through Miracloth and centrifuged at 800 rpm for 5 min. The supernatant was discarded, the pellet re-suspended in 6 mg mL^{-1}potato dextrose broth (PDB) and the concentration adjusted to 10^6 spores mL^{-1}. The inoculum solution was incubated at room temperature for 1.5 hrs. Two days after chemical treatments, tomato seedlings were inoculated by placing a 5-µl drop of inoculum in the centre of each cotyledon. Mock treatments were inoculated with 5-µl drops of the PDB solution.

Bremia lactucae race Bl:32 inoculum solution was prepared by placing infected plant material from seven days post infection in to 50 mL tubes and adding dH_2O. The spore solution was then filtered through Miracloth and the concentration adjusted to 10^5 spores mL^{-1}. Two days after chemical treatments, lettuce seedlings were inoculated with a spray of the spore solution until runoff was imminent. Mock inoculation with dH_2O was applied in the same manner.

2.5 Hyperspectral imaging and processing

Hyperspectral imaging (HSI) was performed with a PSI HC 900 imaging system (Photon Systems Instruments, Czech Republic). The camera in the system, used an imaging CMOS detector with a sensor array of 1920 lines 1000 rows a spectral range of 350-895 nm and a spectral resolution of 1.2 nm. The acquired images were processed with an in house application written in the R language and the application PlantScreen Data Analyser (Photon Systems Instruments, Czech Republic). The processed hyperspectral data was analysed using the Tidyverse R packages (Wickham *et al.*, 2019).

2.5.1 Image acquisition

Seedlings were grown and imaged in fixed locations in a growth chamber for the duration of each experiment. The pots containing the seedlings were placed in Petri dishes, then placed inside trays

with holders that prevented pot movement. At the point of imaging, the samples were uniformly illuminated from above with a broadband halogen lamp. The camera, which was motorised, line-scanned stationary samples at 15 $mm.s^{-1}$. The vertical distance between the camera lens and samples was set to 200 mm, the exposure time to 0.09 s and the spatial resolution was 5 $px.mm^{-1}$. Detached leaves were placed on trays with a non-reflective black mat paper background and similarly line-scanned.

2.5.2 Image calibration

To calibrate raw hyperspectral reflectance images (R_0). A white reference image (R_w) was acquired from a white Teflon standard with a 99.9% reflectance. A black reference image (R_b) was acquired in complete darkness. Then calibrated reflectance images (R) were computed as $R = (R_0-R_b)/(R_w-R_b)$.

2.5.3 Image segmentation

To exclude non-plant material, the calibrated images were segmented. Since plants and non-plant materials like soil and plastics have different hyperspectral reflectance properties, a plant segmentation index (SI) that uses reflectance at three spectral bands where $SI= 1.2(2.5(R_{740}-R_{672})-1.3(R_{740}-R_{556})$ was used. Then an SI threshold of 0.1 was used to erode non-plant material and only retain images of the plant material. Finally the images in each tray were further segmented into individual samples. These segmented images consisted hyperspectral cubes with reflectance values in the band range of 350-895 nm at an interval 1.2 nm for each image pixel. To reduce this large data size, averaged reflectance values per sample were derived and used in subsequent analysis.

2.5.4 Spectral vegetation indices

Using the averaged hyperspectral reflectance data, 115 spectral vegetation indices (SVIs) were derived for each sample. These consisted of previously reported SVIs (Table 2.1), that use VIS and NIR bands of the electromagnetic spectrum. Derivation of the SVIs was performed using the tidyverse (Wickham *et al.*, 2019) and hsdar (Lehnert *et al.*, 2019) R packages.

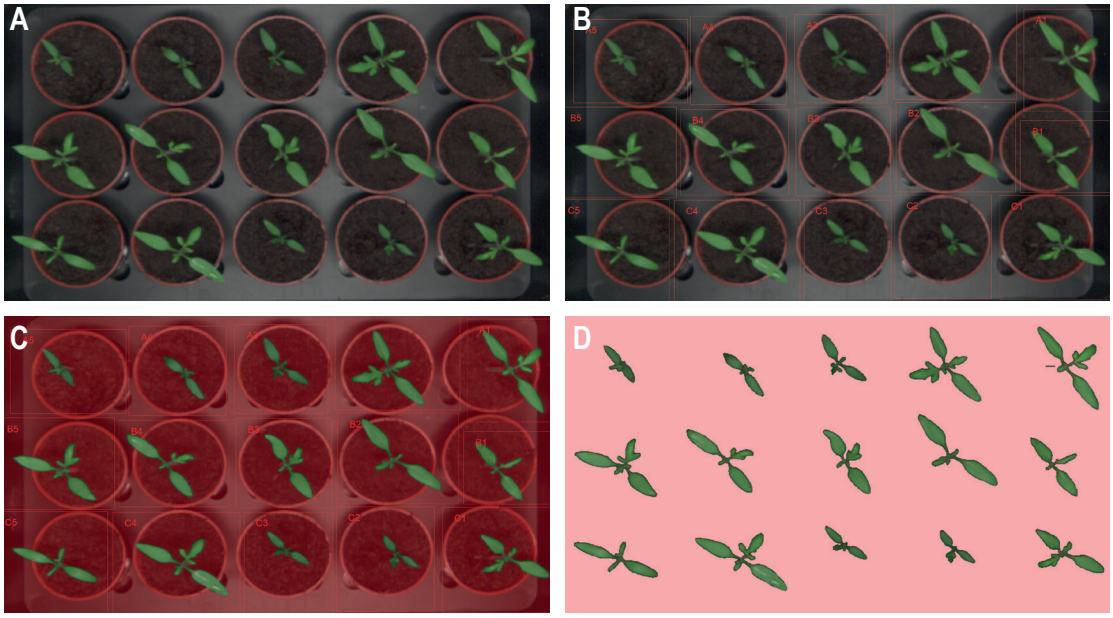

Fig 2.2 | Image segmentation. (**A**) Image of a tray of plants. (**B**) Breaking image up with masks for individual plants. (**C**) Segmenting image to plant (green) and nonplant (red). (**D**) Extracting only plant image data.

Table 2.1 | List of Spectral vegetation indices. Adapted from (Xue and Su, 2017; Harris Geospatial, 2022; Lehnert, 2022)

Index	Formula	Reference
ARI1	$(1/R_{550}) - (1/R_{700})$	(Gitelson, Merzlyak and Chivkunova, 2001)
ARI2	$R_{800}(1/R_{550}) - (1/R_{700})$	
BGI	R_{450}/R_{550}	(Zarco-Tejada *et al.*, 2005)
Boochs	D_{703}	(Boochs *et al.*, 1990)
Boochs2	D_{720}	
BRI	R_{450}/R_{690}	(Zarco-Tejada *et al.*, 2005)
CARI	$R_{700} * abs(a * 670 + R_{670} + b)/R_{670} * (a^2 + 1)^{0.5}$ $a = (R_{700} * R_{550})/150$, $b = R_{550} - (a * 550)$	(Kim, 1994)
Carter	R_{695}/R_{420}	(Carter, 1994)
Carter2	R_{695}/R_{760}	
Carter3	R_{605}/R_{760}	
Carter4	R_{710}/R_{760}	
Carter5	R_{695}/R_{670}	
Carter6	R_{550}	
CI	$R_{675} * R_{690}/R^2_{683}$	(Zarco-Tejada *et al.*, 2003)
CI2	$R_{760}/R_{700} - 1$	(Gitelson, Gritz and Merzlyak, 2003)
ClAInt	$R_{735} \int R_{600}$	(Oppelt and Mauser, 2004)
CRI1	$1/R_{515} - 1/R_{550}$	Gitelson, Gritz and Merzlyak, 2003)
CRI2	$1/R_{515} - 1/R_{770}$	
CRI3	$1/R_{515} - 1/R_{550} * R_{770}$	
CRI4	$1/R_{515} - 1/R_{700} * R_{770}$	
D1	D_{730}/D_{706}	(Zarco-Tejada *et al.*, 2003)
D2	D_{705}/D_{722}	(Zarco-Tejada *et al.*, 2003)
Datt	$(R_{850} - R_{710})/(R_{850} - R_{680})$	(Datt, 1999)
Datt2	R_{850}/R_{710}	
Datt3	D_{754}/D_{704}	
Datt4	$R_{672}/(R_{550} * R_{708})$	(Datt, 1998)
Datt5	R_{672}/R_{550}	
Datt6	$R_{860}/R_{550} * R_{708}$	
DD	$(R_{749} - R_{720}) - (R_{701} - R_{672})$	(Le Maire, François and Dufrêne, 2004)

DDn	$2 * (R_{710} - R_{660} - R_{760})$	(le Maire *et al.*, 2008)
DPI	$D_{688} * D_{710} / D^2_{697}$	(Zarco-Tejada *et al.*, 2003)
DWSI4	R_{550}/R_{680}	(Apan *et al.*, 2004)
EGFN	$(\max(D_{650:750}) + \max(D_{500:550}))/(\max(D_{650:750}) + \max(D_{500:550}))$	(Peñuelas *et al.*, 1994)
EGFR	$\max(D_{650:750})/\max(D_{500:550})$	
EVI	$2.5 * ((R_{800} - R_{670})/(R_{800} - 6 * R_{670} - 7.5 * R_{475} + 1))$	(Huete *et al.*, 1997)
GDVI2	$(R^2_{800} - R^2_{680})/(R^2_{800} + R^2_{680})$	(Wu, 2014)
GDVI3	$(R^3_{800} - R^3_{680})/(R^3_{800} + R^3_{680})$	
GDVI4	$(R^4_{800} - R^4_{680})/(R^4_{800} + R^4_{680})$	
GI	R_{554}/R_{677}	(Smith *et al.*, 1995)
Gitelson	$1/R_{700}$	(Gitelson, Buschmann and Lichtenthaler, 1999)
Gitelson2	$(R_{750} - R_{800}/R_{695} - R_{740}) - 1$	(Gitelson, Gritz and Merzlyak, 2003)
GMI1	R_{750}/R_{550}	(Gitelson and Merzlyak, 1998)
GMI2	R_{750}/R_{700}	
Green NDVI	$(R_{800} - R_{550})/(R_{800} + R_{550})$	(Gitelson, Kaufman and Merzlyak, 1996)
GVI	$(R_{682} - R_{553})/(R_{682} + R_{553})$	(Gandia *et al.*, 2004)
LIC	R_{440}/R_{690}	(Lichtenthaler *et al.*, 1996)
LRDSI1	$6.9*(R_{605}/R_{455})-1.2$	(Ashourloo, Mobasheri and Huete, 2014)
LRDSI2	$4.2 * (R_{695}/R_{455}) - 0.38$	
Maccioni	$(R_{780} - R_{710})/(R_{780} - R_{680})$	(Maccioni, Agati and Mazzinghi, 2001)
MCARI/OSAVI	MCARI2/OSAVI	(Wu *et al.*, 2008)
MCARI	$((R_{700} - R_{670}) - 0.2 * (R_{700} - R_{550})) * (R_{700} - R_{670})$	(Daughtry *et al.*, 2000)
MCARI2	$((R_{700} - R_{670}) - 0.2 * (R_{700} - R_{550})) * (R_{700}/R_{670})$	(Haboudane *et al.*, 2004)
MCARI2/OSAVI2	MCARI2/OSAVI2	(Daughtry *et al.*, 2000)
mND705	$(R_{750} - R_{705})/(R_{750} + R_{705}\} - 2 * R_{445})$	(Sims and Gamon, 2002)
mNDVI	$(R_{800} - R_{680})/(R_{800} + R_{680} - 2 * R_{445})$	
MPRI	$(R_{515} - R_{530})/(R_{515} + R_{530})$	(Hernández-Clemente *et al.*, 2011)
mREIP	Red-edge inflection point using a Gaussian function	(Miller, Hare and Wu, 1990)
MSAVI	$0.5 * (2 * R_{800} + 1 - ((2 * R_{800} + 1)^2 - 8 * (R_{800} - R_{670}))^{0.5})$	(Qi *et al.*, 1994)
mSR	$(R_{800} - R_{445})/(R_{680} - R_{445})$	(Sims and Gamon, 2002)
mSR2	$(R_{750}/R_{705}) - 1/(R_{750}/R_{705} + 1)^{0.5}$	(Chen, 1996)
mSR3	$(R_{800}/(R_{670} - 1))/ (R_{800}/(R_{670} + 1))^{0.5}$	(Chen and Cihlar, 1996)
mSR705	$(R_{750} - R_{445})/(R_{705} - R_{445})$	(Sims and Gamon, 2002)

MTCI	$(R_{754} - R_{709})/(R_{709} - R_{681})$	(Dash and Curran, 2004)
MTVI	$1.2 * (1.2 * (R_{800} - R_{550}) - 2.5 * (R_{670} - R_{550}))$	(Haboudane *et al.*, 2004)
NDVI	$(R_{800} - R_{680})/(R_{800} + R_{680})$	(Tucker, 1979)
NDVI2	$(R_{750} - R_{705})/(R_{750} + R_{705})$	(Gitelson and Merzlyak, 1994)
NDVI3	$(R_{682} - R_{553})/(R_{682} + R_{553})$	(Gandia *et al.*, 2004)
NPCI	$(R_{680} - R_{430})/(R_{680} + R_{430})$	(Peñuelas *et al.*, 1994)
NPQI	$(R_{415} - R_{435})/(R_{415} + R_{435})$	(Zarco-Tejada *et al.*, 2001)
NRI	$(R_{570} - R_{670})/(R_{570} + R_{670})$	(Cao *et al.*, 2015)
OSAVI	$(1 + 0.16) * (R_{800} - R_{670})/(R_{800} + R_{670} + 0.16)$	(Rondeaux, Steven and Baret, 1996)
OSAVI2	$(1 + 0.16) * (R_{750} - R_{705})/(R_{750} + R_{705} + 0.16)$	(Wu *et al.*, 2008)
PhRI	$(R_{550} - R_{531})/(R_{550} + R_{531})$	(Cao *et al.*, 2015)
PRI	$(R_{531} - R_{570})/(R_{531} + R_{570})$	(Gamon, Serrano and Surfus, 1997)
PRI*CI2	PRI*CI2	(Garrity, Eitel and Vierling, 2011)
PRI2	$(R_{570} - R_{539})/(R_{570} + R_{539})$	(Filella *et al.*, 1996)
PRI_norm	$PRI * (-1)/(RDVI * R_{700}/R_{670})$	(Zarco-Tejada *et al.*, 2013)
PSRI	$(R_{678} - R_{500})/R_{750}$	(Merzlyak *et al.*, 1999)
PSSR	R_{800}/R_{635}	(Blackburn, 1998)
PSND	$(R_{800} - R_{470})/(R_{800} - R_{470})$	
RARS	R_{746}/R_{513}	(Chappelle, Kim and McMurtrey, 1992)
RDVI	$(R_{800} - R_{670})/(R_{800} + R_{670})^{0.5}$	(Roujean and Breon, 1995)
REP_LE	Red-edge position by linear extrapolation	(Cho and Skidmore, 2006)
REP_Li	$700 + 40 * ((R_{re} - R_{700})/(R_{740} - R_{700})$ $R_{re} = (R_{670} - R_{780})/2$	(Guyot and Baret, 1988)
RGI	R_{690}/R_{550}	(Zarco-Tejada *et al.*, 2005)
SAVI	$(1 + L)/(R_{800} - R_{670})/(R_{800} + R_{670} + L)$	(Huete, 1988)
SIPI	$(R_{800} - R_{445})/(R_{800} - R_{680})$	(Penuelas, Baret and Filella, 1995)
SIPI2	$(R_{800} - R_{440})/(R_{800} - R_{680})$	(Penuelas *et al.*, 1995)
SIPI3	$(R_{800} - R_{445})/(R_{800} - R_{650})$	(Penuelas, Baret and Filella, 1995)
SPVI	$0.4 * 3.7 * (R_{800} - R_{670}) - 1.2 * ((R_{530} - R_{670})^2)^{0.5}$	(Vincini *et al.*, 2006)
SR	R_{800}/R_{680}	(Jordan, 1969)
SR1	R_{750}/R_{700}	(Gitelson and Merzlyak, 1998)
SR2	R_{752}/R_{690}	
SR3	R_{750}/R_{550}	
SR4	R_{700}/R_{670}	(McMurtrey *et al.*, 1994)

SR5	R_{675}/R_{700}	(Chappelle, Kim and McMurtrey, 1992)
SR6	R_{750}/R_{710}	(Zarco-Tejada and Miller, 1999)
SR7	R_{440}/R_{690}	(Lichtenthaler *et al.*, 1996)
SR8	R_{515}/R_{550}	(Hernández-Clemente, Navarro-Cerrillo and Zarco-Tejada, 2012)
SRPI	R_{430}/R_{680}	(Penuelas *et al.*, 1995)
Sum_Dr1	$\sum_{i=626}^{795} D1i$	(Elvidge and Chen, 1995)
Sum_Dr2	$\sum_{i=680}^{780} D1i$	(Filella and Peñuelas, 1994)
TCARI	$3 * ((R_{700} - R_{670}) - 0.2 * (R_{700} - R_{550}) * (R_{700}/R_{670}))$	(Haboudane *et al.*, 2002)
TCARI/OSAVI	TCARI/OSAVI	
TCARI2	$3 * ((R_{750} - R_{705}) - 0.2 * (R_{750} - R_{550}) * (R_{750}/R_{705}))$	(Wu *et al.*, 2008)
TCARI2/OSAVI2	TCARI2/OSAVI2	
TGI	$-0.5 * (190 * (R_{670} - R_{550}) - 120 * (R_{670} - R_{480}))$	(Hunt *et al.*, 2013)
TVI	$0.5 * (120 * (R_{750} - R_{550}) - 200 * (R_{670} - R_{550}))$	(Broge and Leblanc, 2001)
Vogelmann	R_{740}/R_{720}	(Vogelmann, Rock and Moss, 1994)
Vogelmann2	$(R_{734} - R_{747})/(R_{715} + R_{726})$	
Vogelmann3	D_{715}/D_{705}	
Vogelmann4	$(R_{734} - R_{747})/(R_{715} + R_{720})$	

Chapter 3

Quantification of phytotoxicity by chemical IR agents in lettuce and tomato

Abstract

Chemical IR agents can provide durable and broad-spectrum crop protection. However, many IR agents also tend to repress plant growth at higher doses. These phytotoxic effects are highly variable between plant species and cultivars. Accordingly, safe and effective exploitation of IR agents in crop protection schemes requires a careful characterisation of their growth-repressing effects, in order to minimise undesirable non-target effects. In this Chapter, the dose-dependent phytotoxic activities of IR agents BABA, RBH and ChP were investigated in tomato and lettuce using a hyperspectral sensor. Analysis of the image-derived growth data showed that both BABA and RBH had dose-dependent repressive effects on relative growth rates (RGR), with BABA being generally more phytotoxic than RBH. On the other hand, ChP lacked negative effects on growth in both plant species. Spectral reflectance data revealed that BABA and RBH resulted in dose-dependent spectral patterns. Linking these patterns to the RGR-repressing effects of these agents allowed for the selection of spectral vegetation indices that can rapidly quantify phytotoxicity by IR agents in a non-destructive manner.

3.1 Introduction

Although chemical IR agents provide durable and broad-spectrum crop protection, they are rarely used in agriculture as crop protection agents. One of the main reasons of their under-utilisation can be phytotoxicity of some agents, i.e. the capacity to cause temporary or lasting growth reduction and cellular dysfunction in plants (EPPO, 2014; Werrie *et al.*, 2020). Consequently, effective exploitation of chemical IR agents in crop protection schemes requires minimisation of this non-target effect (Yassin *et al.*, 2021).

This growth repression by chemical IR agents is highly variable between plant species and cultivars. The non-protein β-amino acid BABA is one of the most potent inducers of plant resistance (Cohen, Vaknin and Mauch-Mani, 2016). Unfortunately, this molecule is also phytotoxic, which is the result of its inhibitory effect on the aspartyl-tRNA synthetase enzyme, which leads to the accumulation of uncharged aspartyl-tRNA and ultimately stress-related growth repression (Luna *et al.*, 2014). In Arabidopsis (Wu *et al.*, 2010), tomato (Buswell *et al.*, 2018) and lettuce (Cohen, Vaknin and Mauch-Mani, 2016), BABA has been reported to be phytotoxic in higher concentrations. Yet in other plant species, such as sunflower (Amzalek and Cohen, 2007), soybean (Zhong *et al.*, 2014) and grapevines (Reuveni, Zahavi and Cohen, 2001) BABA was not reported to be phytotoxic. Recently, R-β-homoserine was identified in a screen for resistance-inducing BABA structural analogues with less phytotoxicity. This initial study found no significant phytotoxicity in Arabidopsis and tomato cv. Micro-Tom (Buswell *et al.*, 2018). Another IR agent that has been reported to be less phytotoxic is Chitoplant a water-soluble Chitosan formulation (ChiPro GmbH, Bremen, Germany) (Romanazzi *et al.*, 2013; Younes *et al.*, 2014). Unlike RBH, ChP which is a naturally occurring polysaccharide that has even recently been associated with growth promotion (De Vega *et al.*, 2021). Furthermore, despite many studies that have examined the growth impacts of these chemicals, our understanding of their actions are binary and lack dose-response models of their phytotoxic activities.

The work presented in this chapter will profile the dose-dependent phytotoxic activities of BABA, RBH and ChP in the lettuce (cv. Kavir) and tomato (cv. Money-Maker). To quantify phytotoxic effects of the three IR agents, a HSI camera was used to non-destructively measure plant growth based on image area and investigate physiochemical changes due to chemical treatments through multispectral reflectance.

3.2 Methods

3.2.1 Plant growth, chemical treatments and inoculations

Tomato and lettuce plants were grown and treated with IR agents as described in sections 2.2 and 2.3 respectively. In tomato experiments, six day-old seedlings growing in 4:1 soil : sand mix were treated with increasing doses of the chemicals in the same way as the lettuce seedlings. Two days after chemical treatments, each tomato seedling was mock inoculated with a single 5-µL drop PDB (6 mg mL^{-1}) on each cotyledon. In experiments with lettuce, five days-old seedlings growing in 3:1 soil : sand mix were treated with increasing doses of BABA or RBH (0, 0.125, 0.25, 0.5, 1 and 2% w/v) by soil drenching or with ChP (0, 0.063, 0.125, 0.25, 0.5, 1 and 2 % w/v) by foliar spraying. Two days after chemical treatments, the cotyledons of the lettuce seedlings were mock spray inoculated with dH_2O until run-off was imminent.

3.2.2 Seedling imaging and destructive endpoint sampling

Tomato and lettuce seedlings were imaged with a HSI camera once daily for ten days as described in section 2.5. In experiments with chemical treatments imaging started from the point of chemical application. At the tenth day both tomato and lettuce leaves were detached from their seedlings and imaged while flat by HSI with the adaxial side facing up. For experiments looking at the relationship between seedling green pixel area and fresh weight water-treated seedlings were imaged for 10 days. on the 10^{th} day, aboveground shoot material was harvested and the fresh weights recorded.

3.2.3 Data extraction, analysis and statistical testing

Sample averaged hyperspectral reflectance and green pixel (px) area data, was extracted and processed as described in sections 2.5. All data analysis and statistical tests were performed using R version 4.0.5 (R Core Team, 2021).

3.2.3 .1 Modelling seedling growth rates

Growth data for each seedling consisting of green plant pixel area and time was fitted with generalized additive model (GAM) using the *gam* function of the *mgcv* (version 1.8-38) package (Wood, 2011). To smooth out noise in the growth data, the GAM fitted values were extracted from the model. To ascertain the accuracy of the GAM predicted data a regression analysis was performed to determine the relationship between GAM predicted seeding area and above ground fresh weight. To measure the relative growth rates (RGR) of the seedlings the natural log transformed green area against time data were fitted with linear models and seedling RGR

derived as the slope of the fitted curve.

3.2.3 .2 Dose response modelling

RGR data were fitted with dose response models using the *drc* (version 3.0-1) package (Ritz *et al.*, 2015) and TD_{50} parameters (the dose required to produce 50% of the maximal effect) for the three IR agents was extracted from the fitted models.

3.2.4 Profiling β-amino acid residues by liquid chromatography coupled to quadrupole-orthogonal time-of-flight mass spectrometry

To examine the metabolism of the β-amino acids BABA and RBH over time in tomato and lettuce their residues in plant tissue was measured using liquid chromatography coupled to quadrupole-orthogonal time-of-flight mass spectrometry. Seven-day-old tomato and lettuce seedlings growing in in 3:1 soil : sand mix were treated with BABA (0.5 mM), RBH (0.5 mM) or dH_2O by soil drenching. For each treatment, 24 seedlings grouped in fours were assigned. At 2, 14 and 42 days post-treatment, the above-ground shoot tissue of four plants randomly assigned to each time point were harvested, snap frozen with liquid nitrogen and stored at -80°C. The shoot tissue was freeze-dried, ground in to powder, weighed and then extracted in buffer (MeOH:H2O:Formic acid, 10:89.99:0.01, v/v/v) to make samples at a concentration of 0.1 mg μL^{-1}. The sample extracts were centrifuged at 16,000g at 4 °C for 5 minutes and each supernatant was split in to three aliquots. Using BABA and RBH standards in the range of 0.1 - 100 µM, the samples were analysed in a HPLC-MS coupled system. Sample mass spectra was recorded in positive electro-spray ionization mode on a Waters ACQUITY UPLC system interfaced to a Waters Synapt G2Si HDMS QTof mass spectrometer. Sample separation was performed using Waters ACQUITY HILIC BEH C18 analytical column with 1.7 µm particle size, 50 mm length and 2.1 mm inner diameter. The mobile phase consisted of 20 mM ammonium formate (NH_4HCO_2) with 0.1% formic acid and acetonitrile (CH_3CN) with 0.1% formic acid. NH_4HCO_2 started at a 99% gradient then down to 65% at 4 minutes, 1% at 6 minutes and held there for 1.5 min after which it was returned to 99%. Solvent flow rate was set to 0.3 mL $min^{-1}$and injection volume to 4 µL. Nitrogen was used as the drying and nebulizing gas. The desolvation gas, flow rate was set to 150 L hr^{-1}, the source temperature was set at 100 °C and the final temperature was set to 280 °C. The cone gas flow was set to 20 L hr^{-1}, the cone voltage was 5 V and the capillary voltage was set to 2.5 kV. The instrument was calibrated a range of 20-1200 m/z with a solution of sodium formate and Leucine (Sigma-Aldrich, St. Louis MO, USA) in equal water methanol mix and 0.1% Formic acid.

3.3 Results

3.3.1 Estimating plant growth from images

To determine whether non-destructive quantification of green plant area is suitable for accurately calculating growth rates, lettuce and tomato seedlings were imaged with a HSI camera over 10 days to acquire the top view images of green plant area. Generally green pixel area increased with time (Fig 3.1A). However, seedling stem movements as well as changes in leaf angle over the measurement period lead to within-replicate variation that complicated between-replicate/-treatment analysis of variation. To reduce this noise, GAMs were fitted to the time versus green pixel area data for individual seedlings. Generally the GAMs fitted the data well (Fig 3.1A). Furthermore, end point model predicted values and end point above ground plant fresh weight showed a strong positive correlation (Fig 3.1B) for both tomato (R2 = 0.97) and lettuce (R2 = 0.93). These results indicated that GAM predicted values from image-derived green area could be used to accurately estimate plant growth. Accordingly, quantification of lettuce and tomato growth in subsequent growth analyses was based on GAM-predicted green area.

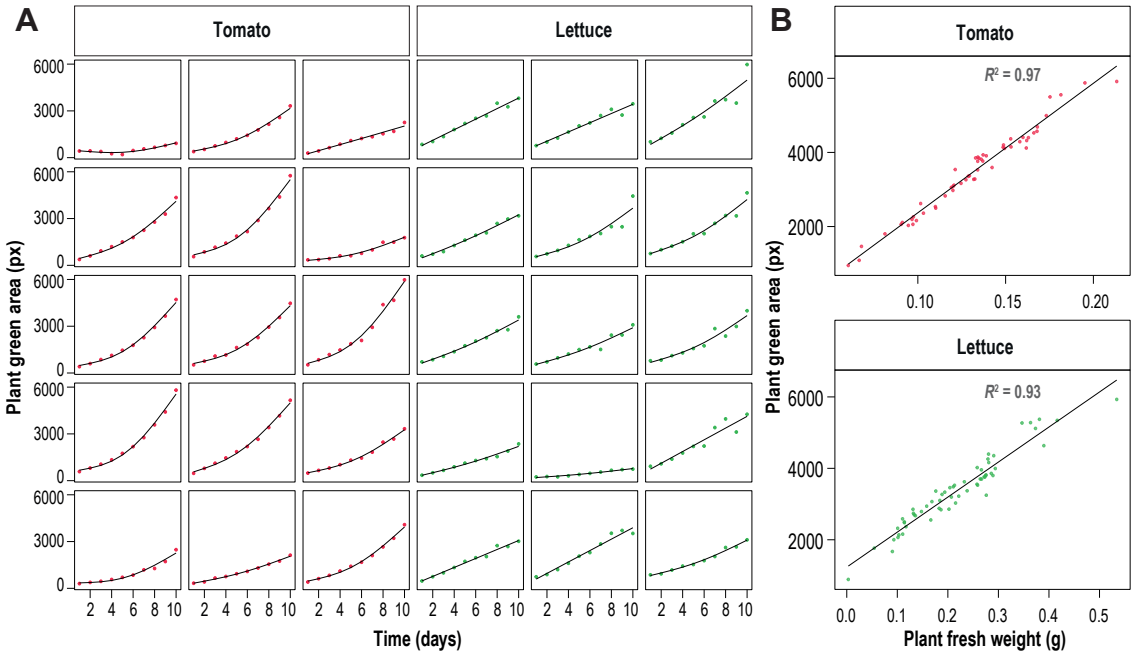

Fig 3.1 | Smoothing tomato and lettuce growth data with GAMs. (**A**) Plots show green area (px) against time (days) for individual lettuce and tomato seedlings. The red (tomato) and green (lettuce) points are the recorded green area and the black lines are the fitted GAM models. (**B**) The correlation between end-point GAM predicted green area and above ground fresh weigh for tomato and lettuce seedlings.

3.3.2 Assessing the phytotoxicity of the chemical IR agents through growth

To assess the effects of BABA, RBH and ChP on tomato and lettuce growth, the green area of seedlings receiving increasing doses of the three chemicals were recorded with a HSI camera for ten days (Fig 3.2). The growth curves of control-treated seedlings (Dose 0) did not plateau indicating the plants continued to grow over the duration of the experiments, as is expected of young plants. Generally, the β-amino acids BABA and RBH caused a dose-dependent decline in growth for both tomato and lettuce, resulting in decreasing slopes of the growth curves with increasing dosages. In tomato, BABA-induced growth repression was more pronounced compared to RBH, whereas in lettuce, the growth-repressing effect of BABA was only marginally stronger than that of RBH. In contrast to both β-amino acids, ChP-treated tomato and lettuce showed little change in growth. Thus, based on the growth curves, BABA and RBH both reduce growth in tomato and lettuce. However, in tomato, and to a lesser extent also lettuce, this phytotoxic effect is stronger by BABA than RBH.

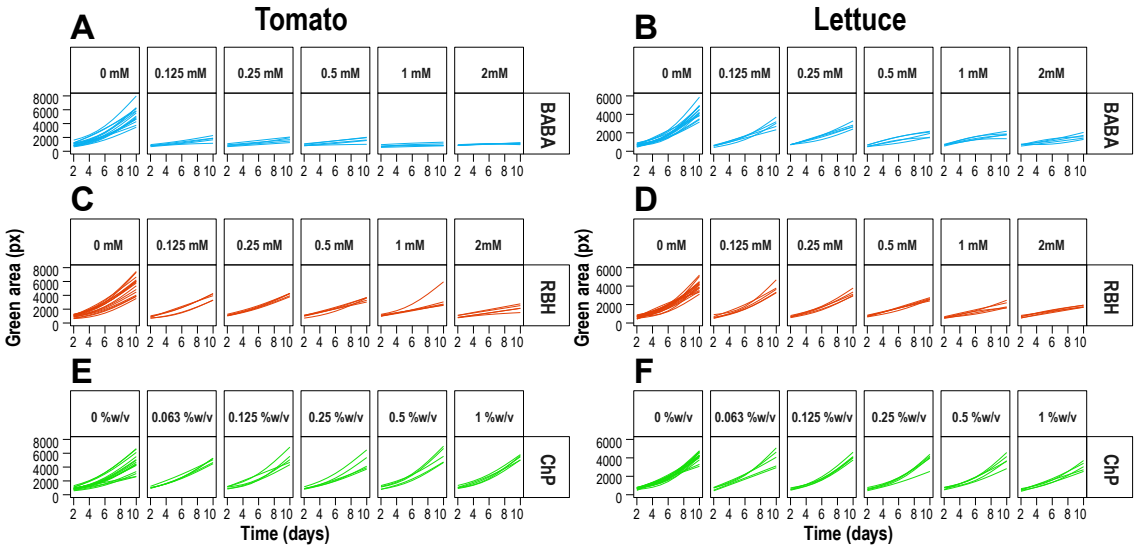

Fig 3.2 | The dose-dependent effects of the IR agents on seedling growth of tomato and lettuce. Shown are GAM-predicted growth curves based on 10 individual time-points. Each plot shows green area (px) against time (days) for individual tomato and lettuce seedlings after soil-drenching with increasing doses of BABA (A and B), RBH (C and D), or spraying the leaves with increases doses of ChP (E and F).

To quantify relative growth rate values (RGRs), log-transformed growth data were fitted with a linear model to derive RGR values from the slope of the fitted curve. To test the effects of chemical dose on RGR, a Kruskal-Wallis test was carried out. Where dose had a significant effect, pairwise comparisons between the controls and each dose using Dunn's test was performed (Fig 3.3). BABA significantly reduced growth at all tested doses in both tomato and lettuce. In RBH

treated tomato and lettuce, all doses above the lowest concentration (0.125 mM) significantly reduced growth. By comparison, ChP dose had no significant effect on growth in either tomato or lettuce. Thus, BABA and RBH both reduce RGR in a dose dependent manner in both tomato and lettuce; however, BABA is more phytotoxic in both species, while ChP is not associated with RGR reduction.

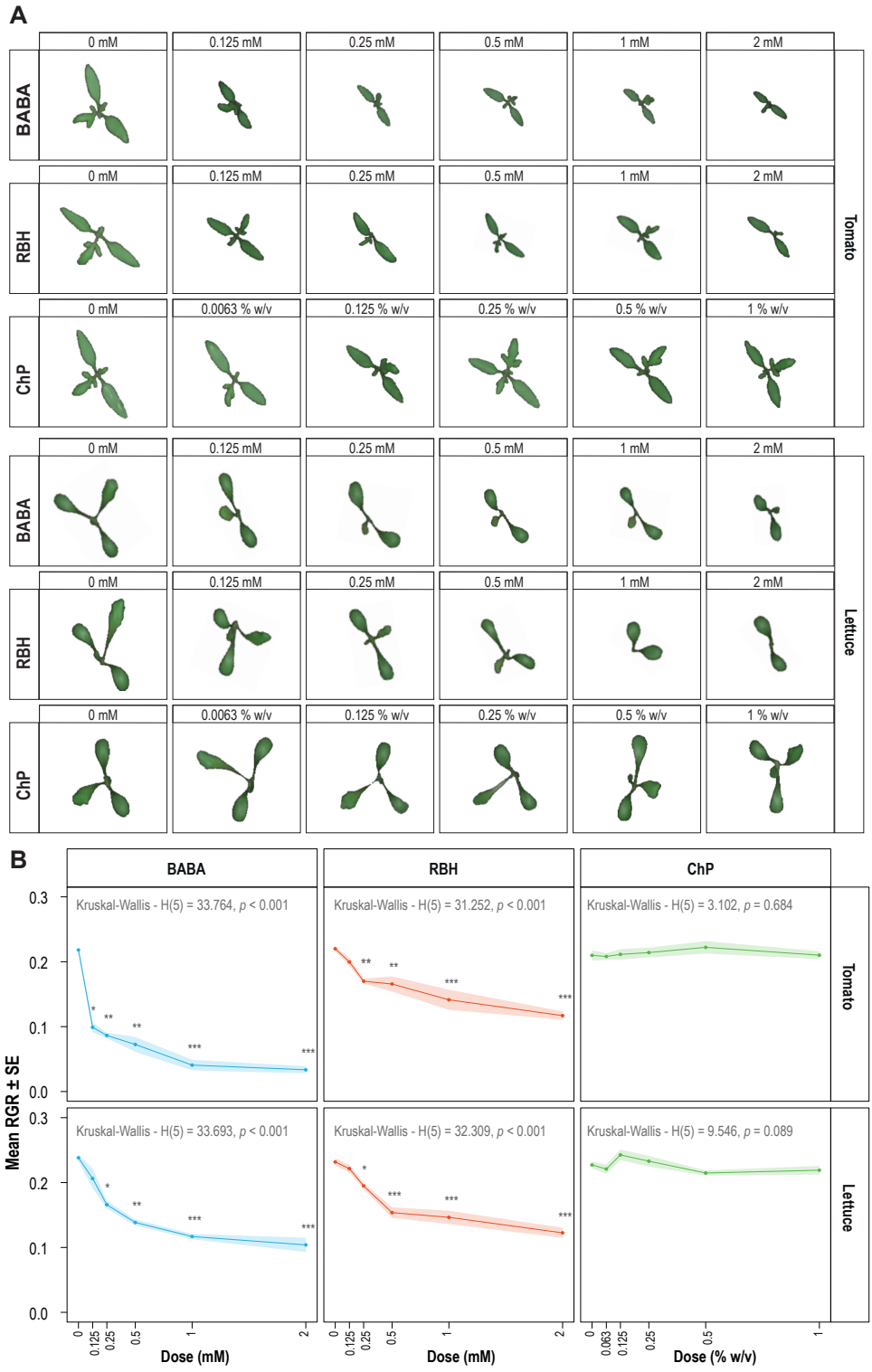

Fig 3.3 | The dose-dependent effects of the IR agents on RGR in tomato and lettuce. (**A**) Sample images of tomato and lettuce seedlings after treatment with increasing IR agent doses. (**B**) The presented curves are mean RGR ± SE. The effect of chemical dose on seedling RGR was tested for statistical significance by Kruskal-Wallis tests. Dose treatments that are statistically different from the control treatment (Dose 0) was carried out by Dunn's tests and denoted as * for $p < 0.05$, ** for $p < 0.01$, and *** for $p < 0.001$.

To compare the phytotoxicity levels of the three IR agents in tomato and lettuce, dose response models were fitted to show the relationship between increasing dose and RGR (Fig 3.4). The dose required to produce 50% of the maximal effect (TD_{50}) was obtained from the fitted models. By this measure, BABA had the lowest TD_{50} values of the three IR agents. In tomato this BABA TD_{50} value was nearly two times lower (0.13 ± 0.02 mM) than that in lettuce (0.25 ± 0.05 mM), suggesting that tomato is more sensitive to BABA than lettuce. By contrast, the TD_{50} value for RBH in lettuce (0.34 ± 0.07 mM) was nearly two times lower than that of tomato (0.57 ± 0.18 mM), suggesting that lettuce is more sensitive to RBH than tomato. The fitted dose response models did not produce significant TD_{50} parameters for ChP in either plant species. Thus, median phytotoxic dose parameters derived from the fitted dose response models suggests that BABA was the more phytotoxic of the two β-amino acids and its phytotoxicity was greater in tomato. RBH, on the other hand, was more phytotoxic in lettuce than tomato, while ChP had no phytotoxicity in tomato or lettuce.

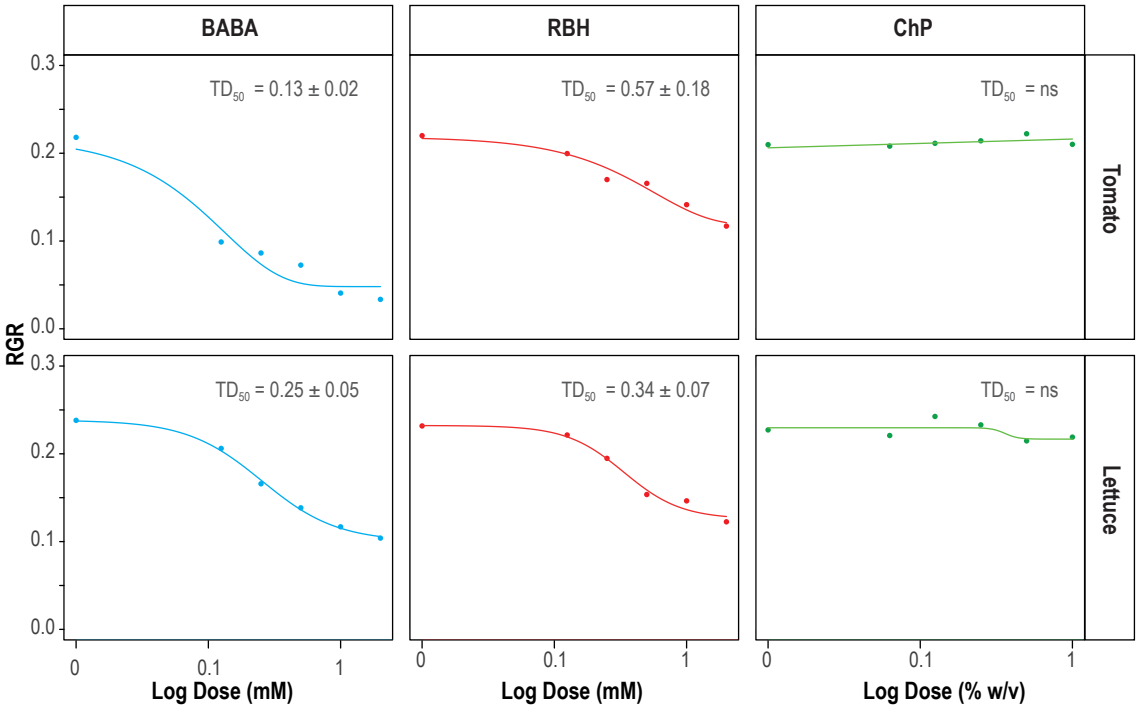

Fig 3.4 | Estimation of phytotoxicity parameters (TD_{50} values) of the three IR agent in tomato and lettuce. The fitted curves are based on mean RGR values per dose, from which TD_{50} values were predicted. In tomato, TD_{50} was estimated at 0.13 ± 0.02 mM ($p < 0.001$) for BABA and at 0.57 ± 0.18 mM ($p = 0.003$) for RBH. In lettuce, TD_{50} values were predicted at 0.25 ± 0.05 mM ($p < 0.001$) for BABA and at 0.34 ± 0.07 mM ($p = 0.071$) for RBH. The TD_{50} value for ChP parameter was not statistically significant in both plant species.

3.3.3 Assessing chemical stress through hyperspectral signatures

Analysis of the tomato and lettuce growth data suggested that BABA and RBH are phytotoxic but have different toxicity profiles in the two species, while ChP was not phytotoxic in either plant species. To delineate stress types and patterns, plants receiving the different treatments were first imaged non-destructively daily for ten days with a HSI camera, then cotyledons and leaves were detached and imaged by HSI for destructive endpoint analysis. To investigate the impact of the chemicals, spectral signatures, which are plots of wavebands against reflectance intensity, were derived from the hyperspectral reflectance data. Fig 3.5 shows end time-point, averaged spectral signatures at each chemical dose, for whole plants, detached cotyledons and true leaves. The samples showed spectral signatures typical of vegetation (Govender, Chetty and Bulcock, 2007; Mahlein *et al.*, 2012). The visible spectrum (VIS) showed generally a low reflectance region, except for the green peak at 550 nm. At the end of the red spectrum, there was a red edge transition zone (680 – 730 nm), which had the usual sharp increase in reflectance. This increase in reflectance then plateaued into the near infrared (NIR) spectrum. Within this general pattern, there were strong dose-dependent shifts in reflectance by BABA and RBH, which were apparent in both plant species. By contrast, the spectral shifts by ChP appeared much more subtle. Furthermore, the magnitude of the spectral shifts by BABA and RBH differed by vegetation type: reflectance changes were most acute in true leaves, followed by whole plants, while cotyledons showed relatively little variation. Thus, treatment with BABA and RBH caused dose-dependent spectral changes correlating with their phytotoxicity (Figs 3.1 - 3.4), which varies by vegetation type. Together, these results demonstrate that the spectral signatures of the seedlings echo the phytotoxic effects of the IR agents.

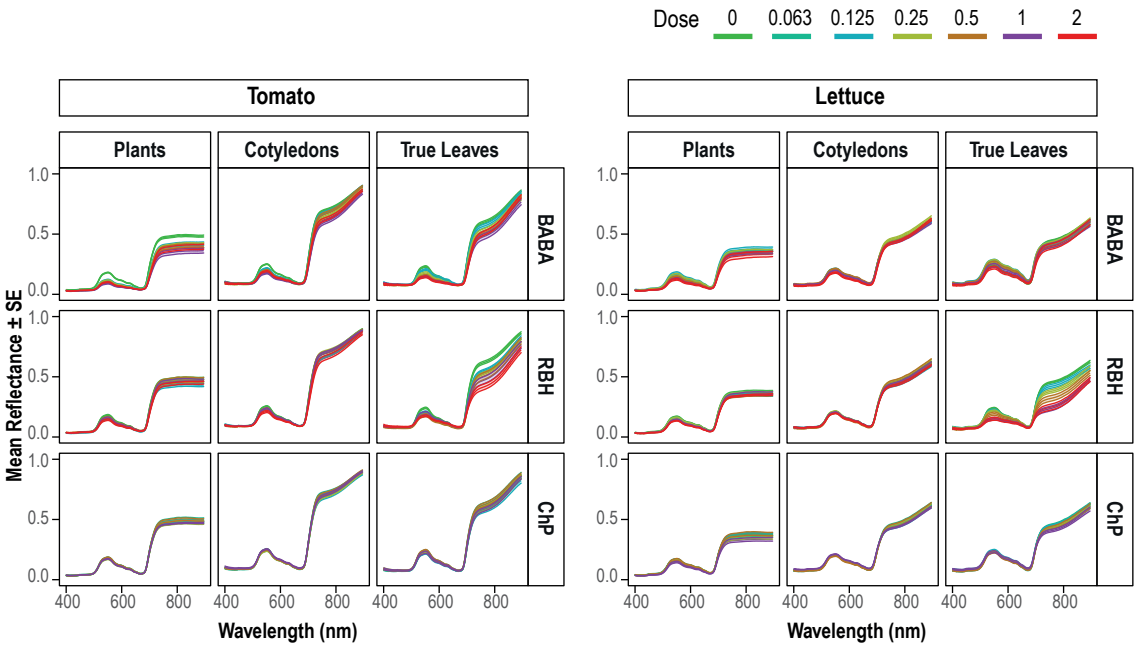

Fig 3.5 | Effects of IR agents on hyperspectral signatures. The presented curves are reflectance intensities at individual wavelengths in the visible spectrum (VIS; 400 – 650 nm) and the near-infrared spectrum (NIR; 650 – 895 nm). Each curve represents the average reflectance of one tomato or lettuce sample upon treatment with a single chemical dose.

3.3.4 Profiling phytotoxicity of IR agents by spectral vegetation indices

Stress caused by IR agents results in dose-dependent spectral shifts (Figs 3.5). To investigate the nature of these stresses further, a small number of bands in the HSI data were used to calculate spectral vegetation indices (SVIs), which are parameters that have been empirically demonstrated to describe specific physio-chemical attributes of plant tissues (Xue and Su, 2017). From these SVIs, three commonly used indices for plant stress markers were selected. Firstly, the Anthocyanin Reflectance Index 2 (ARI2) was selected, which has been developed to estimate concentrations of anthocyanins in vegetation, a well-characterised marker of plant stress (Gitelson, Merzlyak and Chivkunova, 2001). Secondly, the Carotenoid Reflectance Index 2 (CRI2) was selected, which estimates carotenoid concentrations relative to chlorophyll, which have been reported to shift in stressed plant tissues (Gitelson *et al.*, 2002). Thirdly, the Modified Chlorophyll Absorption Ratio Index (MCARI2) was selected, which indicates the depth of chlorophyll absorption and is based on evidence that spectral characteristics of chlorophyll, including fluorescence, change in stressed plant tissues (Haboudane *et al.*, 2004). Kruskal-Wallis tests were carried out to examine whether the chemical IR dose influenced these SVIs significantly. Where there was a statistically significant effect, pairwise comparisons to the controls were performed using Dunn's test (Fig 3.6).

Generally, ARI2 values declined with increasing doses of BABA and RBH, but did not change

much in response to ChP treatment (Fig. 3.6). Between both plant species, BABA had the highest impact on ARI2 in tomato. In whole plants of both tomato and lettuce, increased doses of both BABA and RBH had a statistically significant repressive effect on ARI2 values. In tomato detached true leaves, BABA significantly repressed ARI2 values with increasing dose, whereas BABA failed to have a statistically significant effect on ARI2 in lettuce across all doses. Chemical dose effects on ARI2 values in detached cotyledons were similar to those in true leaves, although generally less variable with lower values. While the dose effect was statistically significant for both chemicals in both plants species, the impact of BABA and RBH on ARI2 on detached cotyledons was greater in lettuce than tomato. ARI2 values varied little with ChP dose, and the only significant change was a slight increase in detached cotyledons treated with 0.125 % (w/v) ChP.

For CRI2, increasing BABA doses caused a complex 'dip-rise effect' in lettuce tissues, while BABA mostly increased CRI2 values in tomato tissues (Fig., 3.7). The effects of increasing RBH doses on CRI2 showed a general upward trend in both plant species, while ChP only increased CRI2 at the highest dose. In whole plants, BABA dose had a statistically significant effect in both species. In lettuce whole plants, CRI2 values decreased at BABA doses of 0.125 and 0.25 mM, but increased from 0.5 to 2 mM. By contrast, BABA dose increased CRI2 values in tomato whole plants, where the size effects on CRI2 were more pronounced overall compared with lettuce. RBH dose had a statistically significant effect in whole plants in both species, mostly causing increasing CRI2 values. However, the effects by RBH in whole tomato plants were less pronounced than those caused by BABA. ChP had no statistically significant effect on CRI2 in whole plants of both species. In detached true leaves of lettuce, the effects of BABA and RBH dose was statistically significant on CRI2. BABA dose caused the same dip-rise effect in detached lettuce leaves as observed in whole plants, while detached tomato leaves showed a steady increase in CRI2 values with BABA dose. At increasing doses of RBH, variation in CRI2 values was less than that observed in detached leaves from BABA-treated plants. In lettuce, RBH dose had no statistically significant effect on CRI2, while in tomato the dose effect was statistically significant only at the higher doses (1 and 2 mM). In cotyledons, the effects of the three chemicals on CRI2 values was relatively mild. However, dose effects on CRI2 were statistically significant for both BABA and ChP in lettuce cotyledons and in tomato for BABA and RBH. The strongest effects were observed for cotyledons from BABA-treated tomato, which showed a statistically significant increase in CRI2 values at the lowest dose of 0.0125 mM.

For MCARI2, effects of IR chemicals were marginal compared to ARI2 and CRI2 (Fig. 3.7). For whole plants, no statistically significant effects were found by either chemical in both lettuce and tomato. In true leaves of lettuce, MCARI2 values decreased with dose for all three chemicals tested, which was statistically significant. For tomato true leaves, only BABA had a significant impact on MCARI2 values, which decreased with increasing BABA dose. For detached cotyledons

of lettuce, only the highest dose of CHP resulted in a significant decrease in MCARI2 value. For tomato cotyledons, RBH dose caused a statistically significant effect on MCARI2, resulting in higher values with increasing dose.

Considering the SVIs (ARI2, CRI2 and MCARI2) selected to profile the stress effects of the IR agents gave a complex picture that reflected chemical plant species and leaf type. The possibility of a single SVI that can serve as proxy of RGR in all the treatment groups was investigated. Taking into account the influences of chemical and plant species on the potential SVI – RGR relationship, the data was separated in to six groups (three chemicals by two plant species). First linear regression was performed to determine the correlations the respective six groups and all available SVIs (115). Following that, only using BABA and RBH treatment data – because ChP does not affect RGR – the median R^2 and interquartile range (IQR) of R^2 was calculated for these four groups (Fig 3.7A). To select SVIs with optimal balance between correlation (high R^2) and spread (low R^2 IQR) a threshold of $R^2 > 0.4$ and R^2 IQR < 0.2 was set. Then the performance of these selected SVIs was investigated in ChP treatment groups by comparing median R^2 for tomato and lettuce plants (Fig 3.7B). While a high R^2 value was better also closeness of the median R^2 values for the tomato and lettuce also important. Finally, when all these consideration were made this process yielded the SVI Triangular Greenness Index (TGI). The correlation between TGI and RGR differed by plant and chemical (Fig 3.7C). The best correlation was in BABA treated plants (tomato, $R^2 = 0.91$, $p < 0.001$; lettuce $R^2 = 0.60$, $p < 0.001$) followed by the RBH treated plants (tomato, $R^2 = 0.50$, $p < 0.001$; lettuce $R^2 = 0.49$, $p < 0.001$), while there was a lack of correlation for ChP treated plants. Overall, TGI against chemical dose (Fig 3.7D) gave results similar to those of RGR against chemical dose for both tomato and lettuce (Fig 3.3).

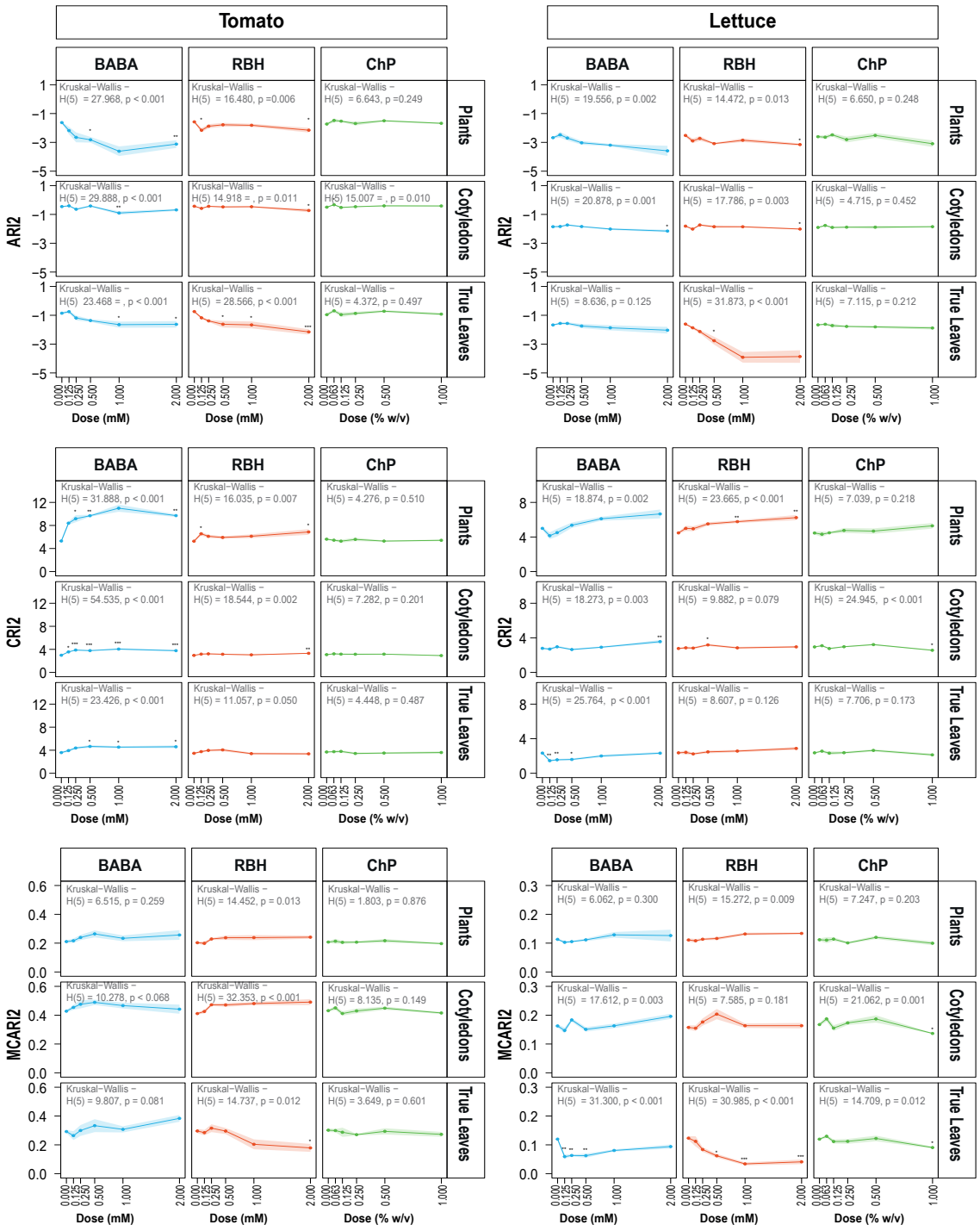

Fig 3.6 | The effects of chemical dose on three stress-related vegetation indices (SVIs). The presented curves are mean ± SE of the SVIs ARI2, CRI2 or MCARI2 at increasing BABA, RBH and ChP doses in tomato tissues (left panels) and lettuce tissues (right panels). Individual panels show the effects of each chemical treatment for either whole plants (upper rows), detached cotyledons (middle rows) or detached true leaves (lower rows). The effect of chemical dose on the SVIs was statistically investigated by Kruskal-Wallis. Where statistically significant, differences between dose treatment and controls was carried out by Dunn's tests (*$p < 0.05$, **$p < 0.01$, and ***$p < 0.001$).

To summarise, all three IR agents had dose-dependent effects on stress-related SVIs. BABA and RBH caused relatively large changes, whereas the effects caused by ChP remained relatively small. It was clear also that the effects on the SVIs were different between BABA and RBH, supporting the notion that both β-amino acids have physiologically different impacts on plants (Buswell *et al.*, 2018). Generally, however, the results suggest that tomato is more sensitive than lettuce to stress by both β-amino acids. Furthermore, the responses by true leaves and cotyledons often differed, whereby true leaves of lettuce showed a stronger SVI response by BABA and RBH than lettuce cotyledons, which was opposite for tomato. Thus, the stress effects of IR agents as quantified by the SVIs is complex and depends on the chemical, plant species and leaf type. However, the SVI TGI gave optimal compromise of plant species and chemical dependents effects to track RGR.

3.3.5 Analysis of BABA and RBH residues in plant tissue over time by liquid chromatography-mass spectrometry

A major concern about the use of agrochemicals is build-up of chemical residues in food crops. Since BABA acts as a general blocker of protein synthesis (Luna *et al.*, 2014) and RBH is a synthetic xenobiotic chemical (Buswell *et al.*, 2018), the translational value of both IR agents is not only determined by their phytotoxicity and IR effectiveness, but also the extent by which these agents form chemical residues in the plant. Moreover, the observed phytotoxicity by both β-amino acids in lettuce and tomato might be related to their accumulation in the leaf tissues. To investigate this relationship further, tomato and lettuce plants were soil-drenched with either BABA (0.5 mM), RBH (0.5 mM) or water (control), after which above ground plant material was harvested at 2, 14 and 42 days. Concentrations of each compound were quantified in methanol extracts from dry plant material using HILIC-Q-TOF (Fig 3.8). In tomato plants, residues of both β-amino acid residue levels remained overall much lower compared to lettuce. In fact, RBH levels did not differ from controls at any time point, indicating that RBH is rapidly metabolised. Interestingly, BABA at 42 days post-treatment residues in tomato reached a level (0.226 ± 0.042 $\mu M.mg^{-1}$) that was statistically higher than the background signal in the control group, suggesting that BABA is less effectively metabolised in older tissues. At two days post-treatment of lettuce, RBH accumulated to slightly higher levels (0.240 ± 0.027 $\mu M.mg^{-1}$) than BABA (0.166 ± 0.03 $\mu M.mg^{-1}$), which was statistically significant compared to the background signal in the controls. At 14 days post-treatment, residues of both β-amino acids peaked in lettuce, with BABA residues being 33% higher (1.570 ± 0.120 $\mu M.mg^{-1}$) than RBH residues (0.942 ± 0.091 $\mu M.mg^{-1}$). At 42 days post-treatment, both BABA and RBH lettuce residue levels declined and were no longer significantly different compared to the background signal in the control-treated plants.

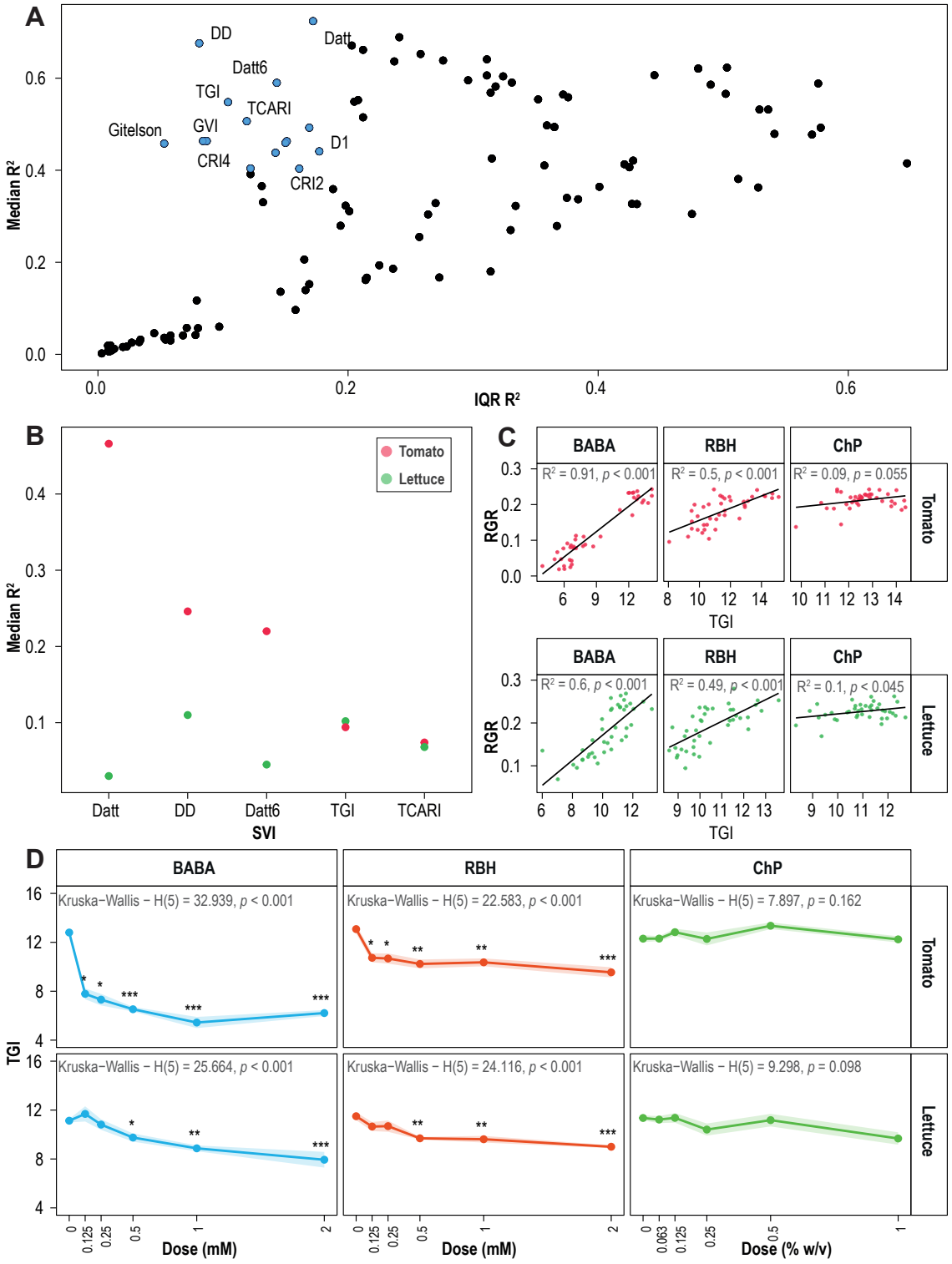

Fig 3.7 | The identification of an SVI proxy for RGR. The process of selecting an SVI that best correlates with RGR in the different treatment groups. (A) The spread (R^2 IQR) and median correlation level (R^2) of SVIs with RGR in BABA and RBH treatment groups. (B) The performance of selected SVIs by closeness of median R^2 in tomato and lettuce. (C) Correlation between TGI and RGR in different treatment groups. (D) The effect of chemical dose on TGI.

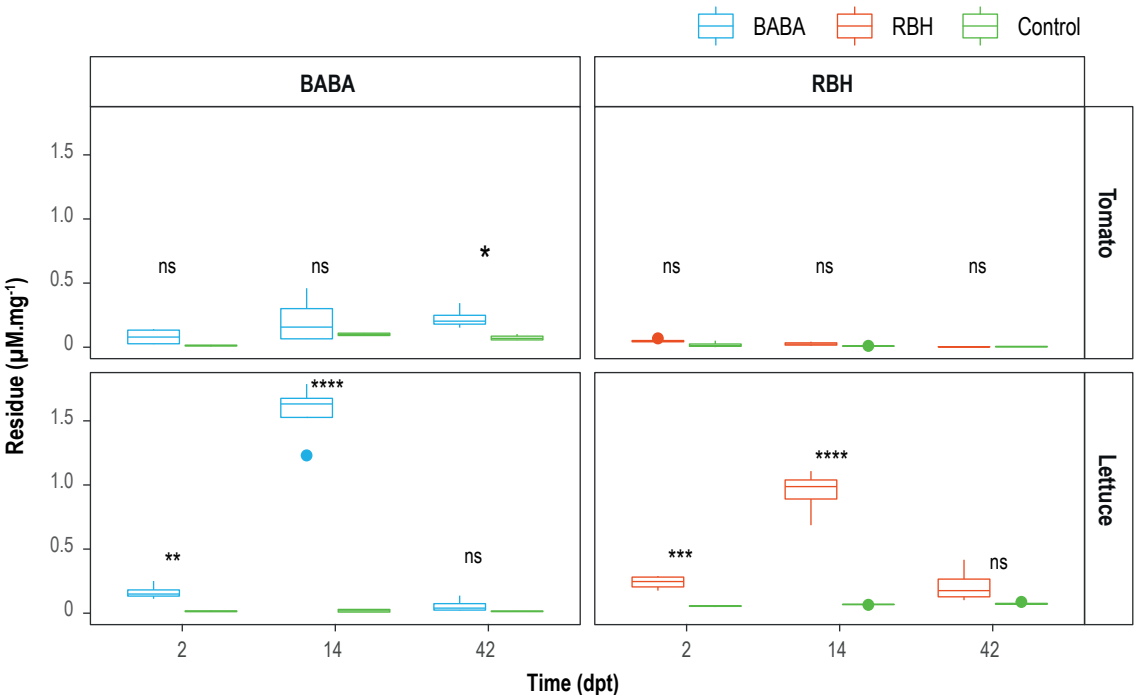

Fig 3.8 | Chemical residues of BABA and RBH in shoot tissues of lettuce and tomato. Boxplots show β-amino acid concentrations (µM/mg DW; n = 4). Tomato or lettuce seedlings were soil-drenched with 0.5 mM BABA or RBH and analysed by HILIC-Q-TOF to estimate β-amino acid concentrations in comparison to water-treated control plants at 2, 14 and 42 days post treatment. Asterisks indicate statistically significant differences between β-amino acid-treated plants and control-treated plants (*$p < 0.05$, **$p < 0.01$, ***$p < 0.001$, ns: not significant).

3.4 Discussion

Phytotoxic effects, when applied in higher doses, have hampered exploitation of some chemical IR agents as crop protection agents. The fact phytotoxicity varies between plant species and cultivars, which necessitates tailored application protocols, is a further hindrance (Yassin *et al.*, 2021). For instance, BABA was found to lack phytotoxicity in some plant species (e.g. sun flower), while it is highly phytotoxic in other species (e.g. tomato) (Amzalek and Cohen, 2007; Wu *et al.*, 2010; Zhong *et al.*, 2014; Buswell *et al.*, 2018). The structural BABA analogue RBH was recently identified as a less toxic IR agent in Arabidopsis and the tomato cultivar MicroTom (Buswell *et al.*, 2018). Similarly, the chitosan formulation ChP has been described as a non-phytotoxic IR agent. To further substantiate these phytotoxic activities of BABA, RBH and ChP, this chapter has presented a dose-dependent analysis of the phytotoxic activities by the IR agents in lettuce (cv. Kavir) and tomato (cv. Moneymaker). Based on non-destructive imaging of plant growth and hyperspectral reflectance, it can be concluded that the degree of phytotoxicity by the three IR agents varies between plant species and tissues. However, in general terms, BABA appeared to be the most phytotoxic of the three agents, followed by RBH, and ChP causing little if any phytotoxicity (Figs 3.4 – 3.6).

The profiling of phytotoxic activities by the IR agents was based on non-destructive phenotyping by HSI. There were two major challenges associated with this approach, which dictated the experimental approaches taken. First, both lettuce and tomato seedlings underwent foliar nyctinasty (Minorsky, 2019), where leaves that have horizontal positions during the light period take vertical positions during the dark. Secondly, as the number of leaves increases over the growth period, leaf overlap occurs which complicate accurate quantification of green plant area. Consequently, the experiments presented in this Chapter were restricted to the light period, using relatively young plants that did not grow beyond the emergence of the first true leaves. These experimental choices made it easier to accurately quantify plant growth over time without destructive sampling. Indeed, the quantification of green plant image appeared to be an excellent proxy for fresh weight as the two were highly correlated (Fig 3.1), enabling precise analysis of relative phytotoxicity of the IR agents, albeit restricted to relatively young plants.

Analysis of the image-derived growth data showed that the both BABA and RBH had-dose dependent repressive effects on RGR, while ChP had no statistically significant repressive effect on RGR (Fig 3.3). BABA was the more phytotoxic of the two β-amino acids (Fig 3.4) and its phytotoxicity was higher in tomato than lettuce. By comparison, RBH phytotoxicity appeared higher in lettuce (Fig 3.6). While BABA phytotoxicity is widely reported, RBH was selected as a molecule lacking this property and was shown to have no growth repression effect in Arabidopsis and tomato cv. Micro-Tom (Buswell *et al.*, 2018). This finding underscores the variable effects

of IR agents between plant species and cultivars, as well as the importance of experimentally selecting chemical IR treatments for target crop species and cultivars. Recent results have revealed that the phytotoxicity of both BABA and RBH is a function of their cellular uptake, which is determined by the LHT1 transporter (Tao *et al.*, 2022). In Arabidopsis, expression of the *LHT1* gene in wild-type plants is sufficiently low to prevent uptake of phytotoxic quantities of RBH, while over-expression of the *LHT1* gene also causes phytotoxicity at increasing doses of RBH. However, while the affinity of LHT1 to BABA is comparable to that of RBH (Tao *et al.*, 2022), BABA is phytotoxic in Arabidopsis wild-type plants whereas RBH is not, which indicates the intracellular toxicity of BABA is higher than RBH. To determine whether the orthologous genes of *LHT1* in lettuce and tomato controls phytotoxicity to BABA and RBH similarly, it would be necessary to over-express these genes and test for increased tolerance. Alternatively, a larger diversity panel of lettuce or tomato varieties, varying in phytotoxicity could be profiled for *LHT1* gene expression to establish a correlation.

The analysis of spectral reflectance data revealed that the two β-amino acids affected spectral signatures of treated plants in a dose dependent manner, while ChP treatments caused little or no changes (Fig 3.6). The shifts in spectral reflectance were more prominent in true leaves than in cotyledons. Similarly, in the derived SVIs, values of ARI2, CRI2 and MCARI2, which have been developed to indicate anthocyanin, carotenoid and chlorophyll content respectively (Gitelson, Merzlyak and Chivkunova, 2001; Gitelson *et al.*, 2002; Haboudane *et al.*, 2004), showed variation between true leaves and cotyledons. In general, SVI values deviated from the control levels in a dose-dependent manner, which was more pronounced in true leaves than in cotyledons. This suggests that the cotyledons are more resilient toward the phytotoxic effects of the IR agents. However, it remains uncertain whether this effect is based on an inherent physiological property of cotyledons, or whether this is because treatment was applied at a point where the cotyledons were mostly developed, and the true leaves were yet to emerge. One possible explanation for the observed difference in tolerance to the β-amino acids is that cotyledons have been shown to have fewer stomata (Geisler and Sack, 2002), and hence would have less uptake via mass flow, which would result in lower cellular uptake of the β-amino acids from the soil and xylem. This possibility could be tested by a time course analysis of β-amino acid residues in cotyledons and true leaves by HPLC-MS method described in section 3.3.5. Nonetheless, TGI was identified as an SVI in which chemical and plant species differences are minimised. TGI was developed analysing HSI data of vegetation canopies from remote sensing satellites has been shown to be highly correlated with leaf chlorophyll content (Hunt *et al.*, 2013). Generally, TGI correlated well with RG, and although not as accurate as deriving RGR from image data, it does serve as a means to assess growth effects when time course data for calculating growth rates are not available or convenient.

If BABA, RBH and ChP are going to be widely exploited as crop protection agents, knowledge of the levels of residues in plant tissues after treatment is important. Analysis of post-treatment BABA and RBH residue levels in plant tissues by HILIC-Q-TOF showed that the absorption and breakdown of the two β-amino acids differed between lettuce and tomato. BABA and RBH were clearly detected in lettuce shoots at 2 days post-treatment, which increased to even higher levels by 14 days post-treatment (Fig 3.9). However, 6 weeks post-treatment, no BABA and RBH could be detected above the background signal, suggesting that both β-amino acids are catabolised in older lettuce tissues. Although RBH is a new IR agent for which there are no previous comparisons, BABA has been reported to be slowly metabolised in Arabidopsis (Jakab *et al.*, 2001; Slaughter *et al.*, 2012), which again underscores the variability IR agent behaviour between plant species and the importance of experimental verification for target crops.

Chapter 4

Quantification of disease protection by chemical IR agents against *Botrytis cinerea* in tomato and *Bremia lactucae* in lettuce.

Abstract

Chemical IR agents can have low and/or variable crop protection efficacies. The performance of these agents often is species- and cultivar-dependent and depends on the nature of the challenging pathogen. In this Chapter, the IR efficacies of BABA, RBH and ChP were tested in tomato against the necrotrophic fungus *B. cinerea* in tomato and in lettuce against the biotrophic oomycete *B. lactucae*. Disease incidence was quantified by traditional (destructive) scoring methods and (non-destructive) remote sensing methods. Multivariate and machine-learning statistical methods were used to analyse the spectral data to disentangle the effects of disease stress and stress caused by the chemical IR agents. This analysis resulted in the selection of a disease-specific spectral vegetation index that allows for a non-destructively quantification of disease progression in the presence and absence of the chemical IR agents. The analyses revealed that only ChP was effective against *B. cinerea* in tomato, whilst all three agents offered protection against *B. lactucae* in lettuce to varying degrees, with BABA showing the strongest IR effect, followed by RBH and then ChP.

4.1 Introduction

Chemical IR agents are under-utilised in crop protection because of potential phytotoxicity (see Chapter 3), relatively low levels of protection compared with conventional pesticides and sometimes variable efficacy (Yassin *et al.*, 2021). It has been shown that the efficacy of IR agents depends on the plant species, cultivar (Hijwegen and Verhaar, 1995; Dann *et al.*, 1998) and identity of the attacking pathogen (Sharma, Butz and Finckh, 2010). Accordingly, it is difficult to generalize about the potential efficacy of an IR chemical and each agent needs to be evaluated experimentally on a point-by-point basis before it can be considered for exploitation against a certain crop disease.

Previously, the IR agents BABA, RBH and ChP were found to be effective against the necrotrophic fungus *B. cinerea* in tomato. BABA, applied as a foliar spray resulted in a dose-dependent reductions in lesion size by *B. cinerea* size in three-week-old tomato plants (cv. Ailsa Craig; Li, Sheng and Shen, 2020). Similarly, soil drench treatments of three-week-old plants of tomato (cv. Moneymaker) with 1 mM BABA resulted in statistically significant reductions in lesion size by *B. cinerea* compared to controls (Luna *et al.*, 2016). RBH has been reported to be effective against *B. cinerea* infection also (Buswell *et al.* 2018). The soil drench treatments of sixteen-day-old seedlings of tomato (cv. MicroTom) with 0.5 mM RBH reduced *B. cinerea* lesion size compared to controls (Buswell *et al.*, 2018). Likewise, ChP was found to suppress *B. cinerea* infection in tomato. The foliar spraying of three-week-old plants of tomato (cv. Moneymaker) with ChP solutions resulted in significantly smaller *B. cinerea* lesion size in comparison to controls (De Vega *et al.*, 2021).

In lettuce, BABA and chitosan provide protection against the biotrophic downy mildew *B. lactucae*. In one-week-old lettuce seedlings (cv. Noga), treatment with a range of BABA doses by foliar spraying or soil drenching both provided protection against *B. lactucae*, but soil drenching provided the stronger protection (Cohen, Rubin and Kilfin, 2010). Similarly, foliar spraying of three-week-old lettuce plants (cv. Balady) resulted in reduced *B. lactucae* symptoms (Abdel-Maksoud Abada, 2017). RBH is relatively new IR agent, and its use in lettuce has not been reported at the time of writing.

To assess the dose-dependent efficacies of the IR agents in the selected pathosystems, optical sensor-based phenotyping was selected for the assessment of disease severity. Traditionally, non-destructive scoring of disease severity is achieved by arbitrary categorisation of disease severity on a discrete scale. However, this method comes with several limitations. Firstly, this type of scoring is subjective and can lead to substantial variation in the observed scores between and within individuals (Bock *et al.*, 2010). Secondly, it can be resource and time intensive (Mutka and

Bart, 2015). Finally, visual scoring misses the pre-symptomatic stages of infection. To improve the accuracy of disease quantification, destructive sampling followed by microscopy analysis is commonly used to obtain a more precise measurement of pathogen colonisation (Fernández-Bautista *et al.*, 2016). However, this is a destructive scoring and is not suitable for following disease progression in the same tissues over time. Some of these limitations can be overcome by using optical sensors to quantify disease. Quantitative data obtained this way are typically more sensitive and consistent than visual scoring, and allow for non-destructive spatial and temporal analysis of the disease progression (Mutka and Bart, 2015).

The type of optical sensor used for detection and quantification of plant disease depends on the type of disease. For the detection of severe and/or advanced disease symptoms, such as chlorosis and necrosis caused by necrotrophic pathogens, simple RGB sensors and low-level data processing is often sufficient. However, the detection of pre-symptomatic infection by biotrophic pathogens is often more complex and requires advanced sensors such as HSI cameras. Such HSI sensors produce large amounts of highly dimensional data, which is computationally challenging to analyse. In addition, the separation of multiple stresses symptoms – such as a phytotoxic chemical and a biotic stress – can be challenging (Mahlein, 2016; Wahabzada *et al.*, 2016). However, with suitable statistical analysis approaches, it is possible to distinguish subtle differences in disease incidence and/or abiotic stress, making optical sensors an attractive method to quantify and disentangle different stresses that are simultaneously imposed on the plant (Mahlein, 2016).

In this chapter, the dose-dependent efficacies of the IR agents BABA, RBH and ChP against *B. cinerea* in tomato (cv. Moneymaker) and *B. lactucae* in lettuce (cv. Kavir) are investigated. Hyperspectral imaging was used to quantify disease development and relate these non-destructive measurements with traditional, destructive measures of infection. This chapter also describes how these methods have been developed and optimised in lettuce to distinguish between spectral changes induced by chemical stress effects from IR agents and spectral changes associated with disease by *B. lactucae*.

4.2 Methods

4.2.1 Plant growth, chemical treatments and inoculations

Tomato and lettuce plants were grown, chemically treated and inoculated as described in sections 2.2, 2.3 and 2.4 respectively. For the tomato experiments, six-day-old seedlings growing in 4:1 soil : sand mix were treated with increasing doses of BABA or RBH by soil drenching (0, 0.125, 0.25, 0.5, 1 and 2 mM; final soil concentration) or with ChP by foliar spraying (0, 0.063, 0.125, 0.25, 0.5 and 1 % w/v). Two days after chemical treatments, tomato seedlings were inoculated by placing single 5-µL droplets of *B. cinerea* spore suspension (10^4 spores mL^{-1}) into each cotyledon. For the lettuce experiments, five day-old seedlings growing in 3:1 soil : sand mix were treated with increasing doses of the chemicals in a similar way. Two days after chemical treatments, the cotyledons of the lettuce seedlings were spray-inoculated with *B. lactucae* spore solution (10^5 spores mL^{-1}) until run-off was imminent. The controls of the chemical treatments (Dose = 0) for BABA and RBH consisted of soil-drenching with a similar volume of dH_2O and for ChP of spraying the leaves with a 0.02% v/v Silwet solution. Mock inoculation of tomato was achieved by placing single 5-µL droplets of 6 $mg.mL^{-1}$ PDB solution; lettuce plants were mock-inoculated by spraying the leaves with dH_2O.

4.2.2 Seedling imaging and destructive endpoint sampling

Tomato and lettuce seedlings were imaged with a HSI camera once daily from the time of chemical treatments as described in section 2.5. In the mock-inoculated tomato experiment, seedlings were imaged up to ten days by HSI from the time of chemical treatments, and on the 10^{th} day, leaves were detached and imaged by HSI with the adaxial side facing up. In the *B. cinerea* inoculated tomato experiment, seedlings were imaged up to five days by HSI, at which point seedlings started to collapse due to *B. cinerea* infection. At this point cotyledons were detached and imaged by HSI with the adaxial side facing up. To measure *B. cinerea* infection lesions, detached cotyledons were imaged with a Nikon D5300 DSLR camera. For mock and *B. lactucae* lettuce experiments, seedlings were imaged with a HSI camera for ten days from the point of chemical application. On the 10^{th} day, leaves were detached and imaged by HSI with the adaxial side facing up.

4.2.3 Assessment of lettuce *B. lactucae* colonisation by trypan-blue staining and microscopy

Trypan blue staining solution (450 mL) was made by mixing 100 mg trypan blue, 50 mL glycerol, 50 mL lactic acid (50 mL) and 50 mg phenol with dH_2O to a total volume of 150 mL.

Then 300 mL of 96% ethanol (v/v) was added. Chloralhydrate solution (500 mL) was made dissolving 300 g chloralhydrate in dH_2O overnight. To stain infected tissue, detached leaves from each seedling were placed in 50 mL Falcon tubes and 5 mL trypan-blue solution added. Samples were incubated in for 60 s in boiling water, 5 min at room temperature, 30 s in boiling water then 3h at room temperature. Samples were destained overnight in 4 mL chloralhydrate solution. Colonisation by *B. lactucae* was scored using a stereomicroscope and a three- level disease rating scheme: (I) no colonisation by *B. lactucae*, (II) colonisation but without sporulation and (III) colonisation and sporulation.

4.2.4 Assessing *B. cinerea* infection severity by lesion area

To assess infection severity by *B. cinerea*, images taken by a DSLR camera were analysed using Photoshop CC 2019, by Adobe© systems Inc. Lesions were measured from images of the detached cotyledons, using the 'magic wand tool' to selectively highlight diseased tissue. The diseased tissue pixel area was measured with the pixel count feature. Pixel values were converted to cm^2 using a standard.

4.2.5 Data extraction, analysis and statistical testing

Hyperspectral reflectance data was extracted, processed and reflectance values for each band at each pixel averaged per sample as described in section 2.5. SVIs (115) were calculated from the averaged hyperspectral reflectance data as described in section 2.5.4. All data analysis and statistical tests were performed using R version 4.0.5 (R Core Team, 2021).

4.2.5.1 Multivariate analysis

Orthogonal partial least-squares discriminant analysis (OPLS-DA) was used to distinguish healthy and *B. lactucae* infected samples and identify an optimal SVI to quantify downy mildew infection. OPLS-DA is a supervised multivariate analysis method used to identify and display differences between two experimental groups. The analysis reports the quantitative relationship between a predictor and a response *Y*. In such data sets, using OPLS-DA, systematic variation in *X* is separated into a predictive part that is linearly correlated to *Y* and an orthogonal part that is uncorrelated to *Y* and thus only the variation that is correlated to the *Y* classification can be selected (Trygg and Wold, 2002; Bylesjö *et al.*, 2006; Liu *et al.*, 2018). In the resulting OPLS-DA model the parameters R^2X and R^2Y measure total variation in *X* and *Y* respectively and represent the model's goodness of fit. The parameter Q^2Y, which is obtained through multiple cross-validations, is a measure of the fraction of *Y* that is predicted *X* and represents the predictive performance of the model (Thévenot *et al.*, 2015). The variable influence on projections (VIP) parameter reveals the importance of a given *X* variable for *Y* and used for variable selection

(Szymańska *et al.*, 2012). Although high R^2 and Q^2 values indicate a good model, it is possible they are attained by chance. To overcome this risk of over fitting, and have a measure of the statistical significance (*p*-value) of the R^2 and Q^2 parameters, a permutation test is conducted. In this process, it is assumed there are no group differences, the samples labels are randomly permuted, and multiple new classification models are calculated. Then the significance of the difference of these models from the original unpermutated model is tested (Thévenot *et al.*, 2015). To further test OPLS-DA model reliability, principal component analysis (PCA) can also be used. PCA is multivariate analysis algorithm, which reduces the variables in a data by geometrically projecting them onto lower dimensions called principal components (PCs). The data can then be plotted based on these few components and group similarities and differences assessed visually (Ringnér, 2008; Jollife and Cadima, 2016). Generally, separation of experimental groups by PCA increases the reliability of the separation achieved by OPLS-DA (Worley and Powers, 2016).

The OPLS-DA model was constructed using the *ropls* R package (Thévenot *et al.*, 2015). The data used consisted of SVIs from detached cotyledons inoculated with water (mock) or *B. lactucae* inoculum solution. The predictor variables *X* consisted of 115 SVIs and the response variable *Y* consisted of the two levels mock or *B. lactucae* inoculated. First, the unsupervised segregation of the samples was checked by PCA prior to OPLS-DA. The parameters R^2Y and Q^2Y along with associated *p*-values were used to evaluate the performance of the model. SVIs having high contribution to the separation of the groups were selected by setting a threshold of VIP ≥ 1.

4.2.5.2 Decision tree classification

Decision tree classification (DTC) was used to categorise samples as uninfected or *B. lactucae* infected and to identify the optimal SVI for this classification. DTC is a supervised machine-learning method that uses algorithms to classify categorical response variables. DTC algorithms recursively partition a response variable into subsets based on the relationship to predictor variables. At each stage, the algorithm partitions the data using the predictor variable and at a threshold value which gives the greatest change in explained deviance. The resulting tree represents a series of steps in which data is split in to smaller and smaller subsets until no further splitting is possible and generally the first selected predictor variable (root node) represents the best classifier (Song and Lu, 2015; Ibrahim *et al.*, 2019).

To generate decision trees, the rpart algorithm from the R package, *rpart* (Therneau and Atkinson, 2019) was employed. The response variable was set as inoculation status (mock or *B. lactucae* inoculated) and 115 distinct SVIs were used as predictor variables. The data was split into training and testing at a ratio of 80:20. Separate decision tree models were created for detached cotyledons and leaves, whole plants at the 7 dpi time point, as well as series of models for whole

plants at eight time points from 0 to 7 dpi. After training DTC models, performance was assessed using the test data. Model overall accuracy (OA) in the test data was calculated using a confusion matrix, as the sum of correct classifications divided by total number of classifications and is scaled 0 – 1 (Story and Congalton, 1986). Further assessment of model performances was made using Cohen's kappa coefficient (*k*). The *k* metric assess the agreement between a model's observed accuracy and the expected accuracy from a random classifier and indicates the proportion of achieved agreement above that expected by chance classifications and is scaled 0 – 1 (Sim and Wright, 2005; McHugh, 2012). Variable importance (*Vimp*) is a measure of the contribution of each predictor variable to model performance. *Vimp* was computed as the level of reduction in predictive accuracy when a variable is removed from the model and is scaled 0 -100 (Therneau and Atkinson, 2015).

4.2.5.3 Measuring relative chemical impacts on SVI values

The chemical impact on SVI (CIS) was formulated as a measure of the change in SVI value due to chemical treatment. The CIS for each SVI was calculated as the sum of absolute change for all doses normalised to a control (Dose= 0) according to the formula $\Sigma|(SVI_{DX} - SVI_{D0})/ SVI_{D0}|$, where SVI_{DX} is the SVI value at the treatment doses for each chemical and SVI_{D0} is the SVI value for the control treatment. This formula returned a single CIS value for each SVI chemical pair and was used as a means to assess the sensitivity of a given chemical treatment.

4.2.5.4 Examination of the relationship between disease scores and SIPI values by Spearman's rank correlation

To examine the relationship between disease scores for *B. lactucae* infection and SIPI values, Spearman's rank correlation was employed. The R package *stats* (R Core Team, 2021) was used to calculate Spearman's rank correlation coefficient rho (ρ) and the associated *p*-value for the significance level of the correlation.

4.3 Results

4.3.1 Assessing the efficacy of the chemical IR agents in tomato against *B. cinerea*

To assess the efficacy of the IR agents against *B. cinerea* in tomato, seedlings were treated with BABA, RBH or ChP doses, and challenged two days later with *B. cinerea.* Since *B. cinerea* is necrotroph whose symptoms are easily visible on plant tissue, infection severity in the cotyledons was first quantified destructively by measuring the area of lesions in detached leaves at two days pot inoculation (dpi) using high-resolution images taken with a DSLR (Fig 4.1). In the BABA- and RBH-treated seedlings, dose had no significant effect on lesion area and disease severity was the same as the control treatments. In contrast, ChP dose had strongly significant effects on *B. cinerea* disease development in tomato seedlings. All ChP doses significantly reduced *B. cinerea* lesion area compared to the control group.

To compare the destructive scoring presented in Fig. 4.1 to non-destructive analysis by HSI, *B. cinerea*-infected seedlings were imaged for five days. However, infection caused cotyledons to collapse and, consequently, they dropped out of view of the HSI camera. Since the onset and progress of disease symptoms was rapid – in some cases cotyledons were severely necrotic by 1 dpi – it made the acquisition of images difficult. Therefore, to investigate the hyperspectral signatures of *B. cinerea* infection, and how the IR agents affect these signatures, cotyledons had to be detached and imaged at two dpi. Fig 4.2 shows hyperspectral signatures from detached cotyledons after receiving treatments of the three IR agents and subsequent challenge with *B. cinerea*. This hyperspectral data was consistent with the lesion area data presented in Fig. 4.2. The signatures of inoculated cotyledons from plants that had been pre-treated with the two β-amino acids (BABA and RBH) were fairly similar to that of inoculated cotyledons from control-treated plants, whereas the signatures of ChP-treated plants were clearly distinct from the controls, showing notably higher reflectance in the green and NIR bands. There was also a strong left shift of the red edge position (Fig. 4.2).

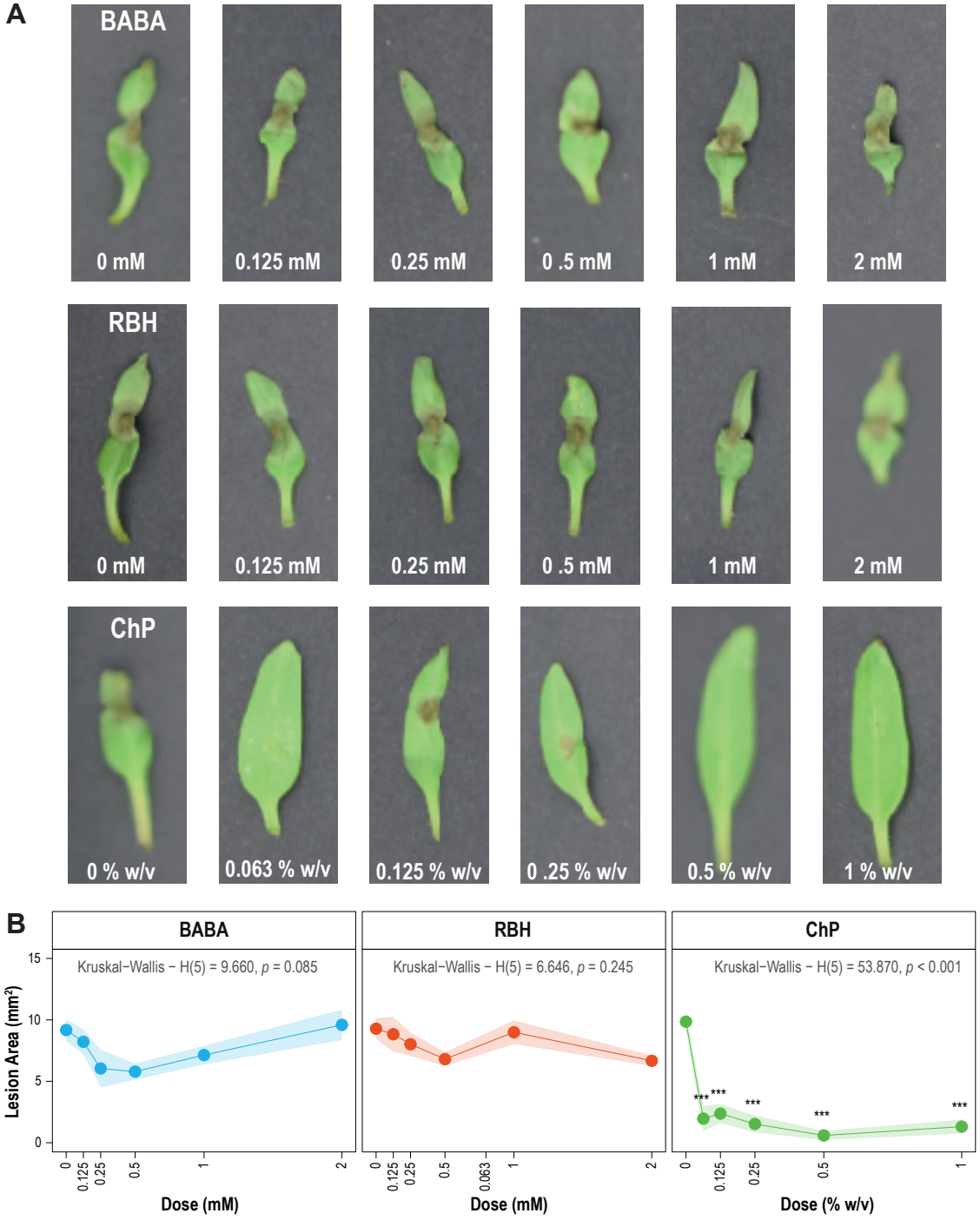

Fig 4.1 | Dose-dependent efficacy of IR agents in tomato against *B. cinerea*. (**A**) Sample images of B. cinerea infected detached cotyledons receiving increasing doses of the IR agents. (**B**) Measurement of lesion area from detached cotyledons quantified by the DSLR at 2 dpi. The plots show mean B. cinerea infection lesion area (mm^2) ± SE. Statistical significance of the effect of chemical dose on lesion area was tested for by Kruskal-Wallis tests. Chemical dose treatments that are statistically different from the control treatment (Dose = 0) was carried out by Dunn's tests and denoted as * for $p < 0.05$, ** for $p < 0.01$, and *** for $p < 0.001$.

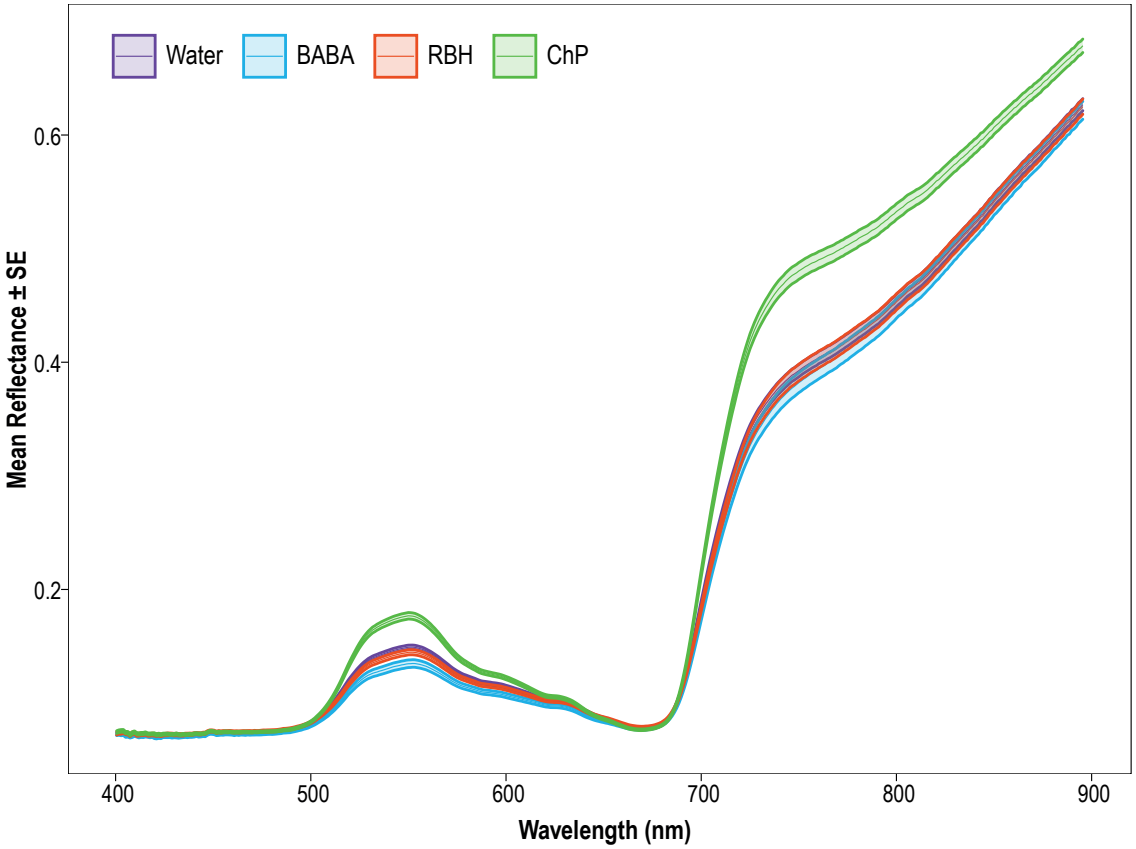

Fig 4.2 | Effects of IR agents on the hyperspectral signatures *B. cinerea* infected tomato cotyledons. The presented curves show mean reflectance ± SE for seedlings treated with all doses of BABA (blue), RBH (red), ChP (green) or water (purple).

Since inoculation with *B. cinerea* causes necrotic lesions that are associated with loss of chlorophyll content (Melouk, 1978), the SVI MCARI2 was selected from the HSI spectra, which provides a measure of chlorophyll content. To determine if IR agent dose influenced MCARI2 values, Kruskal-Wallis tests were carried out and, where dose had a statistically significant effect, pairwise comparisons to the controls were performed, using a Dunn's test. In cotyledons, from seedlings receiving increasing doses of BABA or RBH, no statistically significant effects were found in either group (Fig. 4.3). By contrast, for inoculated cotyledons from seedlings pre-treated with ChP, MCARI2 values increased with rising dosage, which was statistically significant ($p < 0.001$; Kruskal-Wallis test; Fig. 4.3). Furthermore, a post-hoc comparison to the control with Dunn's test showed all ChP doses had significantly higher MCARI2 values (Fig. 4.3).

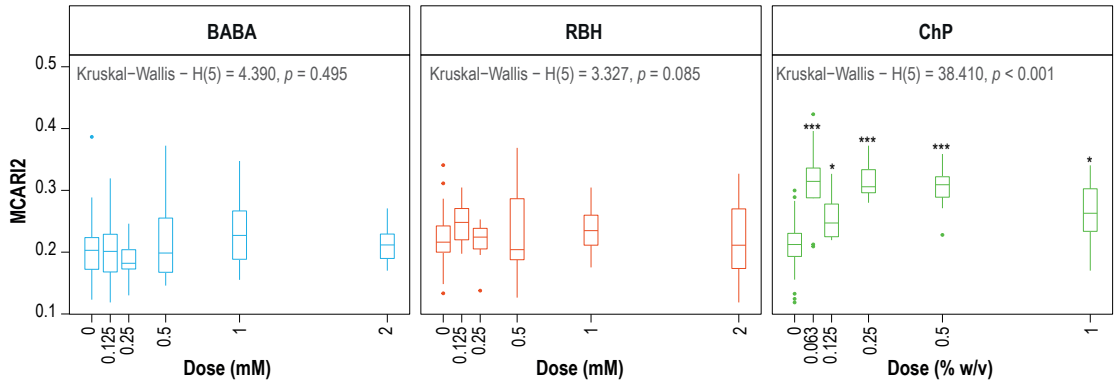

Fig 4.3 | Effects of IR agents on chlorophyll abundance in *B. cinerea* infected tomato cotyledons. The presented boxplots are of MCARI2 values at increasing BABA, RBH and ChP doses in detached tomato cotyledons infected with *B. cinerea*. Kruskal-Wallis tests were carried out to examine if IR agent dose had a significant effect on MCARI2 values. Where there was a statistically significant dose effect, pairwise comparisons to the controls (Dose = 0) were performed using Dunn's test and denoted as * for $p < 0.05$, ** for $p < 0.01$, and *** for $p < 0.001$.

Thus, due to its necrotrophic nature, *B. cinerea* caused major changes to the infected tissue that could be identified easily with both RGB and HSI sensors, enabling quantification of disease severity and the subsequent assessment of the efficacy of the IR agents. The β-amino acids BABA and RBH did not affect lesion size from *B. cinerea* infection (Fig. 4.1). Likewise, the spectral signatures of inoculated cotyledons of plants pre-treated with these chemicals was identical to the inoculated cotyledons from water-treated plants (Fig. 4.2), while MCARI2 values showed chlorophyll content was similar between BABA-, RBH- and water-treated plants (Fig. 4.3). This indicates that both beta-amino acid IR agents failed to alter disease progression. By contrast, plants pre-treated with ChP showed significantly reduced lesion sizes (Fig. 4.1), spectral signatures that are markedly different from the infected controls (Fig. 4.2), and MCARI2 values indicating statistically increased chlorophyll content compared to the controls (Fig.4.3). Together, these results indicate BABA and RBH are ineffective in reducing *B. cinerea* infection, whereas ChP acts a potent IR agent against *B. cinerea* infection.

4.3.2 Assessing *B. lactucae* disease symptoms in lettuce by Trypan-blue scoring

To assess the efficacies of the three IR agents against the biotrophic downy mildew pathogen *B. lactucae*, lettuce seedlings were treated with BABA, RBH or ChP doses and spray-inoculated two days later with conidiospores of *B. lactucae*. Initially, disease severity was scored destructively by collecting leaf tissues at seven dpi for trypan-blue staining and microscopy analysis. This traditional method of trypan-blue scoring served as a standard comparison for the performance of HSI-based methods, and was based on a categorical scale to distinguish between different stages of colonisation by the Oomycete (Asai, Shirasu and Jones, 2015).

In general, colonisation by *B. lactucae* decreased with increasing chemical dose in both leaves and cotyledons (Fig 4.4, top). The effect of dose on disease severity was significant for all three chemicals (BABA $p < 0.001$, RBH $p < 0.001$, ChP $p < 0.003$; Kruskal-Wallis test). Of the three chemicals, BABA was the most potent, such that all BABA treatment groups resulted in significantly lower colonisation rates. None of the leaves from BABA-treated seedlings resulted in *B. lactucae* sporulation (disease score 3) and only a small proportion of leaves receiving the two lowest doses (0.125 and 0.25 mM) showed colonisation by the oomycete (disease score 2) - all higher doses completely prevented infection. RBH was less potent than BABA, where only treatment with 0.125 and 2 mM RBH reduced infection. Most leaves in these treatment groups remained free of colonisation and none of the leaves showed sporulation. In the other RBH treatment groups (0.25, 0.5 and 1 mM), infection was not significantly different from the control group and a proportion of the leaves in each group showed sporulation. Compared to RBH, ChP was the least effective against *B. lactucae*. In all treatment groups, some leaves had the highest disease score and only the highest dose (1% w/v) resulted in statistically significant reductions in infection, although still allowing for sporulation.

To evaluate differences in infection severity between cotyledons and true leaves, disease scores were examined by leaf type. Generally, infection was more severe in cotyledons (Fig 4.4, middle) relative to the true leaves, with a larger proportion of leaves displaying the severe colonisation and formation of conidiospores (level 3). For all three chemicals, the effect of dose on disease severity was significant (BABA $p < 0.001$, RBH $p < 0.001$, ChP $p < 0.001$; Kruskal-Wallis test), where BABA was the most effective. All BABA doses resulted in statistically significant reductions in *B. lactucae* colonisation relative to the control group. Only a small portion of cotyledons from the lowest BABA dose group (0.125 mM) showed signs of colonisation (level 2) and cotyledons from higher dose groups were completely free of pathogen colonisation. Compared to the control group, RBH-treated plants showed reduced strongly reduced levels of *B. lactucae* colonisation at 0.125 and 2 mM, without colonisation, while all other doses appeared statistically ineffective. ChP was effective at the three highest doses (0.25, 0.5 and 1 %w/v), although this protection was relatively mild compared to the control group and still allowed for sporulation by the pathogen.

At the point of inoculation with *B. lactucae*, the first true leaves had not fully emerged. Consequently, these leaves were exposed to lower numbers of *B. lactucae* spores than the cotyledons, which explains why the true leaves showed relatively low levels of colonisation (Fig 4.4, bottom). Of the three chemicals, only BABA had a statistically significant effect of on downy mildew infection ($p < 0.001$; Kruskal-Wallis test). Treatment with BABA 0.5 mM and higher resulted in significantly lower disease scores compared to the control. None of the leaves from BABA-treated plants allowed for sporulation by the pathogen. Although RBH appeared equally effective at supressing sporulation in true leaves at all doses (class 3), these effects were

not statistically significant compared to the control treatment, likely because of the low disease incidence in the control group. The true leaves from plants pre-treated with 0.063 %w/v ChP allowed some sporulation, while higher concentrations of ChP suppressed sporulation fully, although these effects were not statistically significant compared to the control.

In summary, the conventional trypan-blue scoring revealed that BABA is the most potent IR agent in suppressing *B. lactucae* in lettuce (cv. Kavir). Although RBH was less effective than BABA, it managed to suppress sporulation by the Oomycete at two different concentrations, while ChP was the least effective of all and failed to suppress sporulation at all concentrations tested.

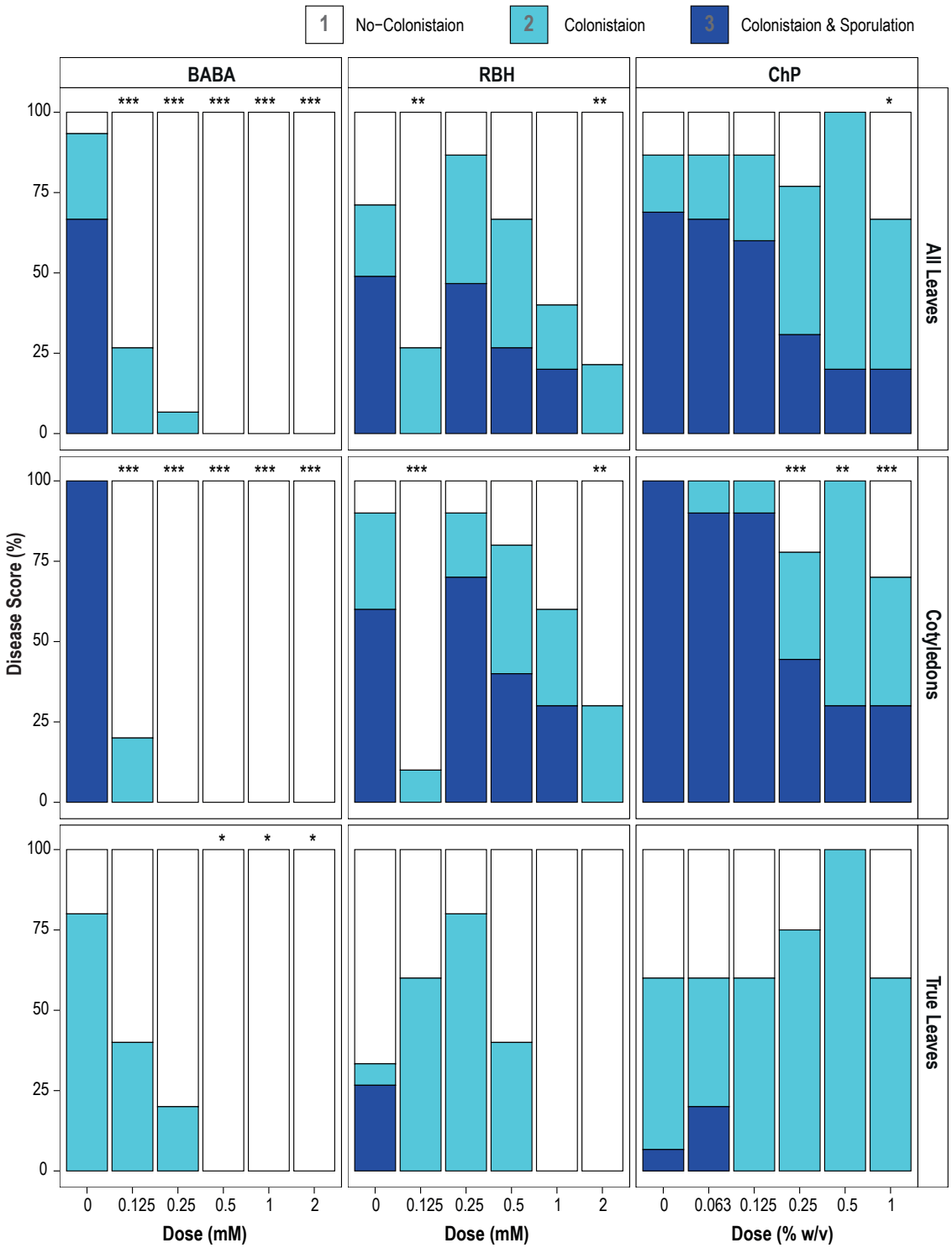

Fig 4.4 | Assessing IR agent efficacy in lettuce against downy mildew disease by trypan-blue scoring. The presented bars show the percentage of the leaves at each disease score (1 = white, 2 = light blue and 3 = dark blue) for each IR agent treatment dose of the. The top panel shows disease scores for all leaves, the middle shows cotyledons and the bottom true leaves. To examine the significance of chemical dose effect on disease score, Kruskal-Wallis tests were carried out. Where dose effect was significant, pairwise comparisons to the controls (Dose = 0) were performed using Dunn's test and denoted as * for $p < 0.05$, ** for $p < 0.01$, and *** for $p < 0.001$.

4.3.2 Disentangling Hyperspectral parameters of *B. lactucae* infection and chemical phytotoxicity in lettuce

The trypan-blue scoring method of evaluating the efficacies of the IR agents was time intensive, destructive and provided limited quantitative data, whereas assessments based on HSI sensor data are non-destructive and generated quantitative data. However, phenotyping disease symptoms by imaging in the lettuce-*B. lactucae* pathosystem is challenging as *B. lactucae* is an obligate biotroph with a relatively long asymptomatic period prior to sporulation, hence causing only subtle changes to its host (Fletcher *et al.*, 2019).

4.3.2.1 The relative effects of *B. lactucae* infection and chemical phytotoxicity on lettuce HSI parameters

The effects of chemical stress could be detected and quantified with a HSI sensor (Figs 3.5, 3.6 and 3.7). To quantify chemical IR, it is important to select a HSI method that can distinguish chemical stress by the IR agents from biological stress from the pathogen. To this end, first the spectral impacts of BABA, which was the most phytotoxic of the three IR agents tested (Chapter 3) was compared to those by *B. lactucae* (Fig 4.5). The hyperspectral signatures of water-treated seedlings differed from that of both BABA- and *B. lactucae*-treated plants. BABA induced differences in the visible region (400-700 nm) whilst *B. lactucae* resulted in more pronounced differences in the NIR (<700 nm). SVIs selected to identify chemical stress (ARI2, CRI2 and MCARI2) showed changes in response to both BABA and *B. lactucae* (Fig 4.5B), rendering them unsuitable to quantify BABA-IR against *B. lactucae.* Since both the chemical IR agent and *B. lactucae* would be applied to the same samples, it was essential to disentangle the effects of *B. lactucae* infection and chemical phytotoxicity.

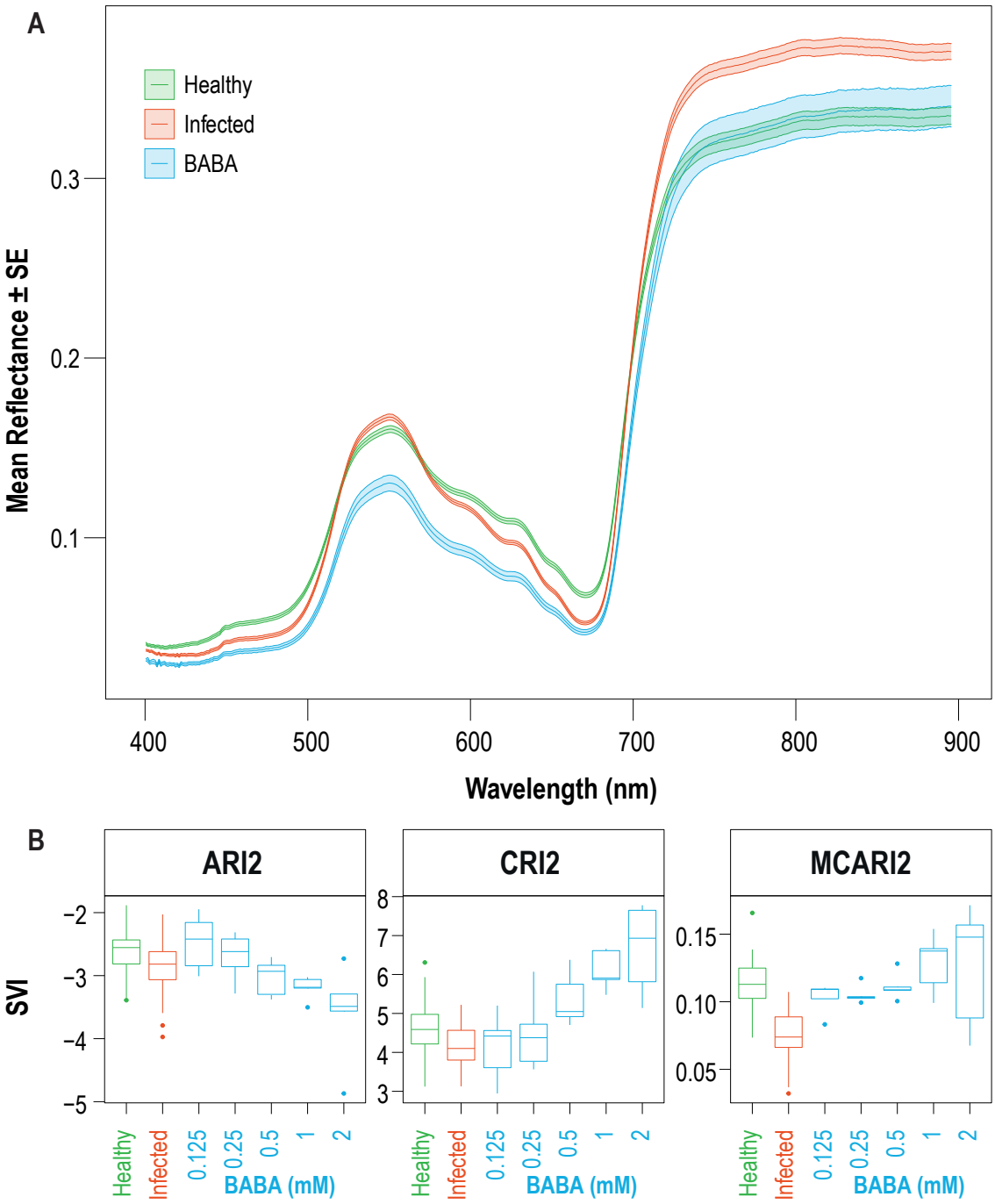

Fig 4.5 | Hyperspectral parameters of *B. lactucae* and chemical stresses in lettuce. (A) The presented curves are mean reflectance intensities at individual wavelengths in the visible spectrum (VIS; 400 – 700 nm) and a portion of the near-infrared spectrum (NIR; 700 – 895 nm). The red curve shows the hyperspectral signature of healthy (water treated) seedlings, the red *B. lactucae* infected and the blue BABA (2 mM) treated. (B) The presented boxplots show SVI values for seedlings receiving increasing BABA doses. ARI2, CRI2 and MCARI2, respectively track anthocyanin, carotenoid and chlorophyll content.

4.3.2.2 Using multivariate statistics to identify SVIs responsive *B. lactucae* symptoms in lettuce

SVIs have been shown to be an effective means of indirectly detecting plant diseases (Mahlein *et al.*, 2013; Lowe, Harrison and French, 2017). To find optimal SVIs for early and quantitative detection of downy mildew disease in lettuce, 115 SVIs were computed from the HSI data of the detached cotyledons experiment, since these showed higher infection rates than true leaves by trypan-blue scoring (Fig 4.4). The 115 SVIs were then subjected to multivariate analysis. To examine the separability of the groups based on SVIs values an unsupervised PCA was performed. In the score plot of PC1 against PC2, samples tended to cluster by inoculation group although there was significant overlap (Fig 4.6A). The first two principal components respectively explained 55.9% and 16.9% of the variance respectively. To determine which SVIs most significantly contribute to the observed separation, a supervised OPLS-DA was performed. As illustrated in Fig 4.6B, the OPLS-DA score plot showed good separation between mock- and *B. lactucae*-inoculated cotyledons. Overall, the performance of the OPLS-DA model was good. Along with a high accuracy score (RMSE = 0.191), the model fitting capacity (R^2X = 0.786 and R^2Y 0.857, $p < 0.001$) and predictive capacity (Q^2Y = 0.847, $p < 0.001$) were both high and statistically significant. To highlight the most robust SVIs driving the observed separation, a VIP threshold of ≥ 1 was set. Ultimately, this yielded 53 SVIs that were deemed to be the discriminant between mock and *B. lactucae* inoculated detached lettuce cotyledons.

4.3.2.3 Identifying *B. lactucae* selective SVIs

HSI quantification of chemical IR against *B. lactucae,* requires SVIs that are responsive to stress by *B. lactucae* but minimally responsive to chemical stress by IR agents. From the initial number of 115 SVIs, OPLS-DA returned 53 SVIs that are *B. lactucae*-responsive (VIP ≥ 1). To select SVIs that are minimally responsive to chemical stress, the same 115 SVIs were analysed for their response to chemical IR treatments by calculating the sum of absolute value change of each SVI in response to all three IR agents (BABA, RBH and ChP). A threshold of chemical impact ≤ 0.1 was set, and 58 SVIs identified that were minimally responsive to chemical IR treatment, of which 9 SVIs were responsive to downy mildew infection (Fig. 4.7). This selection of SVIs could be grouped by function. CI is a measure of chlorophyll content (CI). Four SVIs relate to healthy green vegetation (GDVI_2, GDVI_3, GDVI_4 and mNDVI). Four of these SVIs relate to the ratio of chlorophyll and carotenoids content (SIPI, SIPI2, SIPI3 and SRPI). Fig 4.7B shows the responsiveness to chemical and downy mildew of infection for three SVIs (CI, mNDVI and SIPI) representative of these groupings. The values of these three SVIs from infected (*B. lactucae*), chemical-treated (2 mM RBH; representative for high-end chemical stress) and control (water-treated) were measured over time. As expected, both the chemical stress and control treatment

showed minimal change over time, whereas *B. lactucae* inoculation resulted in progressive changes in the selected SVI values. This demonstrates that the selected SVIs are selective for stress caused by *B. lactucae* infection and robust against chemical stress caused by IR agent, hence suitable for the quantification of chemical IR against downy in lettuce.

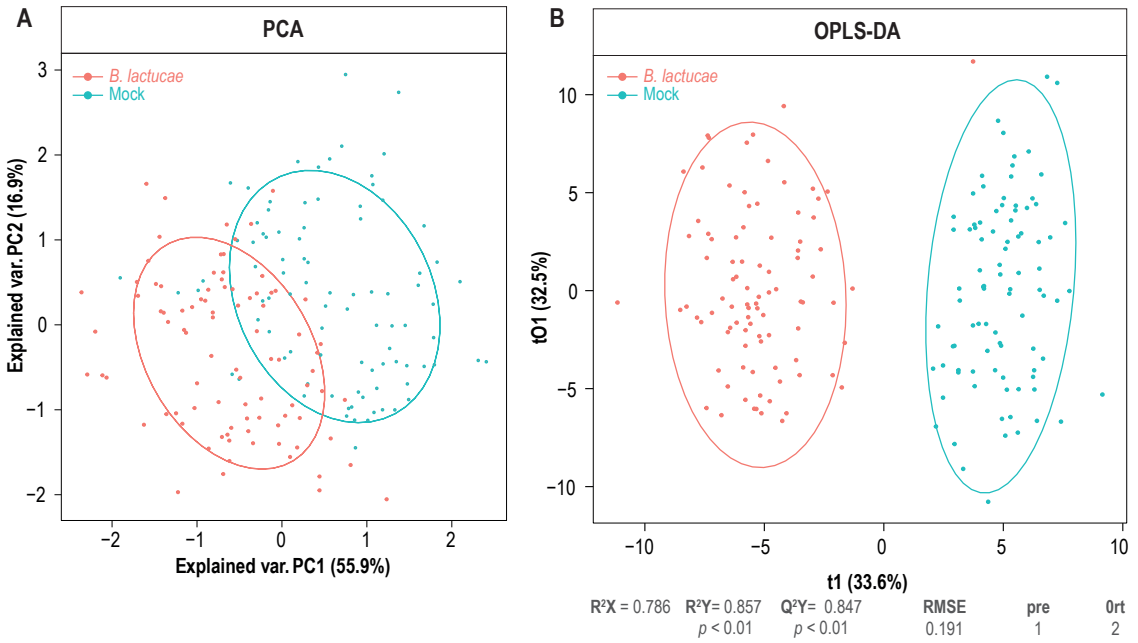

Fig 4.6 | Multivariate statistical analysis of SVIs data from healthy and infected cotyledons. Presented is multivariate analysis using 115 SVIs as predictor variables and inoculation status (mock; blue and *B. lactucae* infected; red) as the response variable. (**A**) PCA variable correlation plot of all samples projected across PC1 and PC2 showing the clustering of the groups. (**B**) OPLS-DA scores plot showing separation of samples by inoculation status. The models goodness of fit (R^2X and R^2Y), predictive capacity (Q^2Y) and accuracy (RMSE) along with associated p-values are shown under the Y-axis.

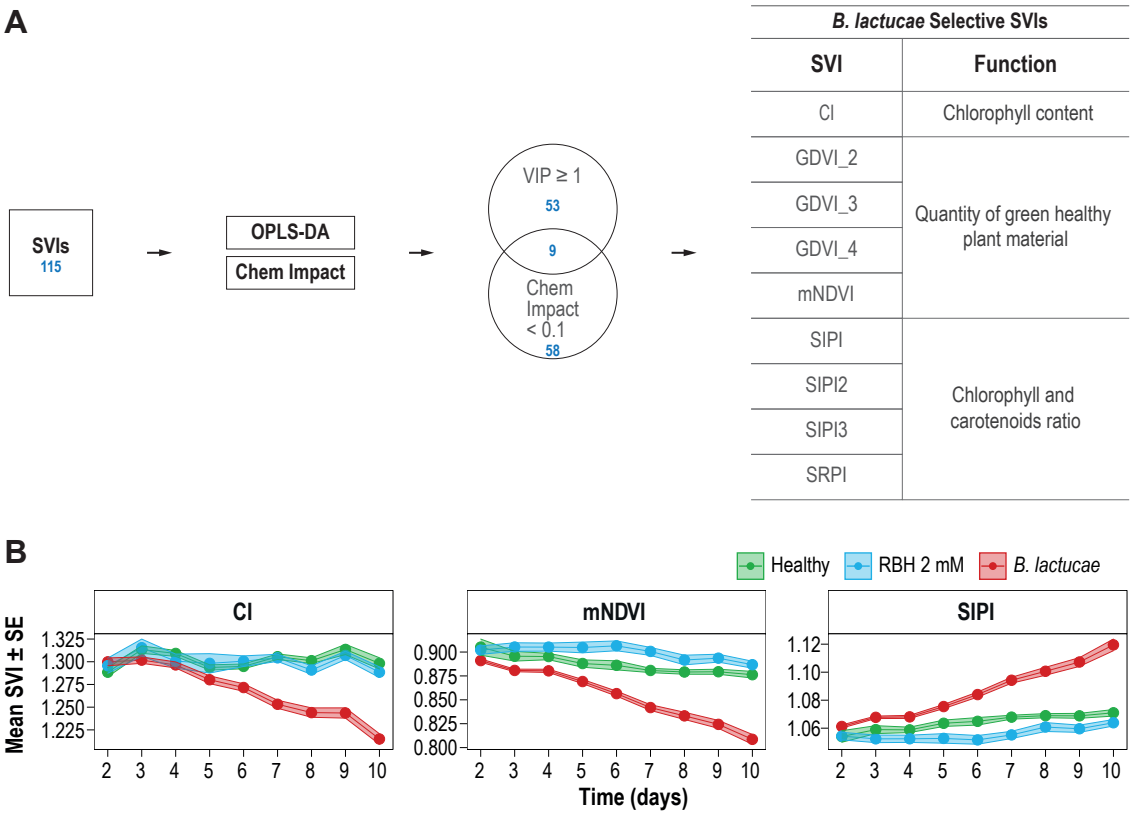

Fig 4.7 | Identification of *B. lactucae* selective SVIs. (A) The process of identifying SVIs responsive to downy mildew infection but minimally responsive to chemical stress. **(B)** The responsiveness to chemical and ***B.*** *lactucae* stress of three SVIs representative of the function groupings of the nine SVIs identified as *B. lactucae* selective.

In addition to multivariate analysis, a machine learning approach was implemented to identify SVIs that are suitable for detecting *B. lactucae* infection in lettuce. Using the entire HSI data set of whole plants (non-destructive) and detached cotyledons and true leaves (destructive) at 7 dpi, decision tree models were created by the 'rpart' algorithm, using inoculation group as the classifier variable and 115 SVIs as the predictor variables. The decision tree models identified three sets of SVIs with high importance in the classification of both groups (Fig 4.8A) and high accuracy in predicting treatment (Fig 4.8B). In whole plants at 7 dpi, the SIPI, mSR, mNDVI and SIPI2 performed best for group classification with equal prediction values (*OA* = 0.94, *k* = 0.88, $p = 0.002$). In detached cotyledons SIPI, mSR and mNDVI performed best, giving equal prediction rates (*OA* = 0.89, *k* = 0.78, $p < 0.001$), while performance was slightly lower than in whole plants. Similarly, classification overall accuracy (*OA*) in true leaves was high, however in contrast to the whole plants and cotyledons, optimal classification was achieved with ARI1 (*OA* = 1.0, k = 1.0, $p < 0.001$), SIPI on the other hand was not identified in the decision tree models.

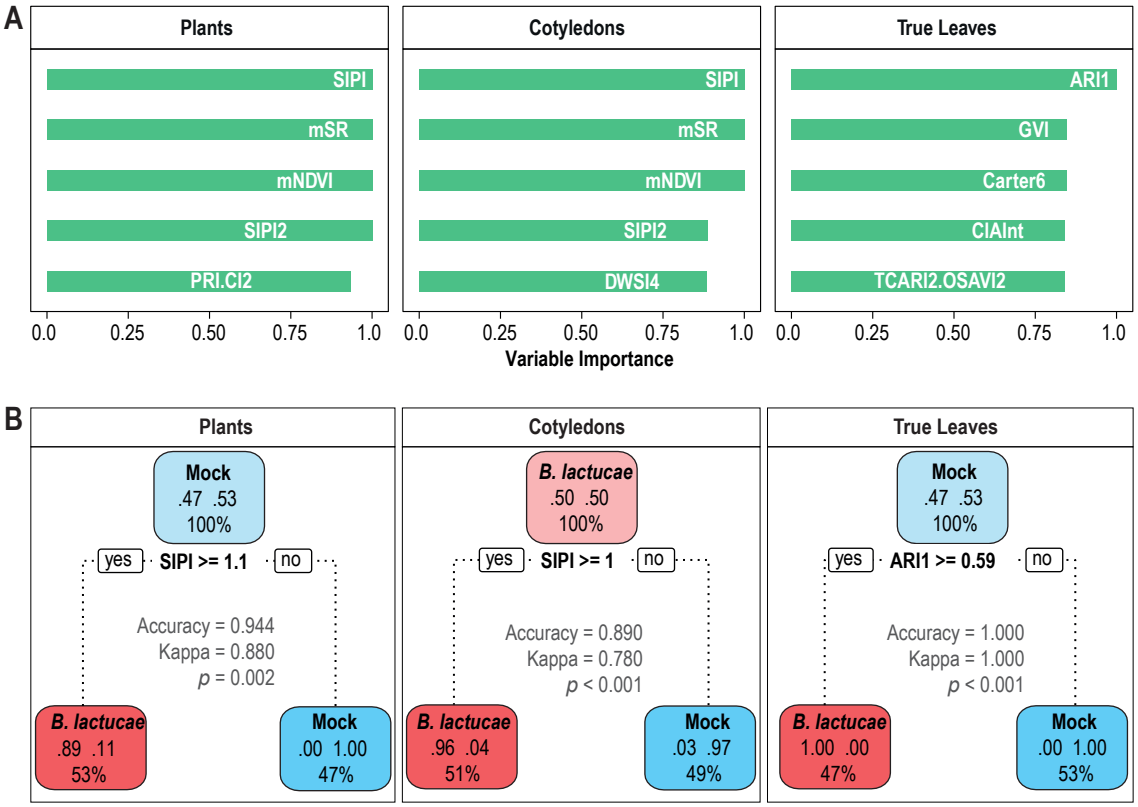

Fig 4.8 | DTC to select SVIs robust at predicting *B. lactucae* infection. **(A)** The variables with the highest *Vimp* values in the classification of the mock and *B. lactucae* inoculated samples. **(B)** Decision tree diagram for the optimal prediction SVI and the associated performance parameters.

To investigate differences of the two groups over a time-course of disease progression, the decision tree algorithm was implemented using the whole plant data from 0 to 7 dpi. The predictive performances of the algorithm over this period are shown in Table 4.1. At the point of inoculation (0 dpi) samples essentially had an equal chance (0.56) of assignment in to either group. However, just a day after inoculation *OA* increased to 0.72. At 4 dpi, which was the point the infected plants showed the first signs of sporulation, and at 7 dpi, when infection was most severe, *OA* was highest at 0.94.

Table 4.1 | Decision tree performance in the classification of inoculation group in lettuce seedlings over time

Time (dpi)	*OA*	*k*	*p*.value
0	0.556	0.153	0.768
1	0.722	0.483	0.237
2	0.722	0.430	0.237
3	0.722	0.430	0.237
4	0.944	0.886	0.002
5	0.833	0.675	0.04
6	0.833	0.620	0.04
7	0.944	0.880	0.002

4.3.3 SIPI: An optimal SVI for measuring *B. lactucae* infection levels in lettuce

Based on the results of the multivariate analysis and the DTC, the SVIs SIPI and mNDVI appeared the best performing for detection of *B. lactucae* infection in cotyledons. Although the performance of both these SVIs to detect *B. lactucae* disease was similar based on OPLS-DA VIP scores and *OA* in DTC, the analysis of chemical impact revealed that SIPI was less responsive to chemical treatment than mNDVI (Table 4.2). This suggested SIPI would be the more suitable SVI for quantifying chemical IR against *B. lactucae*. To validate SIPI as a predictive SVI for *B. lactucae* colonisation, the association between SIPI and disease scores from trypan-blue staining was analysed by correlation analysis between averaged colonisation values and SIPI values per plant. Spearman's rank correlation revealed a positive correlation ($\rho = 0.73$), which is statistically significant ($p < 0.001$; Fig 4.9). Accordingly, SIPI was selected for quantification of chemical IR in lettuce.

Table 4.2 | Performance of the most optimal SVIs in *B. lactucae* symptom detection in lettuce

SVI	OPLS-DA VIP	DTC *OA*	Chem Impact
SIPI	1.634	0.89	0.039
mNDVI	1.639	0.89	0.076

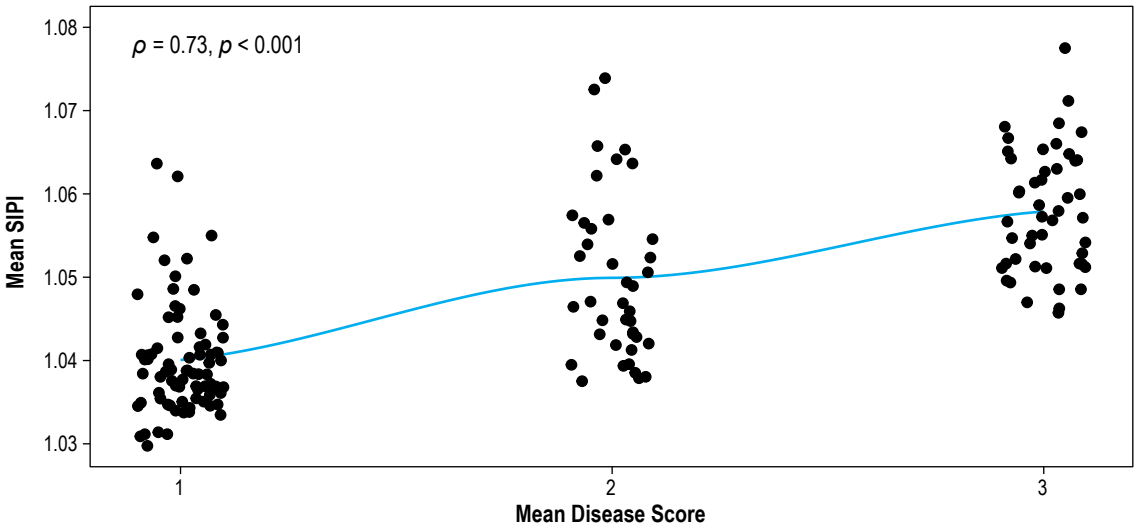

Fig 4.9 | Correlation between SIPI and Disease Score. Shown is a scatter plot of disease score against SIPI value for *B. lactucae* inoculated detached cotyledons. Disease scores and SIPI values are averages of the cotyledons from a single plant. Spearman's rank correlation using Student's t distribution was used to evaluate the strength, direction and significance of the relationship between SIPI and disease score.

4.3.4 Using SIPI to assess the efficacies of the IR agents against *B. lactucae* infection in lettuce

To assess the efficacies of IR agents, HSI analysis of SIPI was used to non-destructively monitor colonisation of water-, RBH-, BABA-, and ChP-treated lettuce by the downy mildew pathogen *B. lactucae*. To this end, lettuce seedlings (cv. Kavir) were treated with increasing doses of the three chemicals and challenged two days later with *B. lactucae* spores (105 spores.mL-1). Subsequently, plants were scanned daily with the HSI camera. This experiment was repeated twice and Fig 4.10 shows the combined SIPI values for seedlings of both experiments at 7 dpi. In BABA-, RBH- or ChP-treated seedlings, SIPI values were the highest in the controls (Dose = 0) and generally decreased with increasing dose of IR agent.

For all three IR agents, dose had a significant effect on SIPI values (BABA $p < 0.001$, RBH $p < 0.001$, ChP $p < 0.032$; Kruskal-Wallis). BABA was the most potent of the three IR agents. In BABA-treated seedlings, SIPI values dropped from the control to the lowest dose (0.125 mM) and did not decline further with increasing doses. This observation was consistent with the pattern observed by the trypan-blue disease scores (Fig 4.4). Since BABA had a high IR potency at all tested doses, a further experiment was conducted to test efficacy at a lower dose range (Fig 4.11). Seedlings were soil-drenched with five different BABA doses in the range 0.004 – 0.063 mM and then infected with downy mildew in a similar manner as described above. At 0.008 mM (16 times lower than the previous lowest tested dose), BABA still significantly lowered SIPI

values compared to the controls. Likewise, RBH showed efficacy against *B. lactucae* infection. However, it was less potent than BABA and not all RBH doses suppressed SIPI values. While the lowest RBH dose (0.125 mM) was effective in reducing SIPI, the second highest dose (0.25 mM) was not, which again supported the trypan-blue disease data (Fig. 4.4). Interestingly, this non-hormetic pattern of disease protection by RBH was observed independently from the HSI data in the two experiments. In comparison to two β-amino acids, ChP was least effective at suppressing downy mildew disease and only statistically suppressed SIPI values at the highest two doses.

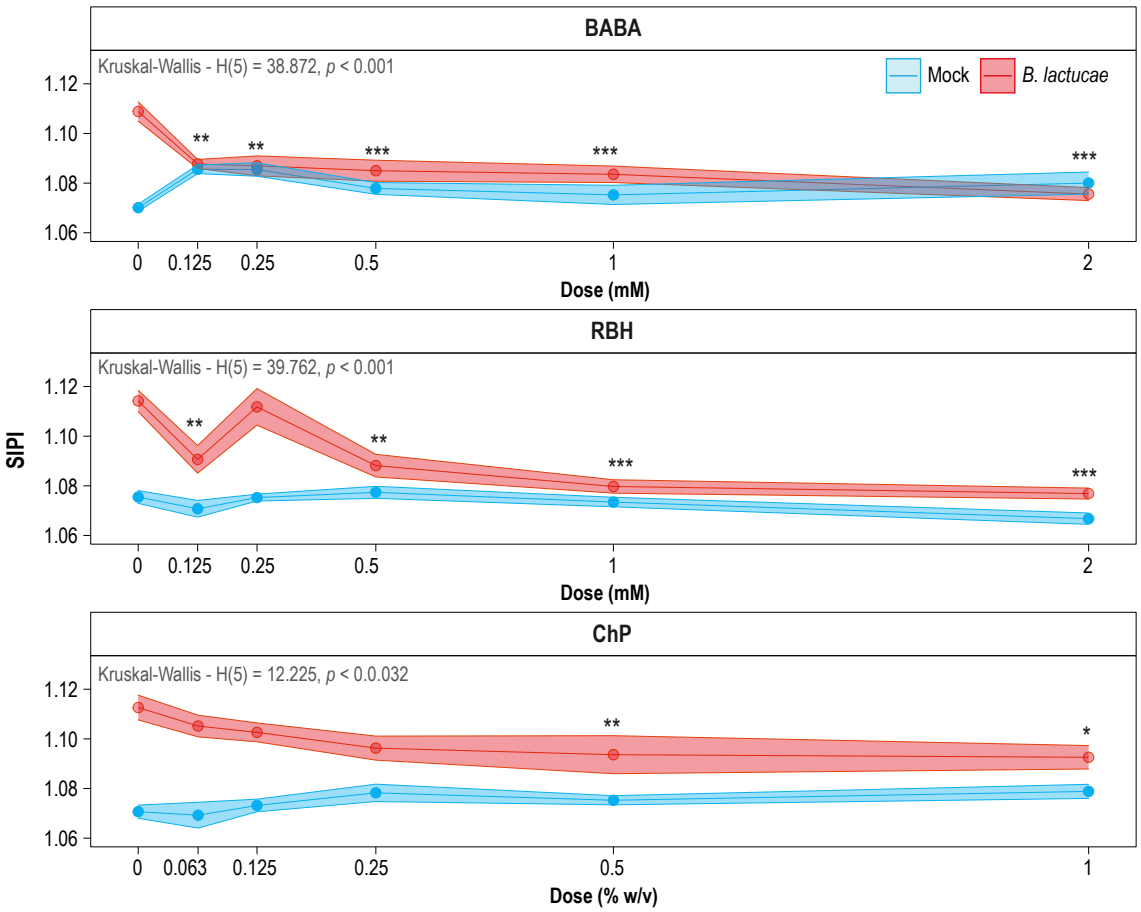

Fig 4.10 | Dose-dependent efficacy of IR agents in lettuce against *B. lactucae*. The plots show mean SIPI values ± SE. The data is of whole plants combined from two independent experiments at 7 dpi. Statistical significance of the effect of chemical dose on SIPI value was tested for by Kruskal-Wallis tests. Chemical dose treatments that are statistically different from the control treatment (Dose = 0) was carried out by Dunn's tests and denoted as * for $p < 0.05$, ** for $p < 0.01$, and *** for $p < 0.001$.

Besides being responsive to disease stress by *B. lactucae*, SIPI was selected because it had relatively low sensitivity to chemical stress by IR agents (i.e. low 'Chemical Impact' value). Indeed, SIPI values of the mock-inoculated seedlings (Fig 4.10 and Fig 4.11) showed minimal change with increasing chemical dose. Nonetheless, SIPI did change in response to the higher doses of BABA (0.125 – 2 mM; Fig. 4.10), whereby values increased relative to the water-treated control group and remained constant across a range of increasing doses. At the lower dose (Fig. 4.11), BABA treatments (0.004 – 0.063 mM), this SIPI response to BABA-induced stress was less pronounced. Although the same effect was observed for RBH and ChP, the increases in SVI occurred at higher doses only and were considerably smaller than the SIPI response to high concentrations of BABA. Thus, SIPI appears to be an appropriate SVI for quantifying the efficacy of IR against downy mildew infection and seems most reliable at relatively low doses of the chemical IR agent.

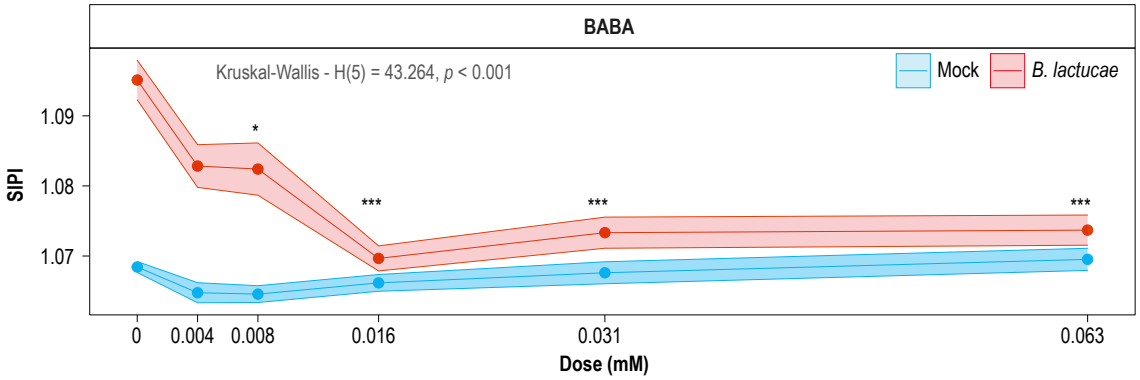

Fig 4.11 | Efficacy of low BABA doses against *B. lactucae* in lettuce. The presented line plots show mean SIPI values ± SE. The data is from whole plants at 7 dpi. Statistical significance of the effect of BABA dose on SIPI value was tested for by Kruskal-Wallis tests. BABA dose treatments that are statistically different from the control treatment (Dose = 0) was carried out by Dunn's tests and denoted as * for $p < 0.05$, ** for $p < 0.01$, and *** for $p < 0.001$.

4.4 Discussion

In addition to the phytotoxic effects discussed in chapter 3, the deployment of chemical IR agents in crop protection has been hindered by low and/or variable efficacy (Yassin *et al.*, 2021). The efficacy of IR agents depends on the challenging pathogen (Sharma, Butz and Finckh, 2010) and is plant species- and cultivar-dependent (Hijwegen and Verhaar, 1995; Dann *et al.*, 1998). Previously, the IR agents BABA, RBH and ChP have all been reported to display efficacy against the necrotrophic fungus *B. cinerea* in different varieties of tomato (Luna *et al.*, 2016; Buswell *et al.*, 2018; Li, Sheng and Shen, 2020; De Vega *et al.*, 2021). Similarly, BABA and ChP have been reported to be effective against the biotrophic oomycete *B. lactucae* in lettuce varieties (Cohen, Rubin and Kilfin, 2010; Abdel-Maksoud Abada, 2017). By contrast, the IR effects of the relatively new IR agent RBH has not been reported outside of tomato and Arabidopsis (Buswell *et al.*, 2018). This Chapter presents the development of image sensor-based methods to quantify grey mould and downy mildew disease symptoms, which subsequently were used to ascertain the dose-dependent efficacies of the IR agents BABA, RBH and ChP in tomato (cv. Moneymaker) and lettuce (cv. Kavir) against *B. cinerea* and *B. lactucae*, respectively.

HSI for the detection and quantification of grey mould (*B. cinerea*) and downy mildew (*B. lactucae*) in tomato and lettuce, respectively, requires different approaches that are dictated by the nature of the these pathogens. *B. cinerea* has a necrotrophic lifestyle and its infection strategy involves the production of cell wall-degrading enzymes and induction of programmed cell death in the host, resulting in tissue collapse and fast-spreading lesions (Williamson *et al.*, 2007). Indeed, *B. cinerea* inoculation of tomato resulted in rapidly spreading necrosis within 24 hours of inoculation. This aggressiveness of *B. cinerea* made imaging of the infection sites in the plants, and hence tracking disease development, difficult. Nevertheless, due to the severe aggressiveness and necrotic symptoms the identification and quantification of disease was relatively straightforward and could be quantified readily from RGB images. Although the opportunity to track the onset and progress of the grey mould by HSI was lost, data gathered from the detached tomato cotyledons captured the biochemical changes caused by the pathogen. In past studies of the protective effects of IR agents against *B. cinerea* in tomato, the common practice has been to use detached true leaves (Audenaert, De Meyer and Höfte, 2002; Luna *et al.*, 2016; De Vega *et al.*, 2021). Similarly, previous HSI approaches to detect of *B. cinerea* infection were often based on detached true leaves (Zhu *et al.*, 2017; Fahrentrapp *et al.*, 2019; Scarboro *et al.*, 2021). This use of detached leaves for image-based phenotyping of disease symptom progress is necessitated by the difficulties of imaging growing plants. However, this approach was not taken in this study. As HSI sensors are sensitive to small physio-chemical changes in vegetation (Li *et al.*, 2015; Mirzaei *et al.*, 2019) and the experimental plants were subjected to both biotic (*B. cinerea*) and abiotic (IR agents) treatments, it was deemed best to minimise the stress effects arising from

wounding and only detach leaves at the end of the experiment. Indeed, how the detachment process would affect the defence status of the leaves was unknown and conclusions based on such results may not translate well to intact plants. Thus, while the high aggressiveness of the pathogen did not allow for the HSI to track *B. cinerea* disease non-destructively, the IR response could be quantified by HIS in intact (non-wounded) plants.

The three IR agents (BABA, RBH and ChP) had markedly different capabilities to protect against grey mould in tomato (cv. Moneymaker). The inoculation of tomato with *B. cinerea* resulted in rapid progression of disease. As early as one-day post inoculation, infected leaves collapsed and this necessitated reliance on destructive end-point measurements. Disease symptoms in the detached cotyledons was assessed with imaging sensors by means of lesion area, hyperspectral signatures and chlorophyll content from MCARI2 values. Together these parameters gave a highly consistent measure of the efficacies of the agents in tomato (cv. Moneymaker) against *B. cinerea*. The β-amino acids BABA and RBH were ineffective. Average lesion area for all treatment doses of the two agents was not significantly different from the water treatment (Fig 4.1), their hyperspectral signatures overlapped with the infected controls (Fig 4.2) and MCARI2 values (chlorophyll content) were as low as the infected controls (Fig 4.2). By contrast, ChP was highly effective at controlling grey mould. All ChP doses significantly lowered lesion area, hyperspectral signatures were distinct from that of diseased controls and MCARI2 values for all doses were significantly higher than for the diseased controls.

The results from the *B. cinerea*-tomato pathosystem underscore the importance of experimental verification in the selection and use of IR agents in crop protection. Previously in the same Moneymaker cultivar, BABA was reported to effectively control *B. cinerea* infection (Luna *et al.*, 2016). A difference between these studies, which could account for the contrasting results, is age. In the Luna *et al.* (2016) study, the age of the plants used was at least one week older than plants used in this study. It is known that plant age influences the outcome of plant-pathogen interactions (Hu and Yang, 2019). The phenomenon of 'age-related resistance' (ARR), in which plants transition from susceptibility to resistance toward pathogens due to developmental changes, has been demonstrated in many plant species, such as Arabidopsis (McDowell *et al.*, 2007), strawberry (Asalf *et al.*, 2014) and tomato (Zhang, Liu and Pan, 2021). It is thought that this relatively low level of disease resistance is a safeguard against yield losses, dwarfism and tissue damage arising from constitutive immune activation during the period of maturation (Brown, 2002; Bomblies and Weigel, 2007; Zhang, Liu and Pan, 2021).

In contrast to the two β-amino acids, ChP showed highly significant efficacy against *B. cinerea in tomato (cv. Moneymaker)* at all the tested doses (0.063 - 1 % w/v). Previously ChP treatment solutions were reported to significantly reduced lesion size in the same pathosystem. Although

concentrations of 0.1 % w/v and higher had antifungal effect, *arresting B. cinerea* hyphal growth, a 0.01 *% w/v* treatment solution induced callose formation and reduced *B. cinerea* lesions whilst not showing any direct antifungal activity *(*De Vega *et al.,* 2021*).* Moreover, De Vega *et al.* (2021) revealed through transcriptomic analysis that ChP primed the induction of plant defence genes as early as nine hours after inoculation. Similarly, ChP has been found to be effective against *B. cinerea* infection in fruits, such as strawberries (Romanazzi *et al.*, 2013), grapes (Muñoz and Moret, 2010) and tomatoes (Zhang *et al.*, 2015). Various studies have shown that this protective effect of ChP is the result of its activation of cellular and molecular defences, such as callose (Kauss, Jeblick and Domard, 1989; De Vega *et al.*, 2021), chitinases (Mauch, Hadwiger and Boller, 1984), peroxidase (Zhang *et al.*, 2015) and lignin (Zhang *et al.*, 2015), as well as having direct antimicrobial activity (Sahariah and Másson, 2017).

Biotrophic pathogens, compared to necrotrophic pathogens, do not cause necrosis during the early stages of infection and, generally, progress more slowly (Koeck, Hardham and Dodds, 2011; Fall, Van Der Heyden and Carisse, 2016; Mahlein, 2016). Considering the chemical stress effects by IR agents, the detection and quantification of relatively subtle disease symptoms by biotrophic *B. lactucae* in lettuce required a more complex data analysis approach. Although this downy mildew disease could be detected by the HSI sensor, the chemical stress by IR agents also had effects on hyperspectral reflectance. Therefore, to quantify IR against downy mildew, it was necessary to separate the two stress responses by HIS and select SVIs that are responsive to stress by *B. lactucae* and not to chemical stress by IR agents. First, OPLS-DA was used to identify SVIs sensitive to downy mildew symptoms, which is a powerful multivariate statistical modelling method that has been previously used to discriminate groups in high-dimensional spectral data (Worley and Powers, 2016). Although OPLS-DA can be prone to statistically unreliable group separation, reliable inferences can be inferred from thoroughly validated models with highly significant fitting capacity (R^2) and predictive capacity (Q^2) (Bylesjö *et al.*, 2006; Worley and Powers, 2016). In this study, the separation of samples from downy mildew- and control-treated samples by OPLS-DA yielded highly significant fitting ($R^2 = 0.857$, $p < 0.001$) and predictive capacities ($Q^2 = 0.847$, $p < 0.001$). Along with SVIs separation by OPLS-DA, a rating for SVI sensitivity to chemical effects was used. Together, these approaches identified SIPI as an SVI, which were responsive to stress by downy mildew disease, while relatively unresponsive to chemical stress by IR agents. Moreover, the use of a DTC method to detect downy mildew validated the result of the multivariate analysis, also returning SIPI as the best SVI to detect downy mildew infection with a high accuracy (*OA* = 0.94, kappa = 0.88). DTC is a method that has been frequently employed for prediction in HSI data (Berhane *et al.*, 2018; Lim, Kim and Jin, 2019; Abbas *et al.*, 2021).

While only ChP was effective in mediating IR in the *B.* cinerea-tomato interaction, all three

agents reduced infection levels by *B. lactucae* in lettuce, albeit to different levels and efficiencies. BABA was the most potent of the three agents; even the smallest dose of 0.008 mM tested reduced *B. lactucae* symptoms (SIPI) to statistically significant levels and was 16 and 64 times more potent than the lowest effective doses of RBH and ChP, respectively. In previous studies, the use of defence mutants has demonstrated that the mechanisms of BABA-IR are diverse and dependent on the pathosystem (Cohen, Vaknin and Mauch-Mani, 2016). For example, in Arabidopsis, BABA is effective against the necrotrophic fungus *B. cinerea*, which acts through a NPR1-dependent SA signalling pathway (Zimmerli, Métraux and Mauch-Mani, 2001). By contrast, against the biotrophic oomycete *Hyaloperonospora arabidopsidis*, BABA-IR can operate independently of SA-, JA-, and ET signalling (Zimmerli *et al.*, 2000; Ton *et al.*, 2005), but instead is dependent on ABA signalling that controls callose accumulation and efficacy (Ton *et al.*, 2005; Schwarzenbacher *et al.*, 2020). Similarly, in lettuce, BABA induced rapid callose encasement of the primary infection structures of *B. lactucae* and prevented its progress into the host (Cohen, Rubin and Kilfin, 2010). Alongside the callose deposition, it has been reported that BABA-primed plants accumulate increased amounts of hydrogen peroxide (H_2O_2) at host cells penetrated by *B. lactucae* (Cohen, Rubin and Kilfin, 2010). This BABA-induced priming of reactive oxygen species (ROS) by BABA has also been reported in tomato against *Pseudomonas syringae* pv. *tomato* (Baysal *et al.*, 2007) and in grapevine against the downy mildew *Plasmopara viticola* (Dubreuil-Maurizi *et al.*, 2010). Rather than acting directly on pathogens, there is increasing evidence that H_2O_2 has a defence-signalling role (Dubreuil-Maurizi *et al.*, 2010; Saxena, Srikanth and Chen, 2016; Černý *et al.*, 2018). In addition, H_2O_2 could act as a substrate for peroxidases in the lignification of cell walls.

At the time of writing, the activity of RBH has not been tested in lettuce. However, similar to BABA-IR, it seems that that RBH-IR acts through mechanisms that are pathosystem- dependent. RBH-IR in Arabidopsis against the necrotrophic fungus *Plectosphaerella cucumerina* has been reported to act through priming of JA- and ET-dependent defences (Buswell *et al.* 2018). In contrast, against the biotrophic downy mildew pathogen *Hyalopersonospora arabidopsidis*, RBH-IR in Arabidopsis was partially dependent on camalexin production and associated with increased defence efficacy of callose depositions, as well as the priming of camalexin induction (Buswell *et al.*, 2018). In contrast to the two β-amino acids, ChP has been reported to display direct antimicrobial activity (Pospieszny, Chirkov and Atabekov, 1991; Rabea *et al.*, 2003), in addition to mediating an IR response in the plant. Nevertheless, ChP only elicits plant defences at lower concentrations (De Vega *et al.*, 2021). In terms of this defence elicitation, the accumulation of PR proteins, phytoalexins and proteinase inhibitors have all been associated with ChP-IR (El Hadrami *et al.*, 2010). Moreover, ChP has been reported to be effective against downy mildew disease in several plant species. For example in pearl millet, ChP yielded high protection against *Sclerospora graminicola* through a mechanism involving nitric oxide (NO) accumulation

(Sharathchandra *et al.*, 2004; Manjunatha *et al.*, 2009). ChP is also effective against *Plasmopara viticola* in grapevine (Romanazzi *et al.*, 2016) and against *B. lactucae* in lettuce (Abdel-Maksoud Abada, 2017).

Since IR agents can protect against diseases whilst also causing phytotoxicity, their use needs careful consideration. All three IR agents tested in this study showed dose-dependent IR efficacy. While ChP did not show deleterious effects in either tomato or lettuce, treatment with BABA and, to a lesser extent, RBH resulted in dose-dependent phytotoxicity in both plant species (Chapter 3). This phytotoxicity can have different causes. For instance, direct up-regulation of plant defences can be metabolically costly and reduce growth and yield (Heil *et al.*, 2000; Martinez-Medina *et al.*, 2016). In addition, some IR agents can have more specific non-target effects on important cellular mechanisms. For instance, BABA has a direct inhibitory effect on aspartyl-tRNA synthetase activity, triggering GCN2-dependent inhibition of gene translation (Luna *et al.*, 2014).

In summary, the work presented in this chapter demonstrates varying dose-dependent efficacies of the IR agents BABA, RBH and ChP in tomato against *B. cinerea* and in lettuce against *B. lactucae*. The traditional disease scoring methods of measuring lesion area and trypan blue staining were compared against HSI methods. Subsequent selection of suitable SVIs from the hyperspectral data proofed equally suitable to distinguish between different levels of disease. As such, the selected SVIs allowed for quantification of the relative efficacies of the IR agents in both pathosystems. This ability was especially useful in the detection of the more subtle symptoms by the biotroph *B. lactucae*. In this case, the use of multivariate statistical and machine learning methods enabled the identification of SIPI as an SVI that is responsive to disease stress by downy mildew, while relatively non-responsive to chemical stress (phytotoxicity) by IR agents. In this endeavour, the importance of tailoring IR agent treatments to the pathosystem became apparent. For instance, the lack of IR by BABA and RBH in tomato against *B. cinerea* is not supported by previous reports in the literature. This discrepancy might be due to differences in tomato cultivar and age of the tested plants. In lettuce, the young age (two-week-old) of seedlings was not an issue and both β-amino acids were highly effective, whereas ChP was less effective. Interestingly, the efficacies in tomato and lettuce also correlates with the observed residue levels (see section 3.3.5 and Fig 3.7) of the agents, which are likely caused by difference in the uptake capacity of the β-amino acids. ChP was effective in both pathosystems but considerably more effective against *B. cinerea* in tomato. Furthermore, the phytotoxic tendency of BABA and RBH necessitates carefully considered treatment strategies that minimise their deleterious side effects whilst still ensuring disease protection. One such strategy is presented in the next Chapter of this thesis.

Chapter 5

Using hyperspectral imaging to quantify the effects of combining chemical IR agents on plant growth and disease protection in the lettuce-Bremia lactucae pathosystem.

Abstract

The efficacy to protect against plant disease by single IR agents generally increases with dose, but often also reduces plant growth. To optimise the balance between IR efficacy and phytotoxicity, it has been proposed to combine IR agents and so obtain additive and/or synergistic levels of IR, while minimising the associated costs on plant growth. However, this approach could equally lead to increased phytotoxicity and/or antagonistic effects on IR by negative signalling-cross between the underpinning defence pathways. With the aim of identifying treatments that suppress disease with no or minimal side effects on plant growth, combinations of relatively low doses of the IR agents BABA, RBH and ChP were characterised by hyperspectral imaging for IR efficacy and growth repression in the lettuce-*B. lactucae* pathosystem. None of the pairwise combinations of BABA, RBH and ChP showed synergistic repression of plant growth. By contrast, the combination of BABA-RBH provided synergistic levels of IR against *B. lactucae*. The latter analysis identified two dose combinations of BABA and RBH that are highly synergistic in terms of disease protection without any adverse effects on plant growth.

5.1 Introduction

Chemical IR agents have the potential to be safer alternatives to traditional chemical biocides. These agents can provide broad-spectrum protection through the augmentation of durable plant defences. Yet, IR agents are not widely used in crop protection. A major reason for this under-utilisation is that they are often associated with detrimental side effects on plant growth and yield. Treatment with IR agents can be metabolically costly resulting in lower biomass and reduced seed production (Heil *et al.*, 2000), or cause genuine phytotoxicity, such as the inhibitory effect of BABA on the aspartyl-tRNA synthetase enzyme (Luna *et al.*, 2014). In chapter 3, it was demonstrated that both BABA and RBH exhibited dose-dependent phytotoxicity in lettuce, while ChP was generally nontoxic (Fig 3.3). Another major reason for the under-utilisation of IR agents is that disease protection can vary, depending on the plant species, the attacking pathogen, mode of application and general growth conditions (Sharma, Butz and Finckh, 2010) (Hijwegen and Verhaar, 1995; Dann *et al.*, 1998). In chapter 4, it was shown that the agents BABA, RBH and ChP all provided varying, but dose dependent, protection against the downy mildew pathogen *B. lactucae* in lettuce (Fig 4.10). Although high doses of the IR agents could be utilised to maximise their efficacy, this strategy can only be beneficial in cases of high disease pressure, where the phytotoxicity costs are outweighed by the provided protection (Heil *et al.*, 2000; Heil and Baldwin, 2002; Walters and Heil, 2007; Walters and Fountaine, 2009).

To optimise the balance between phytotoxicity and efficacy, a variety of approaches have been explored. Several of these approaches used mixed crop protection agent treatment strategies. The combination of the biological control agent *Trichoderma harzianum* and the IR agent Methyl jasmonate (MeJA) provided protection against *Bipolaris sorokiniana* that was superior to either treatment alone (Singh *et al.*, 2019). Another strategy has been the combination IR agents and fungicides. The addition of BABA to the fungicide mancozeb resulted in synergistically increased efficacy and reduced fungicide concentrations were required to achieve the desired protection level (Baider and Cohen, 2003). Also, the strategy of combining different IR agents has been demonstrated to improve efficacy. The mixing of BABA and acibenzolar-S-methyl (ASM) was effective against *Plasmopara viticola* in grapevines at half the recommended doses (Reuveni, Zahavi and Cohen, 2001). Similarly the combination of ASM, BABA and JA enhanced efficacy against powdery mildew in barley and reduced phytotoxicity (Walters *et al.*, 2011).

The strategy of combining IR agents has potential due to the possibility of synergistic interactions on the level of disease protection. A synergistic interaction occurs when the combined effect of two chemicals is greater than the sum of each chemical's individual effect (Roell, Reif and Motsinger-Reif, 2017). BABA-IR involves augmented callose accumulation, which acts independently of SA signalling, but acts via regulation by ABA (Ton and Mauch-Mani, 2004; Ton *et al.*, 2005;

Flors *et al.*, 2008; Schwarzenbacher *et al.*, 2020). RBH-IR is thought to involve the priming of JA- and ET-dependent defences and camalexin production (Buswell *et al.*, 2018). ChP-IR has been shown to lead to the accumulation of proteinase inhibitors, phytoalexins and PR proteins (El Hadrami *et al.*, 2010). According, there is the possibility that combinations of IR agents may simultaneously induce resistance through different pathways and thus act synergistically, although there is the possibility that there might be antagonistic effects by negative signalling-cross talk between the pathways controlling these IR responses (Koornneef and Pieterse, 2008; Vos *et al.*, 2015; Zhou *et al.*, 2016; Proietti *et al.*, 2018). It should be mentioned, however, that these antagonistic effects typically occur at higher concentrations, and additive effects by natural priming responses to rhizobacteria (ISR) and localised pathogen attack (SAR) have been reported as well (van Wees *et al.*, 2000). Despite the promise of combining chemical IR agents, a systematic investigation of their effects is lacking. Consequently, this chapter describes a systematic investigation of the effects of pairwise combinations of the IR agents BABA, RBH and ChP at sub-phytotoxic dose ranges.

5.2 Methods

5.2.1 Plant growth, combined chemical treatments and inoculations

Lettuce plants were grown as described in section 2.2. To assess potential interactions of BABA, RBH and ChP in the lettuce-*B. lactucae* pathosystem, three separate experiments were conducted. Four dose levels each for BABA (0, 0.004, 0.008 and 0.016 mM), RBH (0, 0.063, 0.125 and 0.25 mM) and ChP (0, 0.125, 0.25 and 0.5 % w/v) were selected on the basis of reduced phytotoxicity and IR efficacy. The selected doses of each IR agent pair (BABA:ChP, RBH:ChP and BABA:RBH) were combined in a factorial design, resulting in a 4 x 4 treatment matrix (Fig 5.1) for each pair. Lettuce seedlings (five-days-old) were treated with the combined dose formulations, as described in section 2.3. Two days after chemical applications, the seedlings were inoculated with *B. lactucae* as described in section 2.4.

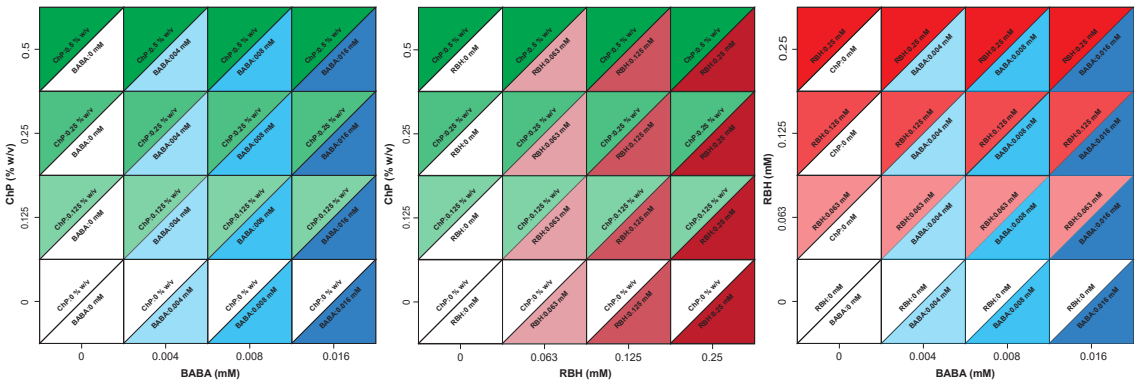

Fig 5.1 | Combined treatment matrices. Shown are the factorial 4 x 4 combination matrices for each IR agent pair (BABA:ChP, RBH:ChP and BABA:RBH).

5.2.2 Hyperspectral data acquisition and analysis

Lettuce seedlings subjected to the various combination treatments were imaged non-destructively on a daily basis up to 10 days with a HSI camera. At the final time point (day 10), leaves were detached and imaged again. Hyperspectral reflectance data were extracted and processed, as described in section 2.5. To investigate the impacts of the combined IR agent treatments, RGR and TGI were selected to assess phytotoxicity by growth impairment effects. SIPI data from detached cotyledons – which tended to show higher infection severity – were selected to evaluate IR efficacies against *B. lactucae*. All data analysis and statistical tests were performed with R version 4.0.5 (R Core Team, 2021). For the single chemical treatments, the effects of dose and inoculation on growth (RGR and TGI) and disease symptoms (SIPI) were tested for statistical significance using two-way ANOVA tests.

To visualise the effects of combining IR agents on RGR and disease symptoms, two separate linear models were fitted in which the two dose covariates behaved either independently or interactively. The Akaike information criterion (AIC), a statistical method for estimating model prediction error (Portet, 2020), was used as a means to select the simplest linear model that fitted the data best. ANOVA was carried out to ascertain whether the two models were significantly different from each other; in each case, the simpler model (i.e. with the lowest AIC value) was selected for subsequent analysis. Model predicted values were extracted and the 95% confidence interval around the predicted data was calculated and plotted to visualise the effects of combined dose treatments.

To determine whether the combined application of IR agents results in interactions that alter phytotoxicity and IR efficacy, two-way ANCOVA tests were conducted for each IR agent pair, allowing the identification of statistically-significant effects and interactions for both RGR and SIPI. A statistically significant result ($p \leq 0.05$) in the interaction term of the ANCOVA test was deemed to indicate synergism. Where a combined chemical pair showed a significant interaction, data from that pair were split in to nine sets. Each data set consisted of the four groups: D_A, D_B, C and D_A:D_B, where D_A and D_B represented the single doses of each IR agent, C was the control ($D_A = 0$ and $D_B = 0$), and D_A:D_B was the mixed treatment. On each data set, a one-way ANOVA test followed by Tukey's test was conducted to establish significant differences between the control, the single treatments and the combined treatment. A synergistic interaction between D_A and D_B was defined as the condition in which effect D_A + effect D_B was significantly less than effect D_A:D_B.

5.3 Results

5.3.1 Treatment effects on lettuce growth

To assess the impacts of the chemical IR agents and inoculation with *B. lactucae* treatments on lettuce growth, RGR and TGI data were used. The data sets were compiled from samples receiving control treatment and low doses of single IR agents, which were predicted to have no or minimal effects on plant growth. In agreement with the results described in Chapter 3, application of low doses of BABA (0.004, 0.008 and 0.016 mM), RBH (0.063, 0.125 and 0.25 mM) and ChP (0.125, 0.25 and 0.5 % w/v) did not have significant growth effects, while *B. lactucae* inoculation resulted in a substantial growth reduction (Fig 5.2). Two-way ANOVA was performed to test the effects of chemical dose and inoculation on RGR, confirming that none of the IR agents had a statistically significant effect on RGR, while the effect of *B. lactucae* inoculation was highly significant (Fig 5.2A). Growth impact as measured by TGI paralleled RGR. There were no significant interactions between the IR agents and inoculation. None of the agents significantly changed TGI values, while inoculation with *B. lactucae* caused significant decreases (Fig 5.2B). Thus, in lettuce seedlings, *B. lactucae* infection lead to a substantial growth reduction, while at the selected low doses, BABA, RBH and ChP did not majorly affect plant growth nor alleviate *B. lactucae*-caused growth impairment.

Table 5.1 | Model selection for the impact of IR agent interactions on RGR

Chem Mix	Model	Inoculation			
		Mock		*B. lactucae*	
		AIC	***p*.val**	**AIC**	***p*.val**
ChP :: BABA	Independent	-418.9	0.545	-400.8	0.845
	Interactive	-410.1		-388.5	
ChP :: RBH	Independent	-422.3	0.347	-376.6	0.273
	Interactive	-416.0		-371.4	
BABA :: RBH	Independent	-439.1	0.489	-427.3	0.844
	Interactive	-430.9		-414.9	

5.3.2 The effects of combining IR agents on lettuce growth

To visualise the effects of combined IR agent treatments on lettuce RGR in the presence and absence of *B. lactucae*, two different linear models were fitted. In one model, the dose covariates of each IR agent pair were set to act independently and in the second, they were set to act

interactively. To ascertain which model fitted the RGR data best, AIC tests were carried out and ANOVA was used to calculate significant differences between models (Table 5.1). For both mock- and *B. lactucae*-inoculated groups the effect of the different IR agent mixes on growth was best described by independent models.

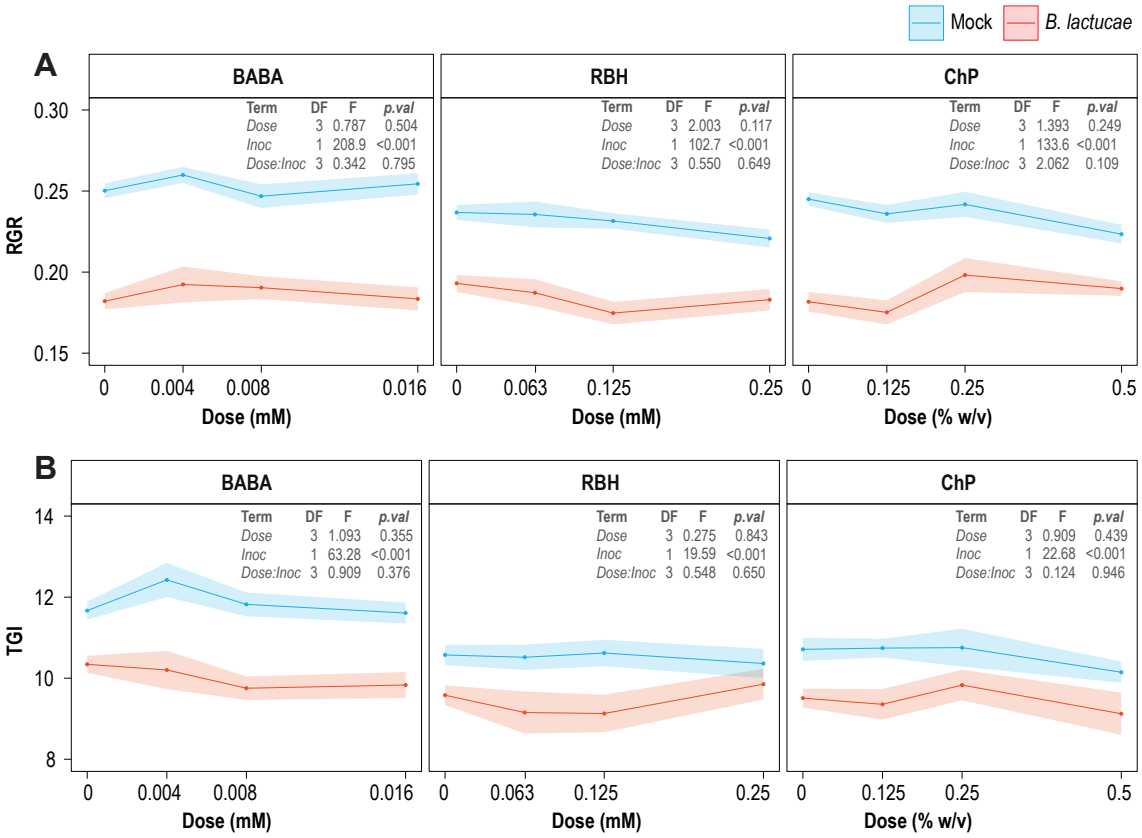

Fig 5.2 | The effects of *B. lactucae* and low doses of IR agents on lettuce growth (RGR and TGI). The presented curves (blue = mock, red = *B. lactucae* inoculation) are mean values ± SE. (**A**) The effect of IR agent dose on RGR. (**B**) The effect of IR agent dose on TGI values in whole plants at 7dpi. The effect of chemical dose and inoculation on group mean RGR and TGI were tested for statistical significance by two-way ANOVA (inserted tables).

Predicted RGR data from the model, along with the original data for each pair of IR agents, are presented in Fig 5.3. As is shown in Fig 5.3A, the very low dose range of BABA did not affect RGR, while ChP caused a slight, dose-dependent decrease in RGR. In the presence *B. lactucae*, the low doses of BABA did not alter RGR; however, the addition of ChP resulted in a small dose-dependent increase in RGR (Fig. 3.5A). In the combined RBH-ChP treatments (Fig 5.3B), both RBH and ChP alone slightly decreased RGR in the mock-inoculated seedlings. By contrast, in the *B. lactucae* inoculated seedlings, RBH caused a decrease in RGR, whereas the addition of increasing ChP doses caused an increase in RGR. When BABA and RBH were combined for mock-inoculated seedlings (Fig 5.3C), RBH reduced RGR in a dose-dependent manner,

which remained similar in the presence with BABA. In *B. lactuca*-incoulated seedlings, RBH still reduced RGR in a dose-dependent manner; however, this trend was reverted in the presence of BABA.

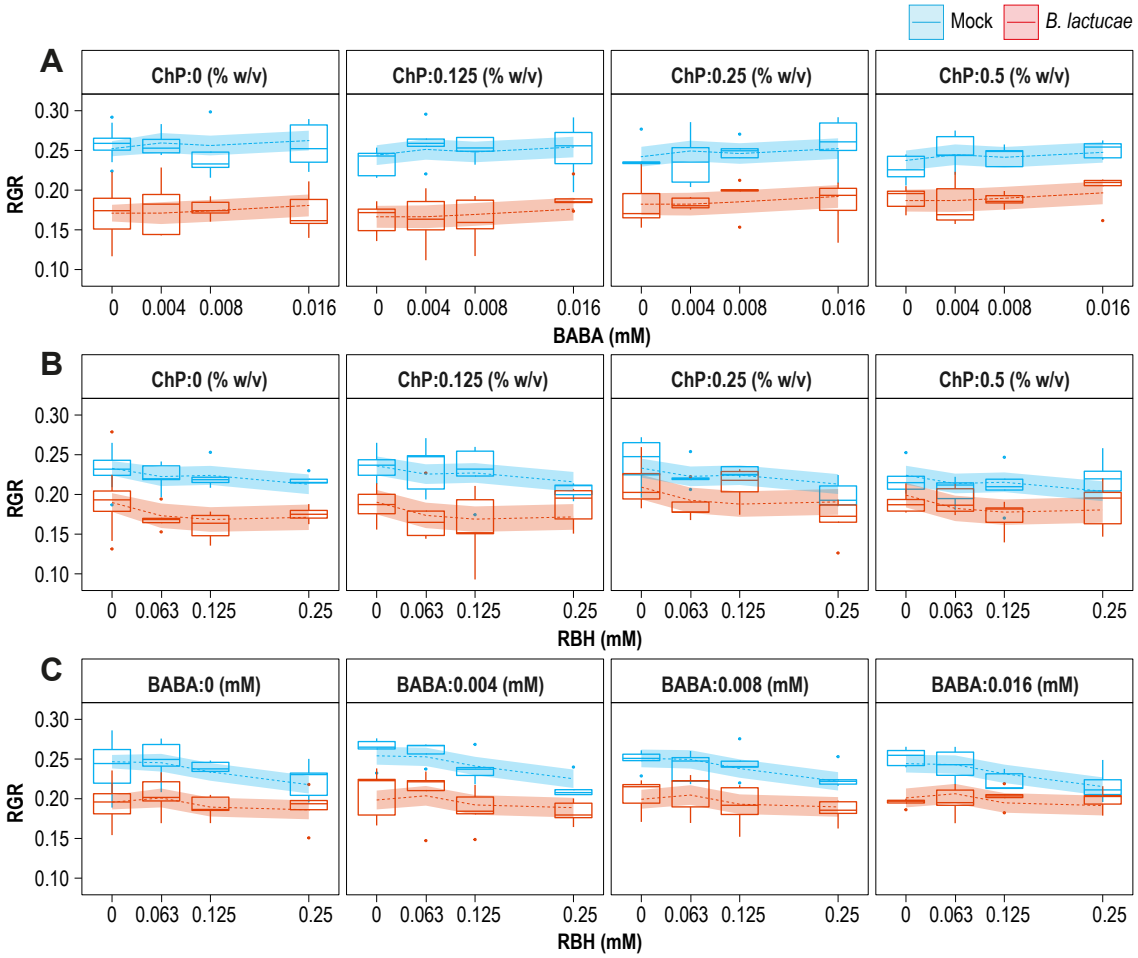

Fig 5.3 | The effects of increasing doses of single and combined IR agents on RGR. Each row (**A-C**) shows the results of a single pair of IR agents; panels show data for one IR agent dose combined with the full range of doses from the second IR agent. Boxplots (blue = mock, red = *B. lactucae* inoculation) show the interquartile range (IQR; box) ± 1.5xIQR (whiskers), including median (horizontal line), of the original (raw) RGR data. Curves show linear model-predicted average RGR values with a 95% confidence interval. In all fitted models, the dose covariates behave independently.

To test the statistical significance of the effects by single and combined doses of IR agents on RGR, two-way ANCOVA was conducted (Table 5.2). For the combined BABA-ChP treatments, the effect of ChP was borderline statistically significant in the presence and absence of *B. lactucae* (p=0.013 and 0.029, respectively), whereas the effect of BABA and the interaction of BABA:ChP were not statistically significant under both conditions. For the combined RBH-ChP treatments, only the effect of RBH was statistically significant in the absence of *B. lactucae*, whereas all other

factors and interactions for this combination did not have an effect. When BABA and RBH were combined, the only significant result came from RBH in the absence of *B. lactucae*. Thus, the results of the two-way ANCOVA indicate that the combined IR agents at the selected dose ranges did not statistically interact, which in turn suggests that there was not synergistic phytotoxicity as a consequence of combining IR agents at low doses.

Table 5.2 | Two-way ANCOVA table showing the effects of combined IR agent treatments on RGR

Chem Mix	Term	Inoculation					
		Mock			*B. lactucae*		
		DF	**F**	***p*.value**	**DF**	**F**	***p*.value**
ChP|BABA	BABA	3	0.518	0.671	3	0.904	0.443
	ChP	1	4.957	0.029	1	6.515	0.013
	BABA::ChP	3	1.152	**0.333**	3	0.151	**0.929**
ChP|RBH	RBH	3	3.693	0.015	3	2.259	0.088
	ChP	1	2.296	0.134	1	2.140	0.147
	RBH::ChP	3	0.963	**0.414**	3	0.352	**0.788**
BABA|RBH	RBH	3	9.387	< 0.001	3	1.884	0.139
	BABA	1	0.373	0.543	1	0.705	0.403
	RBH::BABA	3	0.373	**0.327**	3	0.615	**0.607**

5.3.3 The efficacy of low IR agent doses in lettuce against *B. lactucae*

Low doses of BABA, RBH and ChP were selected to minimise the associated phytotoxicity effects. To evaluate the IR efficacies of these doses against *B. lactucae*, SIPI data from detached cotyledons were quantified at 7 dpi to estimate disease severity in three separate experiments. SIPI values from mock-inoculated samples were consistently lower compared to *B. lactucae*-inoculated groups, which was apparent at all doses and in all three experiments. Generally, SIPI values in the mock-inoculated samples did not show major dose-dependent changes, which supports the robustness of this SVI against chemical stress by IR agents (Chapter 4). In the *B. lactucae*-inoculated samples, the single doses BABA did not alter SIPI values, indicating that these low doses of BABA failed to induce resistance. For RBH and ChP, however, SIPI value showed a small dose-dependent reduction, indicating relatively subtle IR effects.

Two-way ANOVA revealed that *B. lactucae* inoculation had a statistically significant effect in all three experiments. Treatment with BABA did not significantly affect SIPI and there was no statistically significant interaction between BABA and inoculation either (Fig 5.4A), which confirms the lack of BABA-IR at these doses. RBH treatment, on the other hand, did have a statistically significant effect on SIPI and also showed a statistically significant interaction with inoculation (Fig 5.4B). Similarly, ChP treatment had a statistically significant effect on SIPI and showed a significant interaction with inoculation (Fig 5.4C). Together, the results of this ANOVA confirm that increasing doses of RBH and ChP resulted in statistically significant IR effects against *B. lactucae*.

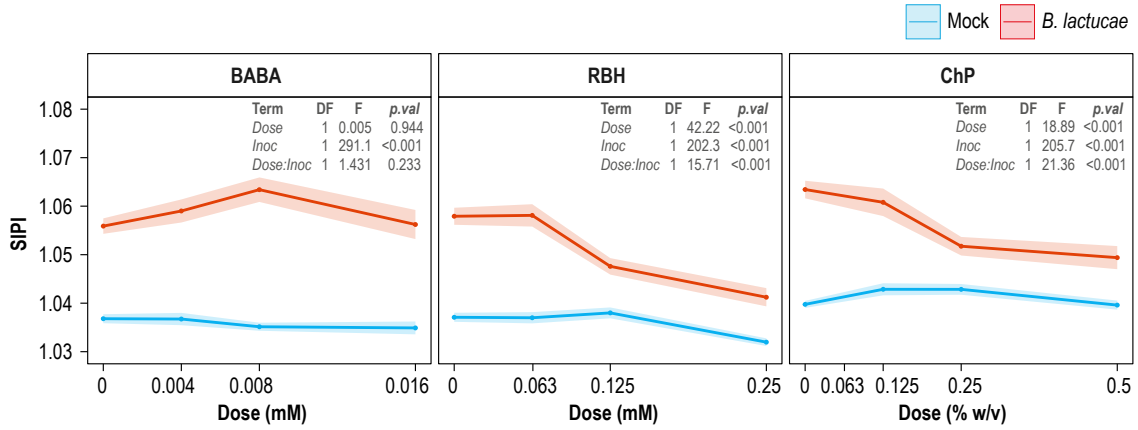

Fig 5.4 | The effects of relatively low doses of single IR agents on SIPI as a marker for *B. lactucae* disease The presented curves (blue = mock, red = *B. lactucae* inoculation) are mean SIPI ± SE in detached cotyledons at 7 dpi. The effects of chemical dose and inoculation on group mean SIPI values was tested for statistical significance by two-way ANOVA (inserted tables).

5.3.4 The efficacy of combined IR agents against *B. lactucae* in lettuce

SIPI is an SVI that is optimal for tracking *B. lactucae* symptoms in lettuce (Chapter 4). To visualise how the combination of IR agents affects SIPI in detached cotyledons, independent and interactive linear models were fitted. Model fit was assessed by AIC tests and significant differences were analysed by ANOVA (Table 5.3). In the BABA-ChP combination, the independent model was the better fit for both mock- and *B. lactucae*- inoculated groups, whereas an interactive model was a better fit for mock- and *B. lactucae*- inoculated groups in the RBH-ChP combination. For the BABA-RBH combination, the independent model was the optimal fit for the mock-inoculated groups, while an interactive model was a better fit the *B. lactucae* inoculated groups.

Table 5.3 | Model selection for the impact of IR agent interactions on SIPI

Chem Mix	Model	Inoculation			
		Mock		*B. lactucae*	
		AIC	***p*.val**	**AIC**	***p*.val**
ChP :: BABA	Independent	-1401.9	0.71142	-1063.7	0.639
	Interactive	-1390.7		-1053.3	
ChP :: RBH	Independent	-1365.5	<0.001	-1106.6	0.024
	Interactive	-1379.2		-1109.2	
BABA :: RBH	Independent	-1350.2	0.067	-1207.9	<0.001
	Interactive	-1349.4		-1244.8	

Fig. 5 shows the effects of combining IR agents on SIPI values in mock- and *B. lactucae*-inoculated plants, using raw data (box plots) and predicted data from the linear model (lines). Generally, SIPI values in mock-inoculated samples stayed constant across increasing IR agent doses. In the *B. lactucae*-inoculated groups, there was a dose-dependent decrease in SIPI values across all three combinations, suggesting IR against *B. lactucae* by combinations of IR agents. For plants treated with the BABA-ChP combinations, this decrease in SIPI values were only caused by ChP dose, while BABA dose had no obvious additional effect. For plants treated with the RBH-ChP combinations, the IR agents appeared to have an additive effect on the reduction in SIPI values. Interestingly, despite the fact that low BABA doses alone did not have an effect, combining BABA with RBH resulted in a stronger reduction of SIPI values by RBH.

To ascertain whether any of the apparent interaction effects from mixed IR agents on SIPI were synergistic, two-way ANCOVA tests were performed (Table 5.4). In mock-inoculated samples, none of the combined IR agents showed a significant interaction and thus did not appear to have synergistic effects on disease suppression. However, in the *B. lactucae* inoculated samples, the combined BABA-RBH treatments showed a statistically significant interaction. This strongly suggests that low doses of BABA and RBH act synergistically to reduce *B. lactucae* infection.

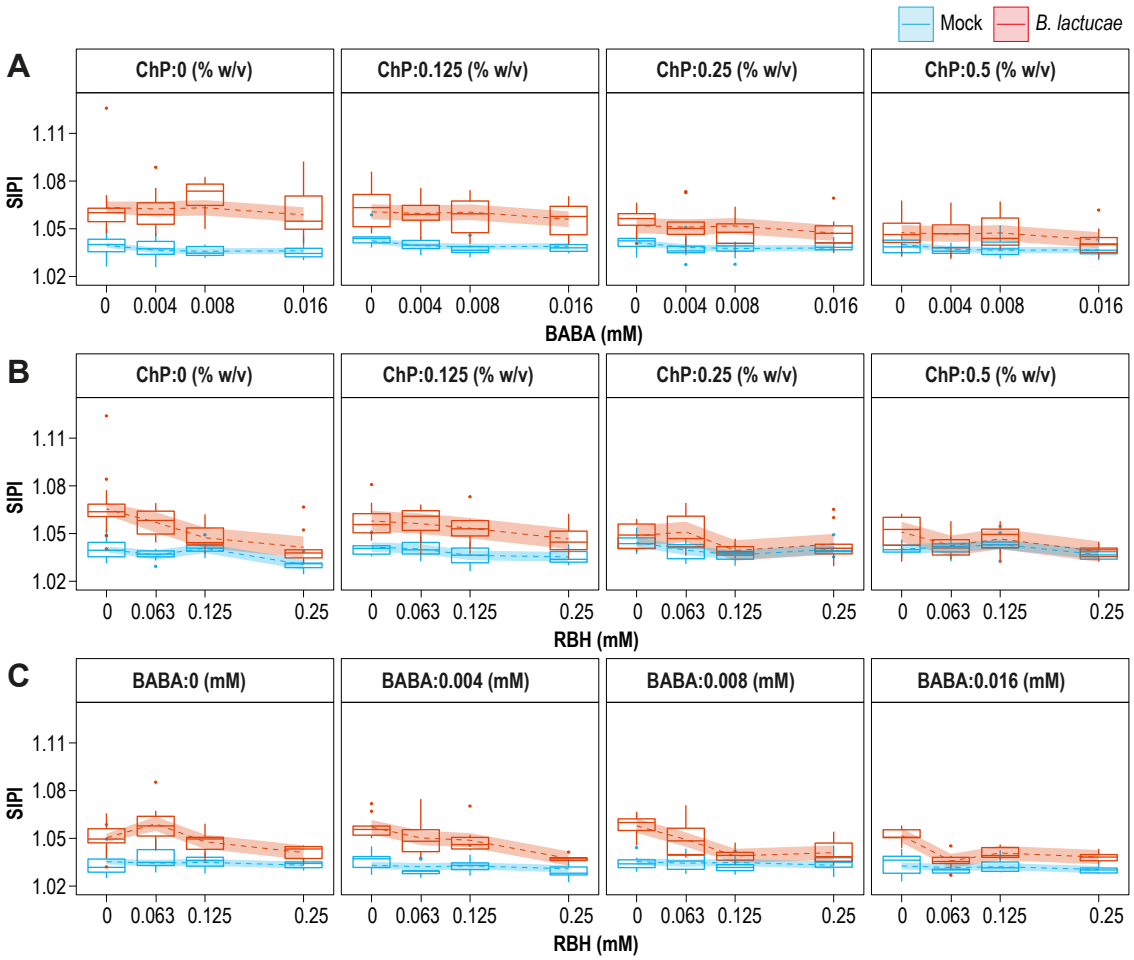

Fig 5.5 | The effects of increasing doses of single and combined IR agents on *B. lactucae* symptoms by HSI. Each row (**A-C**) shows the results of a single pair of IR agents; panels show data for one IR agent dose combined with the full range of doses from the second IR agent. Boxplots (blue = mock, red = *B. lactucae* inoculation) show the interquartile range (IQR; box) ± 1.5xIQR (whiskers), including median (horizontal line), of the original (raw) SIPI data. Curves show linear model predicted mean SIPI with a 95% confidence interval. BABA-ChP and RBH-ChP mixes were fitted with models in which the dose covariates behave independently. The BABA-RBH combination was fitted with an interactive model.

Table 5.4 | Two-way ANCOVA table showing the effects of combined IR agent treatments on SIPI

Chem Mix	Term	Inoculation					
		Mock			*B. lactucae*		
		DF	**F**	***p*.value**	**DF**	**F**	***p*.value**
ChP|BABA	BABA	3	5.057	0.002	3	2.787	0.042
	ChP	1	0.038	0.845	1	45.359	<0.001
	BABA::ChP	3	0.857	**0.465**	3	0.376	**0.771**
ChP|RBH	RBH	3	8.031	<0.001	3	21.458	<0.001
	ChP	1	10.075	0.002	1	25.164	<0.001
	RBH::ChP	3	0.814	**0.488**	3	2.576	**0.056**
BABA|RBH	RBH	3	1.859	0.138	3	28.758	<0.001
	BABA	1	3.547	0.061	1	17.283	<0.001
	RBH::BABA	3	1.233	**0.299**	3	12.826	**<0.001**

In order to compare the effects of BABA and RBH on growth and IR, RGR and SIPI data from the BABA-RBH combination experiment were split into 9 separate dose combination groups and compared to each other. Each group consisted of a control, single BABA dose, single RBH dose and the two doses mixed (Fig 5.6). The groups were analysed for significant differences by one-way ANOVA tests, followed by Tukey tests. As previously suggested by the two-way ANCOVA (Table 5.2), none of the dose pairs showed synergistic action resulting in RGR changes, including the BABA-RBH combination. This indicates that low, non-toxic doses of BABA did not aggravate phytotoxicity by RBH. However, with respect to IR efficacy against *B. lactucae*, two of the BABA-RBH dose combinations showed a strongly synergistic interaction. For plants treated with the combination of 0.008 mM BABA and 0.125 mM RBH, mean SIPI values of the single dose treatments were not significantly lower than the control, indicating that these single low doses did not induce resistance. Nevertheless, SIPI values from plants that had received the combination treatment of 0.008 mM and 0.125 mM RBH were significantly lower than those from plants treated with the single doses and the control solution. A similar pattern was apparent from the combination of 0.016 mM BABA and 0.063 mM RBH with mixed doses decreasing SIPI values significantly compared to the single dose treatments and the control. Crucially, RGR values by these BABA-RBH combinations were statistically similar to the controls. Thus, combining low doses of BABA and RBH induce synergistic levels of IR against *B. lactucae* without compromising plant growth.

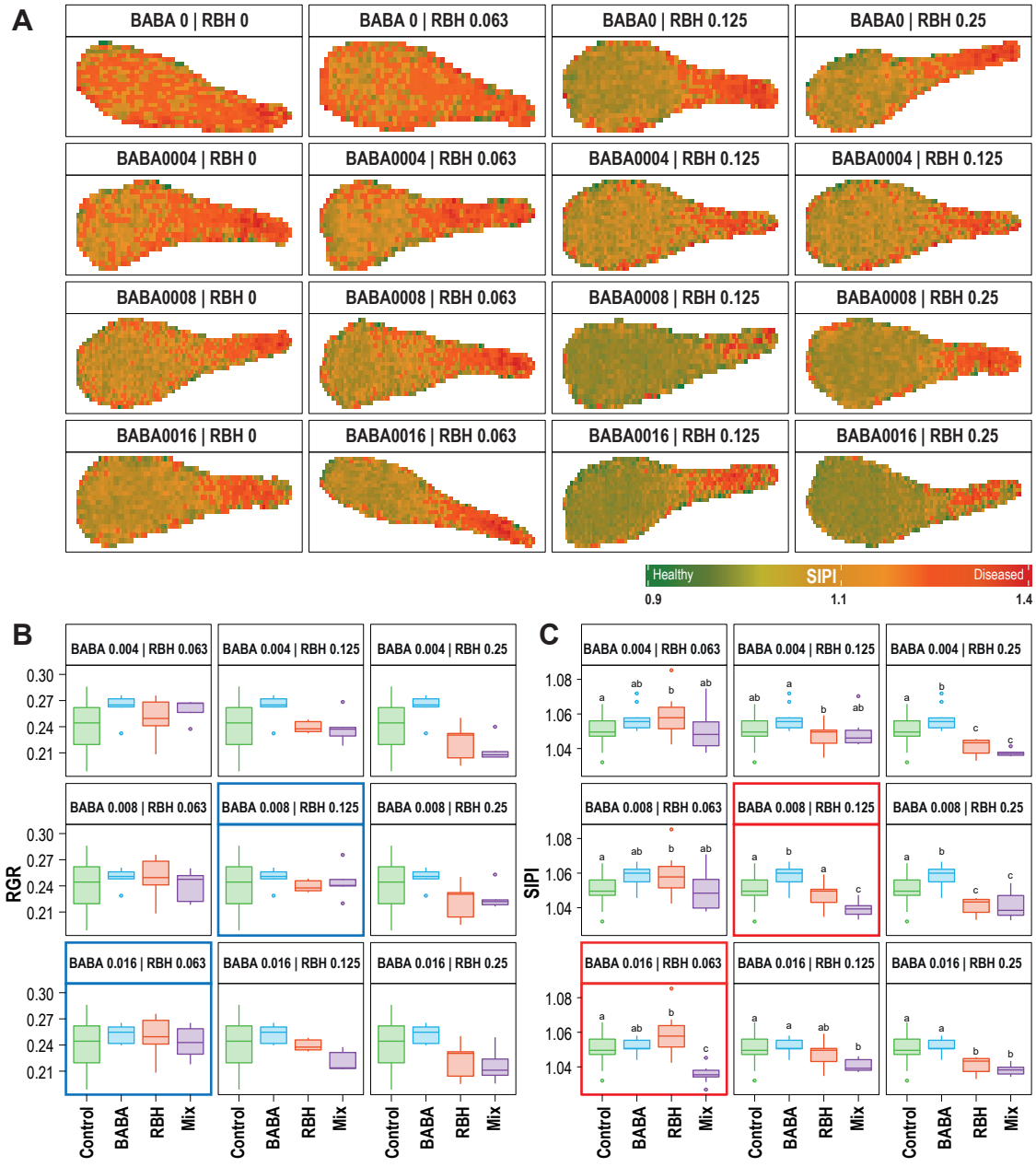

Fig 5.6 | Synergy between low doses of BABA and RBH on IR against *B. lactucae* but not on RGR. (**A**) Heat map of SIPI values in detached cotyledons indicating disease levels (low = green and high = red) for different BABA-RBH mixes. The interquartile range (IQR; box) ± 1.5xIQR (whiskers), including median (horizontal line), of the RGR and SIPI values from control, single and mixed BABA-RBH treatments RGR (**B**) and SIPI (**C**) SIPI. The effects of treatment on group means for RGR and SIPI values were tested for statistical significance by one-way ANOVA followed by Tukey posthoc tests. In each panel, different letters show significant differences among the groups ($p < 0.05$); no letters indicate lack of statistical differences between groups.

5.5 Discussion

Commercial exploitation of chemical IR agents has been hampered by undesirable side-effects on plant performance (Heil *et al.*, 2000) and sometimes variable levels of protection (Yassin *et al.*, 2021). Although the protective efficacy can be increased with dose, this often also leads to more pronounced side-effects on growth and yield (Heil and Baldwin, 2002; Walters and Heil, 2007). Combining different IR treatments are amongst the strategies that have been proposed to optimise the cost-benefit balance by IR agents. Combining IR agents with biocontrol agents (Singh *et al.*, 2019), fungicides (Baider and Cohen, 2003) and other IR agents (Walters *et al.*, 2011) have been reported to lead to improvements in the level of disease protection. Of these, the combination of different IR agents offered the benefit of reducing biocidal activity, while avoiding the challenges of implementing biocontrol procedures. To date, this approach has received limited follow-up investigation.

In this study, the effects of combining chemical IR agents was investigated with the aim to identify combinations that suppress downy mildew disease in lettuce with minimal side-effects on plant growth. Based on the toxicity profiles of BABA, RBH and ChP (section 3.3.2), and relative IR efficacies in lettuce against *B. lactucae* (section 4.3.4), a range of doses with minimal phytotoxicities had been selected. For BABA, the selected doses were 0.004, 0.008 and 0.016 mM. Although the two upper doses slightly reduced SIPI values in *B. lactucae*-inoculated plants in previous experiments (Fig 4.11), none of these doses reduced SIPI in the experiments described in this chapter and thus lacked IR efficacy (Fig 5.4). This variation between experiments further illustrates the variable performance by single IR agents, particularly when applied at lower (non-phytotoxic) doses. On the other hand, the selected doses for RBH (0.063, 0.125, and 0.25 mM) and ChP (0.125, 0.25 and 0.5 % w/v) resulted in relatively low but statistically significant dose-dependent reductions in *B. lactucae* disease (Fig 5.4). At these concentration ranges, RBH and ChP had no statistically significant impacts on growth as measured by RGR and TGI (Fig 5.2). By contrast, *B. lactucae* infection resulted in a dramatic reduction of growth, which was particularly pronounced in the absence of IR agents (Fig 5.2).

To investigate the effects of combing IR agents on growth and IR efficacy, a full-factorial design was used, in which the chemicals were combined in pairs. This design amounted to a total of 48 combinational treatments (Fig 5.1). The use of a HSI sensor enabled efficient profiling of this these treatments for growth (RGR and TGI) and disease by *B. lactucae* (SIPI). From the sensor-captured data, RGR was used as a proxy for phytotoxicity, while SIPI was used to quantify IR efficacy against *B. lactucae*. Of the three agents, ChP was the least effective against *B. lactucae* and BABA was the most effective (Chapter 4; Fig 4.10). However, the combination of the low doses of BABA-ChP did not show in any significant interaction effects. Within these combined treatments,

two-way ANCOVA revealed that ChP alleviated both growth reduction and symptoms by *B. lactucae*, whereas BABA only had a statistically significant effect on symptoms (Table 5.4 and Fig 5.5). Compared to BABA, a relatively higher RBH dose range was used, since this IR agent had lower IR efficacy against *B. lactucae* (Chapter 4; Fig 4.10). The combination of RBH-ChP did not lead to a statistically significant interaction on IR efficacy (Table 5.4), indicating that both agents acted additively on the level of IR against *B. lactucae*. By comparison, the mix of the two β-amino acids BABA and RBH was the most promising. In the absence of infection, there was no statistically significant interaction on plant growth, while in the presence of infection; both agents interacted significantly to mediate synergistic levels of disease suppression.

Further investigation of the BABA-RBH combination confirmed that the treatments of 0.008 mM BABA + 0.125 mM RBH, as well as 0.016 mM BABA + 0.063 mM RBH, resulted in high levels of disease suppression (Fig. 5.6B), even though the single treatments at these concentrations failed to induced resistance. By contrast, the same BABA-RBH dose combinations did not result in growth repression compared to un-treated control plants and the plants treated with the single doses. These results unequivocally demonstrate that the combination of low doses of BABA and RBH has a synergistic effect on IR efficacy even though it does not repress growth. Reuveni *et al.* (2001) showed that the combination of BABA and ASM had an additive level of IR efficacy against the downy mildew pathogen *Plasmopara viticola* in grapevines. Similarly, Walters *et al.* (2011) reported that BABA in combination with ASM and cis-JA improved efficacy against powdery mildew in barley compared to the agents' individual effects. The efficacy of BABA-IR depends on the stress type applied (Cohen, Vaknin and Mauch-Mani, 2016). Against *B. lactucae,* BABA-IR likely acts through a combination of callose-related cell wall defences and SA-dependent defences, as has been reported previously for the interaction between Arabidopsis and the downy mildew pathogen *H. arabidopsidis* (Ton *et al.*, 2005; Schwarzenbacher *et al.*, 2020). Compared to BABA, the IR effects of RBH have been less well characterised, but previous evidence has shown that RBH-IR against *Hpa* induces camalexin and is SA-independent (Buswell *et al.*, 2018). How, and if, low doses of BABA and RBH prime these same defence pathways in lettuce against downy mildew merits further investigation. Three way combinations using the most promosing BABA-RBH combinations with ChP doses, to investigate whether efficacy can be improved further, is worthy of investiagation as well. In the experiments described in this Chapter, the treatment efficacies were measured over relatively short time scales (ten days after application). Hence, ascertaining the durabiltiy of the synergistic IR effects is an important avenue of future research.

Although the results described in this Chapter are extremely encouraging for further development towards application in commercial lettuce protection against downy mildew, it should be noted that the choice of IR agents in the combined treatments requires careful consideration and, arguably, further investigation into the potential costs arising from increased susceptibility to

other stresses. In barley, the combined treatment of BABA, ASM and cis-JA resulted in a strong up-regulation of SA-dependent defences, which was associated with a down-regulation of JA-dependent defences (Walters *et al.*, 2011). This mix, while protecting the barley against powdery mildew, aggravated disease by against the necrotrophic fungus *Ramularia collo-cygni* infection. Although RBH has been reported to prime ET/JA-dependent defences against necrotrophic fungi in Arabidopsis, testing the combined BABA-RBH treatments against other pathogens, herbivores and abiotic stresses is an important future goal before proceeding with application. While the idea of combining IR agents has been around for a while, and the effects of a large number of IR agents have been profiled, there have been a limited number of studies. One reason for this could be that traditional profiling methods for IR agent efficacies are not suited to high throughput screening and testing. However, as demonstrated here, imaging sensor phenotyping has the potential to increase the profiling efficiency of IR agent treatments.

Chapter 6
General discussion

6.1 Optimising IR efficacy through chemical combinations

The overall aim of this research was to explore the possibility of optimising the balance between disease protection and phytotoxicity in chemical IR through a strategy of combining different IR agents. Chemical IR agents could be environmentally safe and durable addition to the available protection strategies against economically damaging crop diseases. Generally, these agents show dose dependent efficacies against a wide range of plant pathogens. However, at the higher doses that provide adequate protection, some also tend to be phytotoxic and this has hampered their full adoption. Thus, identifying IR treatments with a favourable balance between protection and toxicity could facilitate the use of IR agents as mainstream crop protection products.

Such an endeavour would involve phenotyping large number of samples. Fortunately, in recent years, the use of hyperspectral sensors has made large-scale plant phenotyping more efficient (Mahlein *et al.*, 2018). HSI is based on the principle; materials reflect electromagnetic radiation in unique patterns based on their chemical and physical properties. Accordingly, HSI is increasingly used to non-invasively phenotype plants. The use of hyperspectral phenotyping for plants has focused on three main areas. The first is phytopathology, which has benefited the most from HSI, and methods for detecting many plant diseases have been published (Mahlein *et al.*, 2018; Sarić *et al.*, 2022). A second application has been the detection and quantification of abiotic stresses such as chemical contamination (Lassalle *et al.*, 2021). A third application has focussed on measuring physiochemical parameters of plant health such as water and pigment content (Pandey *et al.*, 2017; Terentev *et al.*, 2022). In the hyperspectral phenotyping process, spatial, spectral and temporal details are captured and this usually results in large volumes of data. In such high dimensional data, in which the number of spectral features is larger than the number of observations, various approaches have been utilised to make analysis tractable. A common first step has been reducing the number of spectral bands with the derivation of SVIs, which are ratios of – usually two to four – wave bands that measure one vegetation property while reducing the impact of others (Xue and Su, 2017). SVIs are widely used in phytopathology as they allow the quantitative tracking of disease symptoms (Mahlein *et al.*, 2018). The majority of SVIs have been developed for remote sensing, occasionally new disease-specific SVIs are developed (Mahlein *et al.*, 2013). However, most of the important physiochemical characteristics of vegetation that can

be defined with SVIs have been, and new indices tend to not greatly exceed the performance of existing indices. Machine learning algorithms such as decision tree analysis, support vector machine and random forest have all been used to on both spectral band and SVIs data to detect and quantify plant diseases (Paulus and Mahlein, 2020; Sarić *et al.*, 2022) . Similarly, multivariate statistical models such as principle component analysis and the partial least squares family of models have also been useful in the analysis of highly dimensional HSI (Xie, Yang and He, 2017; Paulus and Mahlein, 2020) . In this work the use of orthogonal partial least squares discriminant analysis and decision tree analysis on SVIs data identified the index SIPI as means of tracking downy mildew stress separately from chemical stress.

With HSI as phenotyping tool, the possibility of optimising chemical IR treatments was explored using the two pathosystems: tomato- *B. cinerea* and lettuce-*B. lactucae*, and the IR agents BABA, RBH and ChP. The problem of optimising chemical IR was approached in three stages. In stage one, the dose dependent phytotoxicity of the three agents was quantified. The use of image derived growth data facilitated the measurement of relatively accurate growth rates, without the need for destructive sampling. Analysis of tomato and lettuce growth data showed that the β-amino acids BABA and RBH had-dose dependent repressive effects on RGR, while the chitin derivative ChP, had no statistically significant repressive effect (Fig 3.3). BABA was more phytotoxic than RBH (Fig 3.4), and its phytotoxicity was higher in tomato than lettuce. From previous studies, we also have a contrast of effects. BABA has been reported to be phytotoxic in Arabidopsis (Wu *et al.*, 2010), tomato (Buswell *et al.*, 2018) and lettuce (Cohen, Vaknin and Mauch-Mani, 2016), while in sunflower (Amzalek and Cohen, 2007), soybean (Zhong *et al.*, 2014) and grapevines (Reuveni, Zahavi and Cohen, 2001) it was found to lack phytotoxicity. As for RBH, while in these experiments it was phytotoxic in tomato cv. Moneymaker, but previously it was found to lack this effect in tomato cv. Micro-Tom (Buswell *et al.*, 2018). From this variation in phytotoxicity between plant species and cultivars, it can be concluded that tailored application protocols are necessary.

Following the profiling of the relative phytotoxicity of the IR agents, in Chapter 4, their relative protective activities were assessed. In tomato cv. Moneymaker, the β-amino acids BABA and RBH failed to provide protection against the necrotrophic fungus *B. cinerea* (Fig 4.1). This was unexpected as in previous studies BABA has been found to be effective in this cultivar against this pathogen (Luna *et al.*, 2016). The plants used in this study were younger than those in the Luna *et al* study. As for RBH, efficacy was reported in the Micro-Tom cultivar (Buswell *et al.*, 2018). These results suggested, in addition to species and cultivar variations in IR agent effects, there may also be plant age related variations. In contrast to the two β-amino acids, ChP was a potent inhibitor of grey mould infection in tomato and provided dose dependent protection. In lettuce, all three agents gave some level of protection against downy mildew infection (Figs 4.4 & 4.10).

However, BABA was far more potent than RBH and ChP, which had similar levels of efficacy.

Since only ChP was effective in tomato against *B. cinerea*, while all three agents showed efficacy in the lettuce against *B. lactucae*, the later was selected for stage three. Smaller doses of BABA, RBH and ChP were combined pairwise in a full factorial design to explore interactions resulting in efficacy and toxicity (Fig 5.1). This evaluation revealed, at the selected dose ranges the agents lacked toxicity (Fig 5.2). Furthermore, when combined none of the mixed pair agents interacted for increased toxicity (Table 5.1). In terms of efficacy, single doses of BABA lacked efficacy against downy mildew, while RBH and ChP had limited efficacy. When used in combination, the mixture between BABA and RBH resulted in synergism (Table 5.4), thus demonstrating the possibility of reducing phytotoxicity while increasing disease efficacy through appropriately formulated IR agent combinations.

6.2 Additional approaches that can improve chemical IR treatments

In addition to combined chemical IR treatments, various other strategies that improve the efficacy of chemical IR agents have also been reported (Fig 6.1). Approaches which range from IR chemicals in combination with plant mutualists or other protection agents to new molecule design or discovery all have individual potential and arguably can best be utilised as components of integrated pest management (IPM). In the IPM strategy, plant pests and diseases are controlled, using all available environmentally benign methods whilst minimising the applications of chemical biocides, to keep them below the economic injury level (EIL) threshold.

6.2.1 Combining biocontrol with chemical IR agents

One promising approach has been the co-treatment of IR agents with biological control agent (BCAs). The use of various *Trichoderma spp* alongside IR agents has resulted in improved disease control. The combination of *Trichoderma harzianum* UBSTH-501 and MeJA gave protection against spot blotch in wheat plants exceeding that provided by each treatment alone (Singh *et al.*, 2019). Similarly, the combination MeJA, SA and *T. harzianum* was shown to give synergistic protection in tomato against *Fusarium oxysporum* (Zehra *et al.*, 2017). In addition to improving the efficacy of IR agents, certain biocontrol organisms have the potential to mitigate the phytotoxicity often associated with the IR agents. For example MeJA which can have high phytotoxicity, when used alongside *T. harzianum* in wheat plants biomass was higher compared to untreated plants, both in the presence and absence of *Bipolaris sorokiniana* infection (Singh *et al.*, 2019).

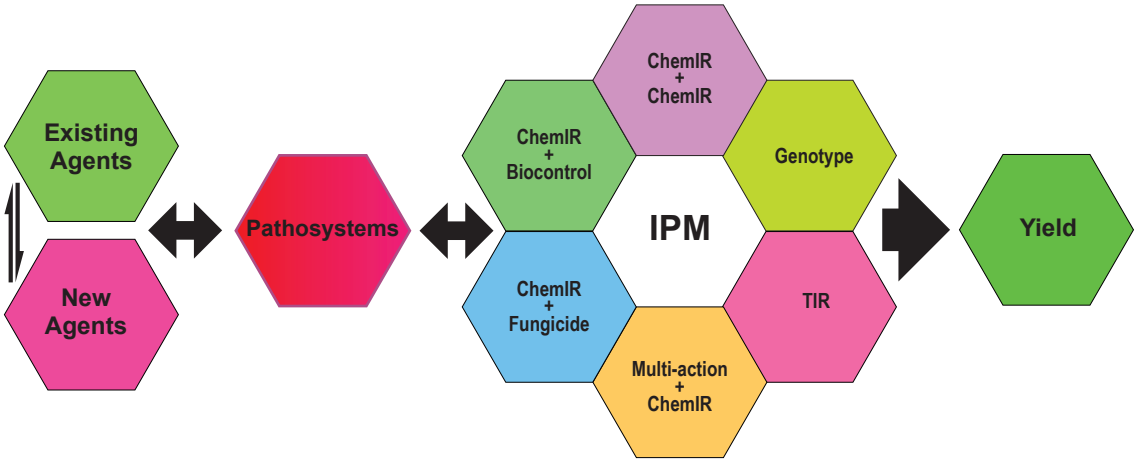

Fig 6.1 | Chemical IR as component of IPM. Existing agents or new agents developed in rational design (Chem-IR) are tested in target pathosystems until effective agent(s) are found. The efficacy can be further improved in combination with other treatments and effective strategies can be further combined. Efficacious treatments can be tested in trans-generationally-primed plants and the cycle repeated until an optimal treatment that can be integrated into an effective IPM strategy is formulated.

Although with good potential, the combining of chemical agents with BCAs must be used with caution. Given the broad-spectrum effectiveness of non-host immunity, chemical treatments intended to trigger IR responses against plant antagonists could also have deleterious effects on plant mutualists. As an example, ASM while having no direct effects on the growth of the rhizobia *Bradyrhizobium japonicum*, did trigger IR against *B. japonicum* in soybean and reduced symbiosis (Faessel *et al.*, 2010). Similarly foliar treatment of soybean with ASM led to a defence response in the plant roots which transiently decreased AMF colonisation (de Román *et al.*, 2011). Nevertheless, chemical IR treatments do not always impact plant mutualists negatively, and it seems that with some chemicals, certain doses and appropriate application methods, they can be used together without disadvantage to plant mutualists. For example, in sunflower, the effects of ASM and BABA on the downy mildew *Plasmopara helianthi* and the AMF *Glomus mosseae* differed by application method. When applied as a soil drench, the chemicals gave a 50-55% protection against the downy mildew - while ASM application decreased *G. mosseae* colonisation, BABA application did not. When applied as a foliar spray, protection increased to 80% and neither chemical impacted *G. mosseae* colonisation. *In vitro*, ASM had an inhibitory effect on *G. mosseae* germination, however BABA promoted germination (Tosi and Zazzerini, 2000). Dose has also been shown to determine toxicity toward mutualists. MeJA root application to cucumber could negatively or positively effect mycorrhizal colonisation, with higher doses reducing growth and lower doses promoting it (Toby Kiers *et al.*, 2010).

6.2.2 Combining chemical IR agents with fungicides

In addition to combing IR agents or IR agents and biocontrol, IR agent-fungicide combinations have shown a complementary potential in which the deleterious effects of both protection products can be reduced. An application of a mixture of BABA and the fungicide mancozeb was significantly more effective at controlling *Phytophthora infestans* in potato and *Pseudoperonospora cubensis* in tomato and cucumber than either BABA or mancozeb alone. The inclusion of BABA in the mancozeb fungicide synergistically increased its efficacy in plants. Application of the BABA and mancozeb mixture did not have a synergistic interaction in controlling the pathogens *in vitro*, thus demonstrating BABA-induced resistance enhanced mancozeb fungicide efficacy with lower doses required to control disease (Baider and Cohen, 2003). In potato, a combination of BABA and the fungicide Fluazinam resulted in a synergistic action against *P. infestans* and full Fluazinam activity was achieved with a 20–25% lower dose under field conditions (Liljeroth *et al.*, 2010). Likewise, ASM efficacy improved in combination with mancozeb. In chickpea plants, repeated ASM application protected against *Didymella rabiei* but also resulted in yield penalties. Instead, using a ASM-mancozeb mix, with reduced application frequency, grain yields were better than those achieved with ASM or mancozeb applications alone (Sharma *et al.*, 2011).

6.2.3 The development of improved IR molecules

Besides the use of combination strategies, other strategies to improve chemical IR have involved the identification and development or of new molecules with enhanced performance. One approach has been the identification of compounds combining biocidal and IR activity. One group of chemicals with such dual modes of action are the strobilurins. These broad-spectrum fungicides were found to also prime plant defences in the presence of disease, while improving yield in the absence of disease. In *NahG* transgenic tobacco deficient in SAR, the strobilurin Pyraclostrobin enhanced resistance to *Pseudomonas syringae* and tobacco mosaic virus (TMV) by priming *PR-1* gene activation (Beck, Oerke and Dehne, 2002; Herms *et al.*, 2002). In an effort to find other dual action compounds the agent 1-isothiocyanato-4-methylsulfinylbutane (SFN) was identified in high-throughput assaying as having dual action. SFN primed *Arabidopsis* defences against *Hyaloperonospora arabidopsidis* and also showed antimicrobial action, directly inhibiting the growth of *H. arabidopsidis* (Schillheim *et al.*, 2018).

Rational molecule design has also resulted in IR agents with improved performance. The combining various IR agents with the cholinium cation to form ionic liquids (ILs) resulted in increased efficacy and reduced phytotoxicity. BABA, ASM and INA ionically bonded to cholinium were tested on the tobacco-TMV pathosystem. ASM and INA, paired with cholinium, had improved disease resistance efficacy. BABA disease efficacy decreased slightly; however, its phytotoxicity,

along with that of ASM, drastically reduced (Schillheim *et al.*, 2018). The screening compound data bases to identify potential new IR agents has also been successful. Chang *et al.*, (2017) virtually screened the Maybridge database, a collection of over 53,000 organic compounds, using the chemical structures of ASM, MeSA and SA to identify three benzotriazole lead compounds. From one of these (L1), which had a 3D structure similar to ASM, two derivatives (3a and 4a) were potent SAR activators. Both L1-3a and 4a gave high protection in a several pathosystems including cucumber- *B. cinerea* and tomato- *P. infestans*.

In addition to screening for structural analogues of known IR molecules, using knowledge of IR receptor structure has been another approach taken to find novel IR ligands. RBH one of the agents used in this research came through such an approach. Buswell *et al.*, (2018), in an attempt to find BABA analogues that induce resistance without stunting plant growth, started with the structure of the BABA receptor IBI1 and through site-directed mutagenesis, found that an (l)-aspartic acid-binding domain was critical for BABA perception. Using ligand-interaction modelling of the binding domain they screened a library of β-amino acids and identified seven resistance-inducing compounds, of which *(R)*-β-homoserine (RBH) had the strongest activity. RBH, like BABA conferred resistance to both biotrophic and necrotrophic pathogens in taxonomically unrelated plant species but without the growth retardation associated with BABA.

6.2.4 Transgenerational IR

Besides, improvements through combination treatments and the development of more efficacious IR molecules. Long lasting transgenerational IR offers another avenue of developing improved treatments. Recently the long-lasting nature of IR has gained renewed attention in the context of epigenetic regulation. For some time it has been known that the seeds or seedlings treated with chemical IR agents develop a long-lasting priming that can be maintained for several weeks (Worrall *et al.*, 2012; Luna *et al.*, 2014). Now there is solid evidence from independent studies that priming can be transmitted epigenetically to following generations. It was reported that the progeny of BABA treated Arabidopsis displayed enhanced resistance to *H. arabidopsidis* and *Pseudomonas syringae*, which was associated with increased responsiveness to priming treatment by BABA ('primed to be primed') (Slaughter *et al.*, 2012). Barley from ASM and saccharin-treated parents exhibited enhanced resistance to infection by *R. commune* (Walters and Paterson, 2012). Also several Arabidopsis-based studies have shown that transgenerational IR relies on a complex interplay of DNA (de)methylation pathways in the plant (Luna and Ton, 2012; López Sánchez *et al.*, 2016; Stassen *et al.*, 2018; Furci *et al.*, 2019; Wilkinson *et al.*, 2019). Despite these promising new insights, the potential of IR agents to exploit transgenerational IR in the field has received limited attention. The main obstacles come from the relative weakness of transgenerational IR, as well as costs arising from increased susceptibly to other (a)biotic stresses that can occur sometimes

(Luna and Ton, 2012; López Sánchez *et al.*, 2020). A potentially more promising strategy for the exploitation of transgenerational IR comes from direct manipulation of the epigenetic makeup of the plant. Furci *et al.* (2019) identified selected hypo-methylated regions of DNA in the Arabidopsis genome, which provided near complete levels of primed resistance against downy mildew and that remained stable over at least eight generations of inbreeding.

6.3 The practicalities of using IR agents in agriculture

IR agents are not the same as conventional biocides where one product can be utilised against a range of pathogens in multiple crops. The selection of optimal IR agents in a given crop must be determined by several interconnected factors. A thorough understanding of species, cultivar and pathogen-dependent responses to chemical IR treatments is crucial to selecting pathosystem-appropriate treatments. Chemical IR agent efficacy in some instances is known to be cultivar dependent. In this research it was found RBH lacked efficacy against *B. cinerea* in tomato cv. Moneymaker, while Buswell *et al* (2018) reported good protection against the same pathogen in tomato cv. Micro Tom. Many similar reports exist in the literature. In several cultivars of spring barley induced resistance to *Rhynchosporium commune* by combined BABA, ASM and MeJA treatment resulted in infection levels that ranged from high to non-existent (Walters *et al.*, 2011). In other studies, chemical IR treatment efficacy was shown to be influenced by cultivar resistance levels. In tobacco infected with *Peronospora hyoscyami f.sp. tabacina*, ASM provided control in partially resistant cultivars, but not susceptible cultivars (Perez *et al.*, 2003). The efficacy of chemical IR agents can also depend on the identity of the attacking pathogen. In tomato, ABA application lead to antagonistic cross-talk between the ABA- and SA-responsive defense pathways, resulting in increased susceptibility to *B. cinerea* (Audenaert, De Meyer and Höfte, 2002), while in *Arabidopsis* pre-treatment with SA caused cross-talk between the SA and JA-dependent defense, causing increased susceptibility to *Alternaria brassicicola* (Spoel, Johnson and Dong, 2007). Furthermore, mixtures of chemical IR agents can have multifarious effects. There could be undesirable outcomes due to the complex cross-talk between plant defence pathways. For example there is considerable evidence that SA and JA dependent defence pathways are antagonistic (Thaler, Humphrey and Whiteman, 2012). There could also be positive effective effects. There is also evidence of the simultaneous expression of SA- and JA-mediated defences (Clarke *et al.*, 2000; Imanishi *et al.*, 2000; van Wees *et al.*, 2000; Betsuyaku *et al.*, 2018). In such mixed agent treatments, the balance between antagonism synergism could be partially dose dependent. The co-application of SA and JA in tobacco and Arabidopsis resulted in synergistic effects on the expression of SA- and JA-dependent defence genes at low concentrations, while higher concentrations of these hormones resulted in antagonism (Mur *et al.*, 2006). Together these examples demonstrate the need for careful, case-by-case selection of optimal pathosystems for the application of IR agent treatments.

With the continuing expansion of our understanding of the mechanistic basis of IR, the characterisation of the action of many chemical IR agents in many pathosystems and the availability of more effective agents, it is reasonable to hope that these agents have the potential to become widely used crop protection products. The strategies discussed here involving different IR agent, BCAs and biocide combinations can be picked and mixed to formulate efficacious treatments that can be incorporated into IPM protocols (Fig 6.1). However, IPM is applied to multiple crops with multiple pathogens, some of which are coincidental in time and/or space. Therefore, it is important to understand the principles whereby IPM components are combined and how these will impact different pathosystems. In the uncontrolled environment of the field where many abiotic and biotic stresses will trigger plant responses that can lead to complex interactions with the agents (Walters and Fountaine, 2009; Bruce, 2014; Walters *et al.*, 2014) this process can be complicated. However, in more controlled environments such as glasshouses or highly controlled vertical farming chambers, their potential is high. Under such controlled conditions, it should be possible to combine IPM measures that include chemical IR agents in a way that has outcomes that are more predictable. Also, under these controlled environments, there is a scope for formulating bespoke treatments that are highly targeted to the biotic stress vulnerabilities of the system. Furthermore, for organic growers that desire natural means of protecting produce, the exploitation of IR agents can fulfil such requirements. Indeed, interest in 'natural' protection products is growing. The global plant Biostimulants (a term used for commercial products that are marketed as stimulants of natural plant growth and/or protection) market is forecast to reach USD4.5 billion by 2027 and have an annual growth rate of 11.2% during the period 2020-2027 (Global Industry Analysts Inc, 2020). In order to provide improved products to this growing market, it is necessary to increase the translation of the growing mechanistic knowledge of IR into applied research that incorporates chemical IR into IPM. Toward that goal, an example from this research has been the identification of a formulation of the IR agents BABA and RBH that can interact synergistically to alleviate downy mildew symptoms without impacting growth, in the economically important crop of lettuce.

6.4 Future work

To further develop and exploit BABA, RBH and ChP as commercial plant protection agents, additional studies are needed. An important hurdle against adoption of these IR agents is their variable effects across pathosystems. Accordingly, further research is needed to investigate the contrasting results reported between this work and past studies. RBH, despite it being a relatively new IR agent, has already been reported to have contrasting effects in terms of phytotoxicity and efficacy against B. cinerea in the tomato cultivars Micro-Tom and Moneymaker (Buswell *et al.*, 2018; Chapter 3). Examining these parameters in other commercial tomato cultivars would be worth pursuing, which may also help genetic breeding schemes for IR efficacy and tolerance. In that regard, it is worth noting a recent publication by Tao *et al.*, (2022) describing the discovery of LHT1 as the cellular uptake transporter of BABA and RBH. This study revealed that the expression of the LHT1 gene not only determined the efficacy of the IR response to RBH and BABA, but also the phytotoxic side-effects upon chemical overstimulation with higher concentrations of both agents. Notably, while Arabidopsis wildtype plants remained tolerant to very high RBH concentrations, transgenic over-expression of LHT1 rendered this plant species sensitive to RBH-induced phytotoxicity. Hence, LHT1 acts as a master regulator of the trade-off between induced resistance by RBH or BABA and growth. Since LHT1 is a conserved amino transporter gene in plants, this study demonstrates that the trade-off between induced resistance and growth by resistance-inducing β-amino acids can be optimized by manipulating LHT1 gene expression, which offers major translational opportunities for breeding programs that aim to exploit BABA- and/or RBH-induced resistance in crops but suffer from phytotoxicity by these agents. Furthermore, the promising synergistic IR efficacy by combinations of low BABA and RBH concentrations should be expanded to other crop-downy mildew pathosystems, while the effectiveness of RBH and BABA against necrotrophic pathogens requires further evaluation. In this work, BABA, unlike multiple past studies (Luna *et al.*, 2016; Wilkinson *et al.*, 2018; Li, Sheng and Shen, 2020) was found to lack efficacy against B. cinerea in tomato, which may be due to plant genotype, age-dependent effects or a combination thereof. Thus, experiments looking into the efficacies and phytotoxicities of all three agents as function of plant genotype and plant age will yield new translatable data that can be used for better exploitation of these IR agents. Finally, exploring and optimising the application methods for these IR agents remains crucial for wider application. Further investigations of differences in the effects of agents as soil, foliar, seed coating or hydroponic growth medium would provide useful information on how best to apply them.

References

Abbas, S. *et al.* (2021) 'Characterizing and classifying urban tree species using bi-monthly terrestrial hyperspectral images in Hong Kong', *ISPRS Journal of Photogrammetry and Remote Sensing*. Elsevier, 177, pp. 204–216. doi: 10.1016/J.ISPRSJPRS.2021.05.003.

Abd El-Rahman, S. S. and Mohamed, H. I. (2014) 'Application of benzothiadiazole and Trichoderma harzianum to control faba bean chocolate spot disease and their effect on some physiological and biochemical traits', *Acta Physiologiae Plantarum*. Springer, 36(2), pp. 343–354. doi: 10.1007/s11738-013-1416-5.

Abdel-Maksoud Abada, K. (2017) 'Potentiality of Inducer Resistance Chemicals and Bioagents in Managing Lettuce Downy Mildew', *American Journal of BioScience*, 5(1). doi: 10.11648/j.ajbio.20170501.12.

Aktar, W., Sengupta, D. and Chowdhury, A. (2009) 'Impact of pesticides use in agriculture: their benefits and hazards', *Interdisciplinary Toxicology*. Slovak Toxicology Society, 2(1), p. 1. doi: 10.2478/V10102-009-0001-7.

Alexandersson, E. *et al.* (2016) 'Plant Resistance Inducers against Pathogens in Solanaceae Species-From Molecular Mechanisms to Field Application.', *International journal of molecular sciences*. Multidisciplinary Digital Publishing Institute (MDPI), 17(10). doi: 10.3390/ijms17101673.

Amzalek, E. and Cohen, Y. (2007) 'Comparative efficacy of systemic acquired resistance-inducing compounds against rust infection in sunflower plants', *Phytopathology*, 97(2). doi: 10.1094/PHYTO-97-2-0179.

Apan, A. *et al.* (2004) 'Detecting sugarcane "orange rust" disease using EO-1 Hyperion hyperspectral imagery', *International Journal of Remote Sensing*. Taylor & Francis Group , 25(2), pp. 489–498. doi: 10.1080/01431160310001618031.

Asaari, M. S. M. *et al.* (2019) 'Analysis of hyperspectral images for detection of drought stress and recovery in maize plants in a high-throughput phenotyping platform', *Computers and Electronics in Agriculture*. Elsevier, 162, pp. 749–758. doi: 10.1016/J.COMPAG.2019.05.018.

Asai, S., Shirasu, K. and Jones, J. (2015) 'Hyaloperonospora arabidopsidis (Downy Mildew) infection Assay in Arabidopsis', BIO-PROTOCOL. Bio-Protocol, LLC, 5(20). doi: 10.21769/BIOPROTOC.1627.

Asalf, B. *et al.* (2014) 'Ontogenic Resistance of Leaves and Fruit, and How Leaf Folding Influences the Distribution of Powdery Mildew on Strawberry Plants Colonized by Podosphaera aphanis', *http://dx.doi.org/10.1094/PHYTO-12-13-0345-R*. The American Phytopathological Society , 104(9), pp. 954–963. doi: 10.1094/PHYTO-12-13-0345-R.

Ashourloo, D., Mobasheri, M. R. and Huete, A. (2014) 'Developing Two Spectral Disease Indices for Detection of Wheat Leaf Rust (Pucciniatriticina)', *Remote Sensing 2014, Vol. 6, Pages 4723-4740*. Multidisciplinary Digital Publishing Institute, 6(6), pp. 4723–4740. doi: 10.3390/RS6064723.

Audenaert, K., De Meyer, G. B. and Höfte, M. M. (2002a) 'Abscisic Acid Determines Basal Susceptibility of Tomato toBotrytis cinerea and Suppresses Salicylic Acid-DependentSignaling Mechanisms', *Plant Physiology*. Oxford University Press, 128(2), p. 491. doi: 10.1104/PP.010605.

Audenaert, K., De Meyer, G. B. and Höfte, M. M. (2002b) 'Abscisic acid determines basal susceptibility of tomato to Botrytis cinerea and suppresses salicylic acid-dependent signaling mechanisms', *Plant Physiology*. American Society of Plant Biologists, 128(2), pp. 491–501. doi: 10.1104/pp.010605.

Bacete, L. *et al.* (2018) 'Plant cell wall-mediated immunity: cell wall changes trigger disease resistance responses', *The Plant Journal*. Blackwell Publishing Ltd, 93(4), pp. 614–636. doi: 10.1111/tpj.13807.

Baider, A. and Cohen, Y. (2003) 'Synergistic interaction between BABA and mancozeb in controlling Phytophthora infestans in potato and tomato and Pseudoperonospora cubensis in cucumber', *Phytoparasitica*. Priel Publishers, 31(4), pp. 399–409. doi: 10.1007/BF02979812.

Baker, N. R. (2008) 'Chlorophyll fluorescence: a probe of photosynthesis in vivo', *Annual review of plant biology*. Annu Rev Plant Biol, 59, pp. 89–113. doi: 10.1146/ANNUREV.ARPLANT.59.032607.092759.

Barzman, M. *et al.* (2015) 'Eight principles of integrated pest management', *Agronomy for Sustainable Development*. Springer-Verlag France, 35(4), pp. 1199–1215. doi: 10.1007/S13593-015-0327-9/FIGURES/8.

Baysal, Ö. *et al.* (2007) 'Enhanced systemic resistance to bacterial speck disease caused by Pseudomonas syringae pv. tomato by dl-β-aminobutyric acid under salt stress', *Physiologia Plantarum*. John Wiley & Sons, Ltd, 129(3), pp. 493–506. doi: 10.1111/J.1399-3054.2006.00818.X.

Beck, C., Oerke, E. C. and Dehne, H. W. (2002) 'Impact of strobilurins on physiology and yield formation of wheat.', *Mededelingen (Rijksuniversiteit te Gent. Fakulteit van de Landbouwkundige en Toegepaste Biologische Wetenschappen)*, 67(2).

Bektas, Y. and Eulgem, T. (2014) 'Synthetic plant defense elicitors.', *Frontiers in plant science*. Frontiers Media SA, 5, p. 804. doi: 10.3389/fpls.2014.00804.

Benhamou, N. and Bélanger, R. R. (1998a) 'Benzothiadiazole-mediated induced resistance to Fusarium oxysporum f. sp. radicis-lycopersici in tomato', *Plant Physiology*. American Society of Plant Biologists, 118(4), pp. 1203–1212. doi: 10.1104/pp.118.4.1203.

Benhamou, N. and Bélanger, R. R. (1998b) 'Induction of systemic resistance to Pythium damping-off in cucumber plants by benzothiadiazole: Ultrastructure and cytochemistry of the host response', *Plant Journal*. Plant J, 14(1), pp. 13–21. doi: 10.1046/j.1365-313X.1998.00088.x.

Berhane, T. M. *et al.* (2018) 'Decision-Tree, Rule-Based, and Random Forest Classification of High-Resolution Multispectral Imagery for Wetland Mapping and Inventory', *Remote sensing*. NIH Public Access, 10(4), p. 580. doi: 10.3390/RS10040580.

Betsuyaku, S. *et al.* (2018) 'Salicylic Acid and Jasmonic Acid Pathways are Activated in Spatially Different Domains Around the Infection Site During Effector-Triggered Immunity in Arabidopsis thaliana', *Plant and Cell Physiology*. Oxford Academic, 59(1), pp. 8–16. doi: 10.1093/pcp/pcx181.

Blackburn, G. A. (1998) 'Spectral indices for estimating photosynthetic pigment concentrations: A test using senescent tree leaves', *International Journal of Remote Sensing*. Taylor & Francis Group , 19(4), pp. 657–675. doi: 10.1080/014311698215919.

Bock, C. H. *et al.* (2010) 'Plant disease severity estimated visually, by digital photography and image analysis, and by hyperspectral imaging', *Critical Reviews in Plant Sciences*. doi: 10.1080/07352681003617285.

Bock, C. H., Chiang, K.-S. and Del Ponte, E. M. (2022) 'Plant disease severity estimated visually: a century of research, best practices, and opportunities for improving methods and practices to maximize accuracy', *Tropical Plant Pathology*. Springer Science and Business Media LLC, 47(1), pp. 25–42. doi: 10.1007/S40858-021-00439-Z/TABLES/3.

Bomblies, K. and Weigel, D. (2007) 'Hybrid necrosis: autoimmunity as a potential gene-flow barrier in plant species', *Nature Reviews Genetics 2007 8:5*. Nature Publishing Group, 8(5), pp. 382–393. doi: 10.1038/nrg2082.

Boochs, F. *et al.* (1990) 'Shape of the red edge as vitality indicator for plants', *International Journal of Remote Sensing*. Taylor & Francis Group, 11(10), pp. 1741–1753. doi: 10.1080/01431169008955127.

Broge, N. H. and Leblanc, E. (2001) 'Comparing prediction power and stability of broadband and hyperspectral vegetation indices for estimation of green leaf area index and canopy chlorophyll density', *Remote Sensing of Environment*. Elsevier, 76(2), pp. 156–172. doi: 10.1016/S0034-4257(00)00197-8.

Brown, J. K. M. (2002) 'Yield penalties of disease resistance in crops', *Current Opinion in Plant Biology*. Elsevier Current Trends, 5(4), pp. 339–344. doi: 10.1016/S1369-5266(02)00270-4.

Brown, S. *et al.* (2007) 'Insensitivity to the Fungicide Fosetyl-Aluminum in California Isolates of the Lettuce Downy Mildew Pathogen, Bremia lactucae', *https://doi.org/10.1094/PDIS.2004.88.5.502*. The American Phytopathological Society , 88(5), pp. 502–508. doi: 10.1094/PDIS.2004.88.5.502.

Bruce, T. J. A. (2014) 'Variation in plant responsiveness to defense elicitors caused by genotype and environment', *Frontiers in Plant Science*. Frontiers Research Foundation, 5(JUL). doi: 10.3389/fpls.2014.00349.

Buswell, W. *et al.* (2018) 'Chemical priming of immunity without costs to plant growth', *New Phytologist*, 218(3), pp. 1205–1216. doi: 10.1111/nph.15062.

Bylesjö, M. *et al.* (2006) 'OPLS discriminant analysis: combining the strengths of PLS-DA and SIMCA classification', *Journal of Chemometrics*. John Wiley & Sons, Ltd, 20(8–10), pp. 341–351. doi: 10.1002/CEM.1006.

Cao, X. *et al.* (2015) 'Detection of powdery mildew in two winter wheat plant densities and prediction of grain yield using canopy hyperspectral reflectance', *PloS one*. PLoS One, 10(3). doi: 10.1371/JOURNAL.PONE.0121462.

Carter, G. A. (1994) 'Ratios of leaf reflectance in narrow wavebands as indicator of plant stress. International Journal of Remote Sensing', *Int.J.Remote Sens.*, 15(3).

Černý, M. *et al.* (2018) 'Hydrogen Peroxide: Its Role in Plant Biology and Crosstalk with Signalling Networks', *International Journal of Molecular Sciences*. Multidisciplinary Digital Publishing Institute (MDPI), 19(9). doi: 10.3390/IJMS19092812.

Chang, K. *et al.* (2017) 'The discovery of new scaffold of plant activators: From salicylic acid to benzotriazole', *Chinese Chemical Letters*. Elsevier B.V., 28(4), pp. 919–926. doi: 10.1016/j.cclet.2017.02.004.

Chappelle, E. W., Kim, M. S. and McMurtrey, J. E. (1992) 'Ratio analysis of reflectance spectra (RARS): An algorithm for the remote estimation of the concentrations of chlorophyll A, chlorophyll B, and carotenoids in soybean leaves', *Remote Sensing of Environment*. Elsevier, 39(3), pp. 239–247. doi: 10.1016/0034-4257(92)90089-3.

Chen, J. M. (1996) 'Evaluation of Vegetation Indices and a Modified Simple Ratio for Boreal Applications', *Canadian Journal of Remote Sensing*. Taylor & Francis, 22(3), pp. 229–242. doi: 10.1080/07038992.1996.10855178.

Chen, J. M. and Cihlar, J. (1996) 'Retrieving leaf area index of boreal conifer forests using Landsat TM images', *Remote Sensing of Environment*. Elsevier, 55(2), pp. 153–162. doi: 10.1016/0034-4257(95)00195-6.

Cho, M. A. and Skidmore, A. K. (2006) 'A new technique for extracting the red edge position from hyperspectral data: The linear extrapolation method', *Remote Sensing of Environment*. Elsevier, 101(2), pp. 181–193. doi: 10.1016/J.RSE.2005.12.011.

Clarke, J. D. *et al.* (2000) 'Roles of salicylic acid, jasmonic acid, and ethylene in cpr-Induced resistance in arabidopsis', *Plant Cell*. Plant Cell, 12(11), pp. 2175–2190. doi: 10.1105/tpc.12.11.2175.

Cohen, Y. (1994) '3-Aminobutyric acid induces systemic resistance against peronospore tabacina', *Physiological and Molecular Plant Pathology*. Academic Press, 44(4), pp. 273–288. doi: 10.1016/S0885-5765(05)80030-X.

Cohen, Y., Rubin, A. E. and Kilfin, G. (2010) 'Mechanisms of induced resistance in lettuce against Bremia lactucae by DL-β-amino-butyric acid (BABA)', *European Journal of Plant Pathology*. Springer, 126(4), pp. 553–573. doi: 10.1007/S10658-009-9564-6/FIGURES/12.

Cohen, Y., Rubin, A. E. and Vaknin, M. (2011) 'Post infection application of DL-3-amino-butyric acid (BABA) induces multiple forms of resistance against Bremia lactucae in lettuce', *European Journal of Plant Pathology*. Springer, 130(1), pp. 13–27. doi: 10.1007/S10658-010-9724-8/FIGURES/7.

Cohen, Y., Vaknin, M. and Mauch-Mani, B. (2016) 'BABA-induced resistance: milestones along a 55-year journey', *Phytoparasitica*. Springer Netherlands, 44(4), pp. 513–538. doi: 10.1007/s12600-016-0546-x.

Conrath, U. *et al.* (2006) 'Priming: Getting Ready for Battle', *Molecular Plant-Microbe Interactions*, 19(10), pp. 1062–1071. doi: 10.1094/MPMI-19-1062.

Cook, R. J. (2000) 'Advances in Plant Health Management in the Twentieth Century', *Annual Review of Phytopathology*. Annual Reviews, 38(1), pp. 95–116. doi: 10.1146/annurev.phyto.38.1.95.

Couto, D. and Zipfel, C. (2016) 'Regulation of pattern recognition receptor signalling in plants', *Nature Reviews Immunology*. Nature Publishing Group, 16(9), pp. 537–552. doi: 10.1038/nri.2016.77.

Créte, R. *et al.* (2020) 'Rotating and stacking genes can improve crop resistance durability while potentially selecting highly virulent pathogen strains', *Scientific Reports 2020 10:1*. Nature Publishing Group, 10(1), pp. 1–17. doi: 10.1038/s41598-020-76788-7.

Crute, I. R. and Harrison, J. M. (1988) 'Studies on the inheritance of resistance to metalaxyl in Bremia lactucae and on the stability and fitness of field isolates', *Plant Pathology*. John Wiley & Sons, Ltd, 37(2), pp. 231–250. doi: 10.1111/J.1365-3059.1988.TB02069.X.

Cui, H., Tsuda, K. and Parker, J. E. (2015) 'Effector-triggered immunity: From pathogen perception to robust defense', *Annual Review of Plant Biology*. Annual Reviews Inc., 66, pp. 487–511. doi: 10.1146/annurev-arplant-050213-040012.

Dash, J. and Curran, P. J. (2004) 'The MERIS terrestrial chlorophyll index', International Journal of Remote Sensing. Taylor and Francis Ltd., 25(23), pp. 5403–5413. doi: 10.1080/0143116042000274015.

Dann, E. *et al.* (1998) 'Effect of treating soybean with 2,6-dichloroisonicotinic acid (INA) and benzothiadiazole (BTH) on seed yields and the level of disease caused by Sclerotinia sclerotiorum in field and greenhouse studies', *European Journal of Plant Pathology*. Springer, 104(3), pp. 271–278. doi: 10.1023/A:1008683316629.

Datt, B. (1998) 'Remote Sensing of Chlorophyll a, Chlorophyll b, Chlorophyll a+b, and Total Carotenoid Content in Eucalyptus Leaves', *Remote Sensing of Environment*. Elsevier, 66(2), pp. 111–121. doi: 10.1016/S0034-4257(98)00046-7.

Datt, B. (1999) 'Visible/near infrared reflectance and chlorophyll content in eucalyptus leaves', *International Journal of Remote Sensing*, 20(14), pp. 2741–2759. doi: 10.1080/014311699211778.

Daughtry, C. S. T. *et al.* (2000) 'Estimating Corn Leaf Chlorophyll Concentration from Leaf and Canopy Reflectance', *Remote Sensing of Environment*. Elsevier, 74(2), pp. 229–239. doi: 10.1016/S0034-4257(00)00113-9.

Deising, H. B., Reimann, S. and Pascholati, S. F. (2008) 'Mechanisms and significance of fungicide resistance', *Brazilian Journal of Microbiology*. Brazilian Society of Microbiology, 39(2), p. 286. doi: 10.1590/S1517-838220080002000017.

Délano-Frier, J. P. *et al.* (2004) 'The effect of exogenous jasmonic acid on induced resistance and productivity in amaranth (Amaranthus hypochondriacus) is influenced by environmental conditions', *Journal of Chemical Ecology*. J Chem Ecol, 30(5), pp. 1001–1034. doi: 10.1023/B:JOEC.0000028464.36353.bb.

Dhondt, S., Wuyts, N. and Inzé, D. (2013) 'Cell to whole-plant phenotyping: the best is yet to come', *Trends in plant science*. Trends Plant Sci, 18(8), pp. 428–439. doi: 10.1016/J.TPLANTS.2013.04.008.

Dietrich, R., Ploss, K. and Heil, M. (2005) 'Growth responses and fitness costs after induction of pathogen resistance depend on environmental conditions', *Plant, Cell and Environment*. John Wiley & Sons, Ltd, 28(2), pp. 211–222. doi: 10.1111/j.1365-3040.2004.01265.x.

Douma, J. C. *et al.* (2017) 'When does it pay off to prime for defense? A modeling analysis', *New Phytologist*. Blackwell Publishing Ltd, 216(3), pp. 782–797. doi: 10.1111/nph.14771.

Dubreuil-Maurizi, C. *et al.* (2010) 'β-Aminobutyric Acid Primes an NADPH Oxidase–Dependent Reactive Oxygen Species Production During Grapevine-Triggered Immunity', *http://dx.doi.org/10.1094/MPMI-23-8-1012*. The American Phytopathological Society , 23(8), pp. 1012–1021. doi: 10.1094/MPMI-23-8-1012.

Elieh-Ali-Komi, D., Hamblin, M. R. and Daniel, E.-A.-K. (2016) 'Chitin and Chitosan: Production and Application of Versatile Biomedical Nanomaterials', *International journal of advanced research*. NIH Public Access, 4(3), p. 411. Available at: /pmc/articles/PMC5094803/ (Accessed: 15 March 2022).

Elvidge, C. D. and Chen, Z. (1995) 'Comparison of broad-band and narrow-band red and near-infrared vegetation indices', *Remote Sensing of Environment*. Elsevier, 54(1), pp. 38–48. doi: 10.1016/0034-4257(95)00132-K.

EPPO (2014) 'PP 1/135 (4) phytotoxicity assessment', *EPPO Bulletin*, 44(3). doi: 10.1111/epp.12134.

Faessel, L. *et al.* (2010) 'Chemically-induced resistance on soybean inhibits nodulation and mycorrhization', *Plant and Soil*. Springer, 329(1), pp. 259–268. doi: 10.1007/s11104-009-0150-7.

Fahrentrapp, J. *et al.* (2019) 'Detection of gray mold leaf infections prior to visual symptom appearance using a five-band multispectral sensor', *Frontiers in Plant Science*. Frontiers Media S.A., 10, p. 628. doi: 10.3389/FPLS.2019.00628/BIBTEX.

Fall, M. L. *et al.* (2015) 'Bremia lactucae infection efficiency in lettuce is modulated by temperature and leaf wetness duration under Quebec field conditions', *Plant Disease*. American Phytopathological Society, 99(7), pp. 1010–1019. doi: 10.1094/PDIS-05-14-0548-RE/ASSET/IMAGES/LARGE/PDIS-05-14-0548-RE_F9.JPEG.

Fall, M. L., Van Der Heyden, H. and Carisse, O. (2016) 'A Quantitative Dynamic Simulation of Bremia lactucae Airborne Conidia Concentration above a Lettuce Canopy', *PloS one*. PLoS One, 11(3). doi: 10.1371/JOURNAL.PONE.0144573.

Fang, Y. and Ramasamy, R. P. (2015) 'Current and Prospective Methods for Plant Disease Detection.', *Biosensors*. Multidisciplinary Digital Publishing Institute (MDPI), 5(3), pp. 537–61. doi: 10.3390/bios5030537.

FAO (2021a) *International Year of Plant Health – Final report*, *International Year of Plant Health – Final report*. FAO. doi: 10.4060/CB7056EN.

FAO (2021b) *The State of Food Security and Nutrition in the World 2021*, *The State of Food Security and Nutrition in the World 2021*. FAO, IFAD, UNICEF, WFP and WHO. doi: 10.4060/CB4474EN.

Farmer, E. E. and Ryan, C. A. (1992) 'Octadecanoid Precursors of Jasmonic Acid Activate the Synthesis of Wound-Inducible Proteinase Inhibitors.', *The Plant Cell*. Oxford University Press (OUP), 4(2), pp. 129–134. doi: 10.1105/tpc.4.2.129.

Fernández-Bautista, N. *et al.* (2016) 'Plant Tissue Trypan Blue Staining During Phytopathogen Infection', *BIO-PROTOCOL*, 6(24). doi: 10.21769/bioprotoc.2078.

Filella, I. *et al.* (1996) 'Relationship between photosynthetic radiation-use efficiency of barley canopies and the photochemical reflectance index (PRI)', *Physiologia Plantarum*. John Wiley & Sons, Ltd, 96(2), pp. 211–216. doi: 10.1111/J.1399-3054.1996.TB00204.X.

Filella, I. and Peñuelas, J. (1994) 'The red edge position and shape as indicators of plant chlorophyll content, biomass and hydric status.', *International Journal of Remote Sensing*. Taylor & Francis Group , 15(7), pp. 1459–1470. doi: 10.1080/01431169408954177.

Fletcher, K. *et al.* (2019) 'Genomic signatures of heterokaryosis in the oomycete pathogen Bremia lactucae', *Nature Communications 2019 10:1*. Nature Publishing Group, 10(1), pp. 1–13. doi: 10.1038/s41467-019-10550-0.

Flors, V. *et al.* (2008) 'Interplay between JA, SA and ABA signalling during basal and induced resistance against Pseudomonas syringae and Alternaria brassicicola', *The Plant journal : for cell and molecular biology*. Plant J, 54(1), pp. 81–92. doi: 10.1111/J.1365-313X.2007.03397.X.

Furci, L. *et al.* (2019) 'Identification and characterisation of hypomethylated DNA loci controlling quantitative resistance in Arabidopsis', *eLife*. NLM (Medline), 8. doi: 10.7554/eLife.40655.

Gamon, J. A., Serrano, L. and Surfus, J. S. (1997) 'The photochemical reflectance index: an optical indicator of photosynthetic radiation use efficiency across species, functional types, and nutrient levels', *Oecologia 1997 112:4*. Springer, 112(4), pp. 492–501. doi: 10.1007/S004420050337.

Gandia, S. *et al.* (2004) 'Retrieval of vegetation biophysical variables from CHRIS/PROBA data in the SPARC campaign', *earth.esa.int*. Available at: https://earth.esa.int/workshops/chris_proba_04/papers/12_Gandia.pdf (Accessed: 21 March 2022).

García-Arenal, F. and McDonald, B. A. (2003) 'An Analysis of the Durability of Resistance to Plant Viruses', *Phytopathology*. The American Phytopathological Society , 93(8), pp. 941–952. doi: 10.1094/PHYTO.2003.93.8.941.

Garrity, S. R., Eitel, J. U. H. and Vierling, L. A. (2011) 'Disentangling the relationships between plant pigments and the photochemical reflectance index reveals a new approach for remote estimation of carotenoid content', *Remote Sensing of Environment*. Elsevier, 115(2), pp. 628–635. doi: 10.1016/J.RSE.2010.10.007.

Geisler, M. J. and Sack, F. D. (2002) 'Variable timing of developmental progression in the stomatal pathway in Arabidopsis cotyledons', *New Phytologist*. John Wiley & Sons, Ltd, 153(3), pp. 469–476. doi: 10.1046/J.0028-646X.2001.00332.X.

Gitelson, A. A. *et al.* (2002) 'Assessing Carotenoid Content in Plant Leaves with Reflectance Spectroscopy¶', *Photochemistry and Photobiology*. John Wiley & Sons, Ltd, 75(3), pp. 272–281. doi: 10.1562/0031-8655(2002)0750272ACCIPL2.0.CO2.

Gitelson, A. A., Buschmann, C. and Lichtenthaler, H. K. (1999) 'The Chlorophyll Fluorescence Ratio F735/F700 as an Accurate Measure of the Chlorophyll Content in Plants', *Remote Sensing of Environment*. Elsevier, 69(3), pp. 296–302. doi: 10.1016/S0034-4257(99)00023-1.

Gitelson, A. A., Gritz, Y. and Merzlyak, M. N. (2003) 'Relationships between leaf chlorophyll content and spectral reflectance and algorithms for non-destructive chlorophyll assessment in higher plant leaves', *Journal of Plant Physiology*. Urban & Fischer, 160(3), pp. 271–282. doi: 10.1078/0176-1617-00887.

Gitelson, A. A., Kaufman, Y. J. and Merzlyak, M. N. (1996) 'Use of a green channel in remote sensing of global vegetation from EOS-MODIS', *Remote Sensing of Environment*. Elsevier, 58(3), pp. 289–298. doi: 10.1016/S0034-4257(96)00072-7.

Gitelson, A. A. and Merzlyak, M. N. (1998) 'Remote sensing of chlorophyll concentration in higher plant leaves', *Advances in Space Research*. Pergamon, 22(5), pp. 689–692. doi: 10.1016/S0273-1177(97)01133-2.

Gitelson, Anatoly A., Merzlyak, M. N. and Chivkunova, O. B. (2001) 'Optical Properties and Nondestructive Estimation of Anthocyanin Content in Plant Leaves¶', *Photochemistry and Photobiology*. John Wiley & Sons, Ltd, 74(1), pp. 38–45. doi: 10.1562/0031-8655(2001)0740038OPANEO2.0.CO2.

Gitelson, A. and Merzlyak, M. N. (1994) 'Quantitative estimation of chlorophyll-a using reflectance spectra: Experiments with autumn chestnut and maple leaves', *Journal of Photochemistry and Photobiology B: Biology*. Elsevier, 22(3), pp. 247–252. doi: 10.1016/1011-1344(93)06963-4.

Global Industry Analysts Inc (2020) *Plant Biostimulants - Global Market Trajectory & Analytics*. Available at: https://www.strategyr.com/market-report-plant-biostimulant-forecasts-global-industry-analysts-inc.asp.

Godard, J. F. *et al.* (1999) 'Benzothiadiazole (BTH) induces resistance in cauliflower (Brassica oleracea var botrytis) to downy mildew of crucifers caused by Peronospora parasitica', *Crop Protection*. Elsevier, 18(6), pp. 397–405. doi: 10.1016/S0261-2194(99)00040-X.

Görlach, J. *et al.* (1996) 'Benzothiadiazole, a novel class of inducers of systemic acquired resistance, activates gene expression and disease resistance in wheat', *Plant Cell*. American Society of Plant Biologists, 8(4), pp. 629–643. doi: 10.1105/tpc.8.4.629.

Govender, M., Chetty, K. and Bulcock, H. (2007) 'A review of hyperspectral remote sensing and its application in vegetation and water resource studies', *Water SA*. doi: 10.4314/wsa.v33i2.49049.

Guyot, G. and Baret, F. (1988) 'Utilisation de la haute resolution spectrale pour suivre l'etat des couverts vegetaux', *Journal of Chemical Information and Modeling*, 53(9).

Haboudane, D. *et al.* (2002) 'Integrated narrow-band vegetation indices for prediction of crop chlorophyll content for application to precision agriculture', *Remote Sensing of Environment*. Elsevier, 81(2–3), pp. 416–426. doi: 10.1016/S0034-4257(02)00018-4.

Haboudane, D. *et al.* (2004) 'Hyperspectral vegetation indices and novel algorithms for predicting green LAI of crop canopies: Modeling and validation in the context of precision agriculture', *Remote Sensing of Environment*. Elsevier, 90(3), pp. 337–352. doi: 10.1016/J.RSE.2003.12.013.

Hadrami, A. El *et al.* (2010) 'Chitosan in Plant Protection', *Marine Drugs*. Multidisciplinary Digital Publishing Institute (MDPI), 8(4), p. 968. doi: 10.3390/MD8040968.

Harris Geospatial (2022) *Alphabetical List of Spectral Indices*. Available at: https://www.l3harrisgeospatial.com/docs/alphabeticallistspectralindices.html (Accessed: 24 March 2022).

Heil, M. *et al.* (2000) 'Reduced growth and seed set following chemical induction of pathogen defence: Does systemic acquired resistance (SAR) incur allocation costs?', *Journal of Ecology*. John Wiley & Sons, Ltd, 88(4), pp. 645–654. doi: 10.1046/j.1365-2745.2000.00479.x.

Heil, M. and Baldwin, I. T. (2002) 'Fitness costs of induced resistance: Emerging experimental support for a slippery concept', *Trends in Plant Science*. Trends Plant Sci, pp. 61–67. doi: 10.1016/S1360-1385(01)02186-0.

Heil, M. and Ton, J. (2008) 'Long-distance signalling in plant defence', Trends in plant science. Trends Plant Sci, 13(6), pp. 264–272. doi: 10.1016/J.TPLANTS.2008.03.005.

Herms, S. *et al.* (2002) 'A strobilurin fungicide enhances the resistance of tobacco against tobacco mosaic virus and Pseudomonas syringae pv tabaci', *Plant Physiology*. American Society of Plant Biologists, 130(1), pp. 120–127. doi: 10.1104/pp.004432.

Hernández-Clemente, R. *et al.* (2011) 'Assessing structural effects on PRI for stress detection in conifer forests', *Remote Sensing of Environment*. Elsevier, 115(9), pp. 2360–2375. doi: 10.1016/J.RSE.2011.04.036.

Hernández-Clemente, R., Navarro-Cerrillo, R. M. and Zarco-Tejada, P. J. (2012) 'Carotenoid content estimation in a heterogeneous conifer forest using narrow-band indices and PROSPECT+DART simulations', *Remote Sensing of Environment*, 127, pp. 298–315. doi: 10.1016/J.RSE.2012.09.014.

Hijwegen, T. and Verhaar, M. A. (1995) 'Effects of cucumber genotype on the induction of resistance to powdery mildew, Sphaerotheca fuliginea, by 2, 6-dichloroisonicotinic acid', *Plant Pathology*. John Wiley & Sons, Ltd, 44(4), pp. 756–762. doi: 10.1111/j.1365-3059.1995.tb01700.x.

Holz, G., Coertze, S. and Williamson, B. (2007) 'The ecology of botrytis on plant surfaces', in *Botrytis: Biology, Pathology and Control*. doi: 10.1007/978-1-4020-2626-3_2.

Hong, E. P. and Park, J. W. (2012) 'Sample Size and Statistical Power Calculation in Genetic Association Studies', *Genomics & Informatics*. Korea Genome Organization, 10(2), p. 117. doi: 10.5808/GI.2012.10.2.117.

Hu, L. and Yang, L. (2019) 'Time to fight: Molecular mechanisms of age-related resistance', *Phytopathology*. American Phytopathological Society, 109(9), pp. 1500–1508. doi: 10.1094/PHYTO-11-18-0443-RVW/ASSET/IMAGES/LARGE/PHYTO-11-18-0443-RVW_F3.JPEG.

Huete, A. R. (1988) 'A soil-adjusted vegetation index (SAVI)', *Remote Sensing of Environment*. Elsevier, 25(3), pp. 295–309. doi: 10.1016/0034-4257(88)90106-X.

Huete, A. R. *et al.* (1997) 'A comparison of vegetation indices over a global set of TM images for EOS-MODIS', *Remote Sensing of Environment*. Elsevier, 59(3), pp. 440–451. doi: 10.1016/S0034-4257(96)00112-5.

van Hulten, M. *et al.* (2006) 'Costs and benefits of priming for defense in Arabidopsis', *Proceedings of the National Academy of Sciences*, 103(14), pp. 5602–5607. doi: 10.1073/pnas.0510213103.

Humplík, J. F. *et al.* (2015) 'Automated phenotyping of plant shoots using imaging methods for analysis of plant stress responses - a review.', *Plant methods*. BioMed Central, 11, p. 29. doi: 10.1186/s13007-015-0072-8.

Hunt, E. R. *et al.* (2013) 'A visible band index for remote sensing leaf chlorophyll content at the canopy scale', *International Journal of Applied Earth Observation and Geoinformation*. Elsevier, 21(1), pp. 103–112. doi: 10.1016/J.JAG.2012.07.020.

Hunter, M. C. *et al.* (2017) 'Agriculture in 2050: Recalibrating Targets for Sustainable Intensification', *BioScience*. Oxford Academic, 67(4), pp. 386–391. doi: 10.1093/BIOSCI/BIX010.

Ibrahim, M. *et al.* (2019) 'Decision Tree Pattern Recognition Model for Radio Frequency Interference Suppression in NQR Experiments', *Sensors (Basel, Switzerland)*. Multidisciplinary Digital Publishing Institute (MDPI), 19(14). doi: 10.3390/S19143153.

ICG (2021) *10 Conflicts to Watch in 2022*. Available at: https://www.crisisgroup.org/global/10-conflicts-watch-2022 (Accessed: 15 March 2022).

IEA (2021) *Global Energy Review*. Available at: https://www.iea.org/reports/global-energy-review-2021 (Accessed: 15 March 2022).

Imanishi, S. *et al.* (2000) 'Aspirin and salicylic acid do not inhibit methyl jasmonate-inducible expression of a gene for ornithine decarboxylase in tobacco BY-2 cells', *Bioscience, Biotechnology and Biochemistry*. Japan Society for Bioscience Biotechnology and Agrochemistry, 64(1), pp. 125–133. doi: 10.1271/bbb.64.125.

Ishii, H. (2006) 'Impact of Fungicide Resistance in Plant Pathogens on Crop Disease Control and Agricultural Environment', *Japan Agricultural Research Quarterly: JARQ*. Japan International Research Center for Agricultural Sciences, 40(3), pp. 205–211. doi: 10.6090/JARQ.40.205.

Jakab, G. *et al.* (2001) 'β-aminobutyric acid-induced resistance in plants', *European Journal of Plant Pathology*, 107(1), pp. 29–37. doi: 10.1023/A:1008730721037.

Jollife, I. T. and Cadima, J. (2016) 'Principal component analysis: a review and recent developments', *Philosophical Transactions of the Royal Society A: Mathematical, Physical and Engineering Sciences*. The Royal Society Publishing, 374(2065). doi: 10.1098/RSTA.2015.0202.

Jones, J. D. G. and Dangl, J. L. (2006) 'The plant immune system', *Nature*. Nature Publishing Group, 444(7117), pp. 323–329. doi: 10.1038/nature05286.

de Jong, H. *et al.* (2019) 'Integrated use of aureobasidium pullulans strain CG163 and acibenzolar-S-methyl for management of bacterial canker in kiwifruit', *Plants*. MDPI AG, 8(8). doi: 10.3390/plants8080287.

Jordan, C. F. (1969) 'Derivation of Leaf-Area Index from Quality of Light on the Forest Floor', *Ecology*. Wiley, 50(4), pp. 663–666. doi: 10.2307/1936256.

Justyna, P. G. and Ewa, K. (2013) 'Induction of resistance against pathogens by β-aminobutyric acid', *Acta Physiologiae Plantarum*. Springer, 35(6), pp. 1735–1748. doi: 10.1007/S11738-013-1215-Z/FIGURES/3.

van Kan, J. A. L. *et al.* (1997) 'Cutinase A of *Botrytis cinerea* is Expressed, but not Essential, During Penetration of Gerbera and Tomato', *Molecular Plant-Microbe Interactions*, 10(1), pp. 30–38. doi: 10.1094/MPMI.1997.10.1.30.

Kauss, H., Jeblick, W. and Domard, A. (1989) 'The degrees of polymerization and N-acetylation of chitosan determine its ability to elicit callose formation in suspension cells and protoplasts of Catharanthus roseus', *Planta 1989 178:3*. Springer, 178(3), pp. 385–392. doi: 10.1007/BF00391866.

Kim, M. S. (1994) 'The use of narrow spectral bands for improving remote sensing estimations of fractionally absorbed photosynthetically active radiation (fapar)', *Master thesis, University of Maryland*.

Knoth, C. *et al.* (2009) 'The synthetic elicitor 3,5-dichloroanthranilic acid induces NPR1-dependent and npr1-independent mechanisms of disease resistance in arabidopsis', *Plant Physiology*. American Society of Plant Biologists, 150(1), pp. 333–347. doi: 10.1104/pp.108.133678.

Koeck, M., Hardham, A. R. and Dodds, P. N. (2011) 'The role of effectors of biotrophic and hemibiotrophic fungi in infection', *Cellular microbiology*. NIH Public Access, 13(12), p. 1849. doi: 10.1111/J.1462-5822.2011.01665.X.

Kogel, K. H. *et al.* (1994) 'Acquired resistance in barley. The resistance mechanism induced by 2, 6-dichloroisonicotinic acid is a phenocopy of a genetically based mechanism governing race-specific powdery mildew resistance', *Plant Physiology*. American Society of Plant Biologists, 106(4), pp. 1269–1277. doi: 10.1104/pp.106.4.1269.

Koornneef, A. and Pieterse, C. M. J. (2008) 'Cross Talk in Defense Signaling', *Plant Physiology*. Oxford Academic, 146(3), pp. 839–844. doi: 10.1104/PP.107.112029.

Kuźniak, E. and Kopczewski, T. (2020) 'The Chloroplast Reactive Oxygen Species-Redox System in Plant Immunity and Disease', *Frontiers in Plant Science*. Frontiers Media S.A., p. 12. doi: 10.3389/fpls.2020.572686.

Lassalle, G. *et al.* (2021) 'Mapping leaf metal content over industrial brownfields using airborne hyperspectral imaging and optimized vegetation indices', *Scientific Reports 2021 11:1*. Nature Publishing Group, 11(1), pp. 1–13. doi: 10.1038/s41598-020-79439-z.

Lechenet, M. *et al.* (2017) 'Reducing pesticide use while preserving crop productivity and profitability on arable farms', *Nature Plants 2017 3:3*. Nature Publishing Group, 3(3), pp. 1–6. doi: 10.1038/nplants.2017.8.

Lehnert, L. W. *et al.* (2019) 'Hyperspectral data analysis in R: The hsdar package', *Journal of Statistical Software*. American Statistical Association, 89. doi: 10.18637/JSS.V089.I12.

Lehnert, L. W. (2022) '"hsdar" - Manage, Analyse and Simulate Hyperspectral Data'. Available at: https://cran.r-project.org/web/packages/hsdar/hsdar.pdf (Accessed: 24 March 2022).

Li, R., Sheng, J. and Shen, L. (2020) 'Nitric oxide plays an important role in β-aminobutyric acid-induced resistance to botrytis cinerea in tomato plants', *Plant Pathology Journal*, 36(2). doi: 10.5423/PPJ.OA.11.2019.0274.

Li, X. *et al.* (2015) 'A hyperspectral index sensitive to subtle changes in the canopy chlorophyll content under arsenic stress', *International Journal of Applied Earth Observation and Geoinformation*. Elsevier, 36, pp. 41–53. doi: 10.1016/J.JAG.2014.10.017.

Lichtenthaler, H. K. *et al.* (1996) 'Detection of Vegetation Stress Via a New High Resolution Fluorescence Imaging System', *Journal of Plant Physiology*. Urban & Fischer, 148(5), pp. 599–612. doi: 10.1016/S0176-1617(96)80081-2.

Liljeroth, E. *et al.* (2010) 'Induced resistance in potato to Phytphthora infestans-effects of BABA in greenhouse and field tests with different potato varieties', *European Journal of Plant Pathology*. Springer, 127(2), pp. 171–183. doi: 10.1007/s10658-010-9582-4.

Lim, J., Kim, K. M. and Jin, R. (2019) 'Tree Species Classification Using Hyperion and Sentinel-2 Data with Machine Learning in South Korea and China', *ISPRS International Journal of Geo-Information 2019, Vol. 8, Page 150*. Multidisciplinary Digital Publishing Institute, 8(3), p. 150. doi: 10.3390/IJGI8030150.

Liu, C. *et al.* (2018) 'Dynamic metrics-based biomarkers to predict responders to anti-PD-1 immunotherapy', *British Journal of Cancer 2018 120:3*. Nature Publishing Group, 120(3), pp. 346–355. doi: 10.1038/s41416-018-0363-8.

López Sánchez, A. *et al.* (2016) 'The role of DNA (de)methylation in immune responsiveness of Arabidopsis', *Plant Journal*. Blackwell Publishing Ltd, 88(3), pp. 361–374. doi: 10.1111/tpj.13252.

López Sánchez, A. *et al.* (2020) 'Costs and benefits of transgenerational acquired resistance in Arabidopsis', *Authorea Preprints*.

Lowe, A., Harrison, N. and French, A. P. (2017) 'Hyperspectral image analysis techniques for the detection and classification of the early onset of plant disease and stress', *Plant Methods*. BioMed Central, 13(1), p. 80. doi: 10.1186/s13007-017-0233-z.

Lucas, J. A., Hawkins, N. J. and Fraaije, B. A. (2015) 'The Evolution of Fungicide Resistance', *Advances in Applied Microbiology*. Academic Press, 90, pp. 29–92. doi: 10.1016/BS.AAMBS.2014.09.001.

Luna, E. *et al.* (2011) 'Callose deposition: A multifaceted plant defense response', *Molecular Plant-Microbe Interactions*. Mol Plant Microbe Interact, pp. 183–193. doi: 10.1094/MPMI-07-10-0149.

Luna, E., van Hulten, M., *et al.* (2014) 'Plant perception of β-aminobutyric acid is mediated by an aspartyl-tRNA synthetase', *Nature Chemical Biology*. Nature Publishing Group, 10(6), pp. 450–456. doi: 10.1038/nchembio.1520.

Luna, E., López, A., *et al.* (2014) 'Role of NPR1 and KYP in long-lasting induced resistance by β-aminobutyric acid', *Frontiers in Plant Science*. Frontiers Research Foundation, 5(MAY). doi: 10.3389/fpls.2014.00184.

Luna, E. *et al.* (2016) 'Optimizing Chemically Induced Resistance in Tomato Against *Botrytis cinerea*', *Plant Disease*. Plant Disease, 100(4), pp. 704–710. doi: 10.1094/PDIS-03-15-0347-RE.

Luna, E. and Ton, J. (2012) 'The epigenetic machinery controlling transgenerational systemic acquired resistance', *Plant Signaling and Behavior*. Taylor & Francis, 7(6), pp. 615–618. doi: 10.4161/psb.20155.

Maccioni, A., Agati, G. and Mazzinghi, P. (2001) 'New vegetation indices for remote measurement of chlorophylls based on leaf directional reflectance spectra', *Journal of Photochemistry and Photobiology B: Biology*. Elsevier, 61(1–2), pp. 52–61. doi: 10.1016/S1011-1344(01)00145-2.

Mageroy, M. H. *et al.* (2020) 'Molecular underpinnings of methyl jasmonate-induced resistance in Norway spruce', *Plant Cell and Environment*. Blackwell Publishing Ltd, 43(8), pp. 1827–1843. doi: 10.1111/pce.13774.

Mahlein, A. K. *et al.* (2012) 'Hyperspectral imaging for small-scale analysis of symptoms caused by different sugar beet diseases', *Plant Methods*. BioMed Central, 8(1), p. 3. doi: 10.1186/1746-4811-8-3.

Mahlein, A. K. *et al.* (2013) 'Development of spectral indices for detecting and identifying plant diseases', *Remote Sensing of Environment*. Elsevier, 128, pp. 21–30. doi: 10.1016/J.RSE.2012.09.019.

Mahlein, A. K. (2016) 'Plant Disease Detection by Imaging Sensors - Parallels and Specific Demands for Precision Agriculture and Plant Phenotyping', *Plant disease*. Plant Dis, 100(2), pp. 241–254. doi: 10.1094/PDIS-03-15-0340-FE.

Mahlein, A. K. *et al.* (2018) 'Hyperspectral Sensors and Imaging Technologies in Phytopathology: State of the Art', *Annual review of phytopathology*. Annu Rev Phytopathol, 56, pp. 535–558. doi: 10.1146/ANNUREV-PHYTO-080417-050100.

le Maire, G. *et al.* (2008) 'Calibration and validation of hyperspectral indices for the estimation of broadleaved forest leaf chlorophyll content, leaf mass per area, leaf area index and leaf canopy biomass', *Remote Sensing of Environment*. Elsevier, 112(10), pp. 3846–3864. doi: 10.1016/J.RSE.2008.06.005.

Le Maire, G., François, C. and Dufrêne, E. (2004) 'Towards universal broad leaf chlorophyll indices using PROSPECT simulated database and hyperspectral reflectance measurements', *Remote Sensing of Environment*. Elsevier, 89(1), pp. 1–28. doi: 10.1016/J.RSE.2003.09.004.

Malerba, M. and Cerana, R. (2016) 'Chitosan Effects on Plant Systems', *International Journal of Molecular Sciences 2016, Vol. 17, Page 996*. Multidisciplinary Digital Publishing Institute, 17(7), p. 996. doi: 10.3390/IJMS17070996.

Manjunath, K. R. *et al.* (2013) 'Discrimination of mangrove species and mudflat classes using in situ hyperspectral data: a case study of Indian Sundarbans', *http://dx.doi.org/10.1080/15481603.2013.814275*. Taylor & Francis , 50(4), pp. 400–417. doi: 10.1080/15481603.2013.814275.

Manjunatha, G. *et al.* (2009) 'Nitric oxide is involved in chitosan-induced systemic resistance in pearl millet against downy mildew disease', *Pest Management Science*. John Wiley & Sons, Ltd, 65(7), pp. 737–743. doi: 10.1002/PS.1710.

Martinez-Medina, A. *et al.* (2016) 'Recognizing Plant Defense Priming', *Trends in Plant Science*. Elsevier Ltd, pp. 818–822. doi: 10.1016/j.tplants.2016.07.009.

Mauch, F., Hadwiger, L. A. and Boller, T. (1984) 'Ethylene: Symptom, Not Signal for the Induction of Chitinase and beta-1,3-Glucanase in Pea Pods by Pathogens and Elicitors', *Plant physiology*. Plant Physiol, 76(3), pp. 607–611. doi: 10.1104/PP.76.3.607.

McDowell, J. M. *et al.* (2007) 'Genetic Analysis of Developmentally Regulated Resistance to Downy Mildew (Hyaloperonospora parasitica) in Arabidopsis thaliana', *http://dx.doi.org/10.1094/MPMI-18-1226*. The American Phytopathological Society , 18(11), pp. 1226–1234. doi: 10.1094/MPMI-18-1226.

McHugh, M. L. (2012) 'Interrater reliability: the kappa statistic', *Biochemia Medica*. Croatian Society for Medical Biochemistry and Laboratory Medicine, 22(3), p. 276. doi: 10.11613/bm.2012.031.

McMurtrey, J. E. *et al.* (1994) 'Distinguishing nitrogen fertilization levels in field corn (Zea mays L.) with actively induced fluorescence and passive reflectance measurements', *Remote Sensing of Environment*. Elsevier, 47(1), pp. 36–44. doi: 10.1016/0034-4257(94)90125-2.

Melouk, H. A. (1978) 'Determination of Leaf Necrosis Caused by Cercospora arachidicola Hori in Peanut as Measured by Loss in Total Chlorophyll', *Peanut Science*. Allen Press, 5(1), pp. 17–18. doi: 10.3146/I0095-3679-5-1-4.

Merzlyak, M. N. *et al.* (1999) 'Non-destructive optical detection of pigment changes during leaf senescence and fruit ripening', *Physiologia Plantarum*. John Wiley & Sons, Ltd, 106(1), pp. 135–141. doi: 10.1034/J.1399-3054.1999.106119.X.

Miller, J. R., Hare, E. W. and Wu, J. (1990) 'Quantitative characterization of the vegetation red edge reflectance 1. An inverted-Gaussian reflectance model', *International Journal of Remote Sensing*. Taylor & Francis Group , 11(10), pp. 1755–1773. doi: 10.1080/01431169008955128.

Minorsky, P. V. (2019) 'The functions of foliar nyctinasty: a review and hypothesis', *Biological Reviews*. John Wiley & Sons, Ltd, 94(1), pp. 216–229. doi: 10.1111/BRV.12444.

Mirzaei, M. *et al.* (2019) 'Eco-Friendly Estimation of Heavy Metal Contents in Grapevine Foliage Using In-Field Hyperspectral Data and Multivariate Analysis', *Remote Sensing 2019, Vol. 11, Page 2731*. Multidisciplinary Digital Publishing Institute, 11(23), p. 2731. doi: 10.3390/RS11232731.

Mishra, P. *et al.* (2017) 'Close range hyperspectral imaging of plants: A review', *Biosystems Engineering*. Academic Press, 164, pp. 49–67. doi: 10.1016/J.BIOSYSTEMSENG.2017.09.009.

Mottet, A. *et al.* (2017) 'Livestock: On our plates or eating at our table? A new analysis of the feed/food debate', *Global Food Security*. Elsevier, 14, pp. 1–8. doi: 10.1016/J.GFS.2017.01.001.

Mundt, C. C. (2014) 'Durable resistance: A key to sustainable management of pathogens and pests', *Infection, Genetics and Evolution*. Elsevier, 27, pp. 446–455. Available at: http://www.ncbi.nlm.nih.gov/pubmed/24486735 (Accessed: 26 October 2017).

Muñoz, Z. and Moret, A. (2010) 'Sensitivity of Botrytis cinerea to chitosan and acibenzolar-S-methyl', *Pest management science*. Pest Manag Sci, 66(9), pp. 974–979. doi: 10.1002/PS.1969.

Mur, L. A. J. *et al.* (2006) 'The outcomes of concentration-specific interactions between salicylate and jasmonate signaling include synergy, antagonism, and oxidative stress leading to cell death', *Plant Physiology*. American Society of Plant Biologists, 140(1), pp. 249–262. doi: 10.1104/pp.105.072348.

Mutka, A. M. and Bart, R. S. (2015) 'Image-based phenotyping of plant disease symptoms', *Frontiers in Plant Science*. Frontiers, 5, p. 734. doi: 10.3389/fpls.2014.00734.

Naveed, Z. A. *et al.* (2020) 'The PTI to ETI Continuum in Phytophthora-Plant Interactions', *Frontiers in Plant Science*. Frontiers Media S.A., p. 593905. doi: 10.3389/fpls.2020.593905.

Nicolopoulou-Stamati, P. *et al.* (2016) 'Chemical Pesticides and Human Health: The Urgent Need for a New Concept in Agriculture', *Frontiers in Public Health*. Frontiers Media S.A., 4, p. 148. doi: 10.3389/FPUBH.2016.00148/BIBTEX.

Nordskog, B. *et al.* (2007) 'Impact of Diurnal Periodicity, Temperature, and Light on Sporulation of Bremia lactucae', *http://dx.doi.org/10.1094/PHYTO-97-8-0979*. The American Phytopathological Society , 97(8), pp. 979–986. doi: 10.1094/PHYTO-97-8-0979.

Oppelt, N. and Mauser, W. (2004) 'Hyperspectral monitoring of physiological parameters of wheat during a vegetation period using AVIS data', *International Journal of Remote Sensing* . Taylor & Francis Group , 25(1), pp. 145–159. doi: 10.1080/0143116031000115300.

Pandey, P. *et al.* (2017) 'High Throughput In vivo Analysis of Plant Leaf Chemical Properties Using Hyperspectral Imaging', *Frontiers in Plant Science*. Frontiers, 8, p. 1348. doi: 10.3389/fpls.2017.01348.

Paulus, S. and Mahlein, A. K. (2020) 'Technical workflows for hyperspectral plant image assessment and processing on the greenhouse and laboratory scale', *GigaScience*. Oxford Academic, 9(8), pp. 1–10. doi: 10.1093/GIGASCIENCE/GIAA090.

Pel, M. J. C. and Pieterse, C. M. J. (2013) 'Microbial recognition and evasion of host immunity', *Journal of Experimental Botany*, 64(5), pp. 1237–1248. doi: 10.1093/jxb/ers262.

Penuelas, J. *et al.* (1995) 'Reflectance assessment of mite effects on apple trees', *International Journal of Remote Sensing*. Taylor & Francis Group, 16(14), pp. 2727–2733. doi: 10.1080/01431169508954588.

Peñuelas, J. *et al.* (1994) 'Reflectance indices associated with physiological changes in nitrogen- and water-limited sunflower leaves', *Remote Sensing of Environment*. Elsevier, 48(2), pp. 135–146. doi: 10.1016/0034-4257(94)90136-8.

Penuelas, J., Baret, F. and Filella, I. (1995) 'Semi-empirical indices to assess carotenoids/chlorophyll a ratio from leaf spectral reflectance', *Photosynthetica*, 31(2).

Perez, L. *et al.* (2003) 'Efficacy of acibenzolar-S-methyl, an inducer of systemic acquired resistance against tobacco blue mould caused by Peronospora hyoscyami f. sp. tabacina', *Crop Protection*. Elsevier, 22(2), pp. 405–413. doi: 10.1016/S0261-2194(02)00198-9.

Pertot, I. *et al.* (2017) 'A critical review of plant protection tools for reducing pesticide use on grapevine and new perspectives for the implementation of IPM in viticulture', *Crop Protection*. Elsevier, 97, pp. 70–84. doi: 10.1016/J.CROPRO.2016.11.025.

Petrasch, S. *et al.* (2019) 'Grey mould of strawberry, a devastating disease caused by the ubiquitous necrotrophic fungal pathogen Botrytis cinerea', *Molecular Plant Pathology*. Wiley-Blackwell, 20(6), p. 877. doi: 10.1111/MPP.12794.

Pieterse, C. M. *et al.* (1996) 'Systemic resistance in Arabidopsis induced by biocontrol bacteria is independent of salicylic acid accumulation and pathogenesis-related gene expression.', *The Plant cell*. American Society of Plant Biologists, 8(8), pp. 1225–37. doi: 10.1105/TPC.8.8.1225.

Pieterse, C. M. J. *et al.* (1998) 'A novel signaling pathway controlling induced systemic resistance in arabidopsis', *Plant Cell*, 10(9). doi: 10.1105/tpc.10.9.1571.

Pieterse, C. M. J. *et al.* (2012) 'Hormonal modulation of plant immunity', *Annual Review of Cell and Developmental Biology*. Annu Rev Cell Dev Biol, 28, pp. 489–521. doi: 10.1146/annurev-cellbio-092910-154055.

Pieterse, C. M. J. *et al.* (2014) 'Induced systemic resistance by beneficial microbes', *Annual Review of Phytopathology*. Annual Reviews Inc., 52, pp. 347–375. doi: 10.1146/annurev-phyto-082712-102340.

Portet, S. (2020) 'A primer on model selection using the Akaike Information Criterion', *Infectious Disease Modelling*. KeAi Publishing, 5, p. 111. doi: 10.1016/J.IDM.2019.12.010.

Pospieszny, H., Chirkov, S. and Atabekov, J. (1991) 'Induction of antiviral resistance in plants by chitosan', *Plant Science*. Elsevier, 79(1), pp. 63–68. doi: 10.1016/0168-9452(91)90070-O.

Prashar, A. and Jones, H. G. (2014) 'Infra-Red Thermography as a High-Throughput Tool for Field Phenotyping', *Agronomy 2014, Vol. 4, Pages 397-417*. Multidisciplinary Digital Publishing Institute, 4(3), pp. 397–417. doi: 10.3390/AGRONOMY4030397.

Pritchard, L. and Birch, P. R. J. (2014) 'The zigzag model of plant-microbe interactions: Is it time to move on?', *Molecular Plant Pathology*. Blackwell Publishing Ltd, 15(9), pp. 865–870. doi: 10.1111/mpp.12210.

Proietti, S. *et al.* (2018) 'Genome-wide association study reveals novel players in defense hormone crosstalk in Arabidopsis', *Plant, Cell & Environment*. John Wiley & Sons, Ltd, 41(10), pp. 2342–2356. doi: 10.1111/PCE.13357.

Qi, J. *et al.* (1994) 'A modified soil adjusted vegetation index', *Remote Sensing of Environment*. Elsevier, 48(2), pp. 119–126. doi: 10.1016/0034-4257(94)90134-1.

Qi, J. *et al.* (2017) 'Apoplastic ROS signaling in plant immunity', *Current Opinion in Plant Biology*. Elsevier Ltd, pp. 92–100. doi: 10.1016/j.pbi.2017.04.022.

R Core Team (2021) 'R: A Language and Environment for Statistical Computing', *R Foundation for Statistical Computing*. Available at: https://www.r-project.org/.

Rabea, E. I. *et al.* (2003) 'Chitosan as Antimicrobial Agent: Applications and Mode of Action', *Biomacromolecules*. American Chemical Society , 4(6), pp. 1457–1465. doi: 10.1021/BM034130M.

Rajamuthiah, R. and Mylonakis, E. (2014) 'Effector triggered immunity activation of innate immunity in metazoans by bacterial effectors', *Virulence*. Landes Bioscience, pp. 697–702. doi: 10.4161/viru.29091.

Reuveni, M., Zahavi, T. and Cohen, Y. (2001) 'Controlling downy mildew (Plasmopara viticola) in field-grown grapevine with β-aminobutyric acid (BABA)', *Phytoparasitica*. Springer, 29(2), pp. 125–133. doi: 10.1007/BF02983956.

Ringnér, M. (2008) 'What is principal component analysis?', *Nature Biotechnology 2008 26:3*. Nature Publishing Group, 26(3), pp. 303–304. doi: 10.1038/nbt0308-303.

Ristaino, J. B. *et al.* (2021) 'The persistent threat of emerging plant disease pandemics to global food security', *Proceedings of the National Academy of Sciences of the United States of America*. National Academy of Sciences, 118(23). doi: 10.1073/PNAS.2022239118/SUPPL_FILE/PNAS.2022239118.SAPP.PDF.

Ritz, C. *et al.* (2015) 'Dose-response analysis using R', *PLoS ONE*, 10(12). doi: 10.1371/journal.pone.0146021.

Rodriguez-Salus, M. *et al.* (2016) 'The synthetic elicitor 2-(5-Bromo-2-Hydroxy-Phenyl)- thiazolidine-4-carboxylic acid links plant immunity to hormesis1', *Plant Physiology*. American Society of Plant Biologists, 170(1), pp. 444–458. doi: 10.1104/pp.15.01058.

Roell, K. R., Reif, D. M. and Motsinger-Reif, A. A. (2017) 'An introduction to terminology and methodology of chemical synergy-perspectives from across disciplines', *Frontiers in Pharmacology*. Frontiers Research Foundation, 8(APR), p. 158. doi: 10.3389/FPHAR.2017.00158/BIBTEX.

de Román, M. *et al.* (2011) 'Elicitation of foliar resistance mechanisms transiently impairs root association with arbuscular mycorrhizal fungi', *Journal of Ecology*. John Wiley & Sons, Ltd, 99(1), pp. 36–45. doi: 10.1111/j.1365-2745.2010.01752.x.

Romanazzi, G. *et al.* (2013) 'Effectiveness of postharvest treatment with chitosan and other resistance inducers in the control of storage decay of strawberry', *Postharvest Biology and Technology*. Elsevier, 75, pp. 24–27. doi: 10.1016/J.POSTHARVBIO.2012.07.007.

Romanazzi, G. *et al.* (2016) 'Impact of alternative fungicides on grape downy mildew control and vine growth and development', *Plant Disease*. American Phytopathological Society, 100(4), pp. 739–748. doi: 10.1094/PDIS-05-15-0564-RE/ASSET/IMAGES/LARGE/PDIS-05-15-0564-RE_T5.JPEG.

Rondeaux, G., Steven, M. and Baret, F. (1996) 'Optimization of soil-adjusted vegetation indices', *Remote Sensing of Environment*. Elsevier, 55(2), pp. 95–107. doi: 10.1016/0034-4257(95)00186-7.

Ross, A. F. (1961) 'Systemic acquired resistance induced by localized virus infections in plants', *Virology*, 14(3). doi: 10.1016/0042-6822(61)90319-1.

Roujean, J. L. and Breon, F. M. (1995) 'Estimating PAR absorbed by vegetation from bidirectional reflectance measurements', *Remote Sensing of Environment*. Elsevier, 51(3), pp. 375–384. doi: 10.1016/0034-4257(94)00114-3.

Sahariah, P. and Másson, M. (2017) 'Antimicrobial Chitosan and Chitosan Derivatives: A Review of the Structure-Activity Relationship', *Biomacromolecules*. American Chemical Society, 18(11), pp. 3846–3868. doi: 10.1021/ACS.BIOMAC.7B01058/SUPPL_FILE/BM7B01058_SI_001.PDF.

Sarić, R. *et al.* (2022) 'Applications of hyperspectral imaging in plant phenotyping', *Trends in Plant Science*. Elsevier Current Trends, 27(3), pp. 301–315. doi: 10.1016/J.TPLANTS.2021.12.003.

Saxena, I., Srikanth, S. and Chen, Z. (2016) 'Cross talk between H2O2 and interacting signal molecules under plant stress response', *Frontiers in Plant Science*. Frontiers Media S.A., 7(APR2016), p. 570. doi: 10.3389/FPLS.2016.00570/BIBTEX.

Scarboro, C. G. *et al.* (2021) 'Quantification of gray mold infection in lettuce using a bispectral imaging system under laboratory conditions', *Plant Direct*. John Wiley & Sons, Ltd, 5(3), p. e00317. doi: 10.1002/PLD3.317.

Schillheim, B. *et al.* (2018) 'Sulforaphane modifies histone H3, unpacks chromatin, and primes defense', *Plant Physiology*. American Society of Plant Biologists, 176(3), pp. 2395–2405. doi: 10.1104/pp.17.00124.

Schwarzenbacher, R. E. *et al.* (2020) 'The IBI1 Receptor of β-Aminobutyric Acid Interacts with VOZ Transcription Factors to Regulate Abscisic Acid Signaling and Callose-Associated Defense', *Molecular plant*. Mol Plant, 13(10), pp. 1455–1469. doi: 10.1016/J.MOLP.2020.07.010.

Schwarzenbacher, R. E., Luna, E. and Ton, J. (2014) 'The discovery of the BABA receptor: scientific implications and application potential', *Frontiers in Plant Science*. Frontiers Media SA, 5(JUN), pp. 450–456. doi: 10.3389/FPLS.2014.00304.

Schweizer, P., Buchala, A. and Métraux, J. P. (1997) 'Gene-expression patterns and levels of jasmonic acid in rice treated with the resistance inducer 2,6-dichloroisonicotinic acid', *Plant Physiology*. American Society of Plant Biologists, 115(1), pp. 61–70. doi: 10.1104/pp.115.1.61.

Sharathchandra, R. G. S. *et al.* (2004) 'A Chitosan formulation Elexa™ induces downy mildew disease resistance and growth promotion in pearl millet', *Crop Protection*. Elsevier, 23(10), pp. 881–888. doi: 10.1016/J.CROPRO.2003.12.008.

Sharma, K., Butz, A. F. and Finckh, M. R. (2010) 'Effects of host and pathogen genotypes on inducibility of resistance in tomato (Solanum lycopersicum) to Phytophthora infestans', *Plant Pathology*. John Wiley & Sons, Ltd, 59(6), pp. 1062–1071. doi: 10.1111/j.1365-3059.2010.02341.x.

Sharma, K. D. *et al.* (2011) 'Control of chickpea blight disease caused by Didymella rabiei by mixing resistance inducer and contact fungicide', *Crop Protection*. Elsevier, 30(11), pp. 1519–1522. doi: 10.1016/j.cropro.2011.07.003.

Shrestha, S. *et al.* (2016) 'Single seed near-infrared hyperspectral imaging in determining tomato (Solanum lycopersicum L.) seed quality in association with multivariate data analysis', *Sensors and Actuators B: Chemical*. Elsevier, 237, pp. 1027–1034. doi: 10.1016/J.SNB.2016.08.170.

Sim, J. and Wright, C. C. (2005) 'The Kappa Statistic in Reliability Studies: Use, Interpretation, and Sample Size Requirements', *Physical Therapy*. Oxford Academic, 85(3), pp. 257–268. doi: 10.1093/PTJ/85.3.257.

Simko, I. *et al.* (2013) 'Identification of QTLs conferring resistance to downy mildew in legacy cultivars of lettuce', *Scientific Reports 2013 3:1*. Nature Publishing Group, 3(1), pp. 1–10. doi: 10.1038/srep02875.

Sims, D. A. and Gamon, J. A. (2002) 'Relationships between leaf pigment content and spectral reflectance across a wide range of species, leaf structures and developmental stages', *Remote Sensing of Environment*. Elsevier, 81(2–3), pp. 337–354. doi: 10.1016/S0034-4257(02)00010-X.

Singh, U. B. *et al.* (2019) 'Trichoderma harzianum-and methyl jasmonate-induced resistance to bipolaris sorokiniana through enhanced phenylpropanoid activities in bread wheat (Triticum aestivum L.)', *Frontiers in Microbiology*. Frontiers Media S.A., 10. doi: 10.3389/fmicb.2019.01697.

Slaughter, A. *et al.* (2012) 'Descendants of Primed Arabidopsis Plants Exhibit Resistance to Biotic Stress', *PLANT PHYSIOLOGY*, 158(2), pp. 835–843. doi: 10.1104/pp.111.191593.

Smith, J. E. *et al.* (2014) 'Resistance to Botrytis cinerea in Solanum lycopersicoides involves widespread transcriptional reprogramming', *BMC Genomics*. BioMed Central Ltd., 15(1), pp. 1–18. doi: 10.1186/1471-2164-15-334/FIGURES/9.

Smith, R. C. G. *et al.* (1995) 'Forecasting wheat yield in a Mediterranean-type environment from the NOAA satellite', *Australian Journal of Agricultural Research*. CSIRO PUBLISHING, 46(1), pp. 113–125. doi: 10.1071/AR9950113.

Song, Y. Y. and Lu, Y. (2015) 'Decision tree methods: applications for classification and prediction', *Shanghai Archives of Psychiatry*. Shanghai Mental Health Center, 27(2), p. 130. doi: 10.11919/J.ISSN.1002-0829.215044.

Sós-Hegedűs, A. *et al.* (2014) 'Soil Drench Treatment with ß-Aminobutyric Acid Increases Drought Tolerance of Potato', *PLoS ONE*. Edited by Z. Chan. Public Library of Science, 9(12), p. e114297. doi: 10.1371/journal.pone.0114297.

Spoel, S. H. and Dong, X. (2012) 'How do plants achieve immunity? Defence without specialized immune cells', *Nature Reviews Immunology*. Nature Publishing Group, 12(2), pp. 89–100. doi: 10.1038/nri3141.

Spoel, S. H., Johnson, J. S. and Dong, X. (2007) 'Regulation of tradeoffs between plant defenses against pathogens with different lifestyles', *Proceedings of the National Academy of Sciences of the United States of America*. National Academy of Sciences, 104(47), pp. 18842–18847. doi: 10.1073/pnas.0708139104.

Stassen, J. H. M. *et al.* (2018) 'The relationship between transgenerational acquired resistance and global DNA methylation in Arabidopsis', *Scientific Reports*. Nature Publishing Group, 8(1), p. 14761. doi: 10.1038/s41598-018-32448-5.

Sticher, L., Mauch-Mani, B. and Métraux, and J. (1997) 'Systemic acquired resistance', *Annual Review of Phytopathology*, 35(1), pp. 235–270. doi: 10.1146/annurev.phyto.35.1.235.

Story, M. and Congalton, R. G. (1986) 'Accuracy assessment: a user's perspective.', *Photogrammetric Engineering & Remote Sensing*, 52(3).

Sytar, O. *et al.* (2017) 'Applying hyperspectral imaging to explore natural plant diversity towards improving salt stress tolerance', *Science of The Total Environment*. Elsevier, 578, pp. 90–99. doi: 10.1016/J.SCITOTENV.2016.08.014.

Szymańska, E. *et al.* (2012) 'Double-check: validation of diagnostic statistics for PLS-DA models in metabolomics studies', *Metabolomics*. Springer, 8(Suppl 1), p. 3. doi: 10.1007/S11306-011-0330-3.

Tao, C.-N. *et al.* (2022) 'A single amino acid transporter controls the uptake of priming-inducing beta-amino acids and the associated trade-off between induced resistance and plant growth', *bioRxiv*. Cold Spring Harbor Laboratory, p. 2022.03.17.484770. doi: 10.1101/2022.03.17.484770.

Terentev, A. *et al.* (2022) 'Current State of Hyperspectral Remote Sensing for Early Plant Disease Detection: A Review', *Sensors (Basel, Switzerland)*. Multidisciplinary Digital Publishing Institute (MDPI), 22(3). doi: 10.3390/S22030757.

Thaler, J. S., Humphrey, P. T. and Whiteman, N. K. (2012) 'Evolution of jasmonate and salicylate signal crosstalk', *Trends in Plant Science*. Trends Plant Sci, pp. 260–270. doi: 10.1016/j.tplants.2012.02.010.

Therneau, T. and Atkinson, B. (2019) 'rpart: Recursive partitioning and regression trees. R package version 4.1-15.', *https://CRAN.R-project.org/package=rpart.*

Therneau, T. M. and Atkinson, E. J. (2015) 'An Introduction to Recursive Partitioning Using the RPART Routines', *Mayo Clinic Division of Biostatistics*. doi: 10.1017/CBO9781107415324.004.

Thevenet, D. *et al.* (2017) 'The priming molecule β -aminobutyric acid is naturally present in plants and is induced by stress', *New Phytologist*, 213(2), pp. 552–559. doi: 10.1111/nph.14298.

Thévenot, E. A. *et al.* (2015) 'Analysis of the Human Adult Urinary Metabolome Variations with Age, Body Mass Index, and Gender by Implementing a Comprehensive Workflow for Univariate and OPLS Statistical Analyses', *Journal of proteome research*. J Proteome Res, 14(8), pp. 3322–3335. doi: 10.1021/ACS.JPROTEOME.5B00354.

Thordal-Christensen, H. (2020) 'A holistic view on plant effector-triggered immunity presented as an iceberg model', *Cellular and Molecular Life Sciences*. Springer Science and Business Media Deutschland GmbH, pp. 3963–3976. doi: 10.1007/s00018-020-03515-w.

Tisdall, S. (2022) 'The world in 2022: another year of living dangerously', *The Guardian*. Available at: https://www.theguardian.com/world/2021/dec/29/the-world-in-2022-another-year-of-living-dangerously (Accessed: 15 March 2022).

Toby Kiers, E. *et al.* (2010) 'Manipulating the jasmonate response: How do methyl jasmonate additions mediate characteristics of aboveground and belowground mutualisms?', *Functional Ecology*. John Wiley & Sons, Ltd, 24(2), pp. 434–443. doi: 10.1111/j.1365-2435.2009.01625.x.

Ton, J. *et al.* (2002) 'Differential Effectiveness of Salicylate-Dependent and Jasmonate/Ethylene-Dependent Induced Resistance in *Arabidopsis*', *Molecular Plant-Microbe Interactions*. The American Phytopathological Society , 15(1), pp. 27–34. doi: 10.1094/MPMI.2002.15.1.27.

Ton, J., Jakab, G., Toquin, V., Flors, V., Iavicoli, A., Maeder, Muriel N, *et al.* (2005) 'Dissecting the beta-aminobutyric acid-induced priming phenomenon in Arabidopsis.', *The Plant cell*. American Society of Plant Biologists, 17(3), pp. 987–99. doi: 10.1105/tpc.104.029728.

Ton, J., Jakab, G., Toquin, V., Flors, V., Iavicoli, A., Maeder, Muriel N., *et al.* (2005) 'Dissecting the beta-aminobutyric acid-induced priming phenomenon in Arabidopsis', *The Plant cell*. Plant Cell, 17(3), pp. 987–999. doi: 10.1105/TPC.104.029728.

Ton, J., Flors, V. and Mauch-Mani, B. (2009) 'The multifaceted role of ABA in disease resistance', *Trends in Plant Science*. Trends Plant Sci, 14(6), pp. 310–317. doi: 10.1016/j.tplants.2009.03.006.

Ton, J. and Mauch-Mani, B. (2004) 'Beta-amino-butyric acid-induced resistance against necrotrophic pathogens is based on ABA-dependent priming for callose', *The Plant journal : for cell and molecular biology*. Plant J, 38(1), pp. 119–130. doi: 10.1111/J.1365-313X.2004.02028.X.

Tosi, L. and Zazzerini, A. (2000) 'Interactions between Plasmopara helianthi, Glomus mosseae and two plant activators in sunflower plants', *European Journal of Plant Pathology*. Springer, 106(8), pp. 735–744. doi: 10.1023/A:1026543126341.

Trotel-Aziz, P. *et al.* (2006) 'Chitosan stimulates defense reactions in grapevine leaves and inhibits development of Botrytis cinerea', *European Journal of Plant Pathology*. doi: 10.1007/s10658-006-0005-5.

Trygg, J. and Wold, S. (2002) 'Orthogonal projections to latent structures (O-PLS)', *Journal of Chemometrics*. John Wiley & Sons, Ltd, 16(3), pp. 119–128. doi: 10.1002/CEM.695.

Tsuda, K. and Katagiri, F. (2010) 'Comparing signaling mechanisms engaged in pattern-triggered and effector-triggered immunity', *Current Opinion in Plant Biology*. Curr Opin Plant Biol, pp. 459–465. doi: 10.1016/j.pbi.2010.04.006.

Tucker, C. J. (1979) 'Red and photographic infrared linear combinations for monitoring vegetation', *Remote Sensing of Environment*. Elsevier, 8(2), pp. 127–150. doi: 10.1016/0034-4257(79)90013-0.

De Vega, D. *et al.* (2021) 'Chitosan primes plant defence mechanisms against Botrytis cinerea, including expression of Avr9/Cf-9 rapidly elicited genes', *Plant Cell and Environment*, 44(1). doi: 10.1111/pce.13921.

Vincini, M. *et al.* (2006) 'Angular dependence of maize and sugar beet VIs from directional CHRIS/Proba data', in *Paper presented at the Proc. 4th ESA CHRIS PROBA Workshop*. Available at: https://www.academia.edu/download/40620798/Angular_dependence_of_maize_and_sugar_be20151203-15468-z5m8ly.pdf (Accessed: 23 March 2022).

Vogelmann, J. E., Rock, B. N. and Moss, D. M. (1994) 'Red edge spectral measurements from sugar maple leaves', *International Journal of Remote Sensing*. Taylor & Francis Group , 14(8), pp. 1563–1575. doi: 10.1080/01431169308953986.

Vos, I. A., Moritz, L., Pieterse, Corné M. J., *et al.* (2015) 'Impact of hormonal crosstalk on plant resistance and fitness under multi-attacker conditions', *Frontiers in Plant Science*. Frontiers Media S.A., 6(AUG), p. 639. doi: 10.3389/fpls.2015.00639.

Wahabzada, M. *et al.* (2016) 'Plant Phenotyping using Probabilistic Topic Models: Uncovering the Hyperspectral Language of Plants', *Scientific Reports 2016 6:1*. Nature Publishing Group, 6(1), pp. 1–11. doi: 10.1038/srep22482.

Walter, A., Liebisch, F. and Hund, A. (2015) 'Plant phenotyping: From bean weighing to image analysis', *Plant Methods*. BioMed Central Ltd., 11(1), pp. 1–11. doi: 10.1186/S13007-015-0056-8/FIGURES/3.

Walters, D. *et al.* (2005) 'Induced Resistance for Plant Disease Control: Maximizing the Efficacy of Resistance Elicitors', *Phytopathology*. The American Phytopathological Society , 95(12), pp. 1368–1373. doi: 10.1094/PHYTO-95-1368.

Walters, D. and Heil, M. (2007) 'Costs and trade-offs associated with induced resistance', *Physiological and Molecular Plant Pathology*. Academic Press, pp. 3–17. doi: 10.1016/j.pmpp.2007.09.008.

Walters, D. R. (2010) 'Induced resistance: Destined to remain on the sidelines of crop protection?', *Phytoparasitica*. Springer, pp. 1–4. doi: 10.1007/s12600-009-0067-y.

Walters, D. R., Havis, N. D., Paterson, L., *et al.* (2011) 'Cultivar effects on the expression of induced resistance in spring barley', *Plant Disease*. The American Phytopathological Society , 95(5), pp. 595–600. doi: 10.1094/PDIS-08-10-0577.

Walters, D. R., Havis, N. D., Sablou, C., *et al.* (2011) 'Possible trade-off associated with the use of a combination of resistance elicitors', *Physiological and Molecular Plant Pathology*. Academic Press, 75(4), pp. 188–192. Available at: https://www.sciencedirect.com/science/article/pii/S088557651100021X (Accessed: 3 December 2017).

Walters, D. R. *et al.* (2014) 'Control of foliar pathogens of spring barley using a combination of resistance elicitors', *Frontiers in Plant Science*. Frontiers Research Foundation, 5(MAY). doi: 10.3389/fpls.2014.00241.

Walters, D. R. and Fountaine, J. M. (2009) 'Practical application of induced resistance to plant diseases: an appraisal of effectiveness under field conditions', *The Journal of Agricultural Science*. Cambridge University Press, 147(05), p. 523. doi: 10.1017/S0021859609008806.

Walters, D. R., Newton, A. C. and Lyon, G. D. (2014) *Induced Resistance for Plant Defense: A Sustainable Approach to Crop Protection*, *Induced Resistance for Plant Defense: A Sustainable Approach to Crop Protection*. doi: 10.1002/9781118371848.

Walters, D. R. and Paterson, L. (2012) 'Parents lend a helping hand to their offspring in plant defence', *Biology Letters*. Royal Society, 8(5), pp. 871–873. doi: 10.1098/rsbl.2012.0416.

Wang, K. *et al.* (2015) 'Response of direct or priming defense against Botrytis cinerea to methyl jasmonate treatment at different concentrations in grape berries', *International Journal of Food Microbiology*. doi: 10.1016/j.ijfoodmicro.2014.11.006.

van Wees, S. C. *et al.* (2000) 'Enhancement of induced disease resistance by simultaneous activation of salicylate- and jasmonate-dependent defense pathways in Arabidopsis thaliana.', *Proceedings of the National Academy of Sciences of the United States of America*. National Academy of Sciences, 97(15), pp. 8711–6. doi: 10.1073/pnas.130425197.

Van Wees, S. C., Van der Ent, S. and Pieterse, C. M. (2008) 'Plant immune responses triggered by beneficial microbes', *Current Opinion in Plant Biology*. doi: 10.1016/j.pbi.2008.05.005.

Weiberg, A. *et al.* (2013) 'Fungal Small RNAs Suppress Plant Immunity by Hijacking Host RNA Interference Pathways', *Science (New York, N.Y.)*. NIH Public Access, 342(6154), p. 118. doi: 10.1126/SCIENCE.1239705.

Werrie, P. Y. *et al.* (2020) 'Phytotoxicity of essential oils: Opportunities and constraints for the development of biopesticides. A review', *Foods*. doi: 10.3390/foods9091291.

White, R. F. (1979) 'Acetylsalicylic acid (aspirin) induces resistance to tobacco mosaic virus in tobacco', *Virology*. Virology, 99(2), pp. 410–412. doi: 10.1016/0042-6822(79)90019-9.

Wickham, H. *et al.* (2019) 'Welcome to the Tidyverse', *Journal of Open Source Software*, 4(43). doi: 10.21105/joss.01686.

Wilkinson, S. W. et al. (2018) 'Long-lasting β-aminobutyric acid-induced resistance protects tomato fruit against Botrytis cinerea', Plant Pathology. John Wiley & Sons, Ltd, 67(1), pp. 30–41. doi: 10.1111/PPA.12725.

Wilkinson, S. W. *et al.* (2019) 'Surviving in a Hostile World: Plant Strategies to Resist Pests and Diseases', *Annual Review of Phytopathology*. Annual Reviews, 57(1), pp. 505–529. doi: 10.1146/annurev-phyto-082718-095959.

Williamson, B. *et al.* (2007) 'Botrytis cinerea: the cause of grey mould disease', *Molecular plant pathology*. Mol Plant Pathol, 8(5), pp. 561–580. doi: 10.1111/J.1364-3703.2007.00417.X.

Wood, S. N. (2011) 'Fast stable restricted maximum likelihood and marginal likelihood estimation of semiparametric generalized linear models', *Journal of the Royal Statistical Society. Series B: Statistical Methodology*, 73(1). doi: 10.1111/j.1467-9868.2010.00749.x.

World Bank (2022) *Food security and COVID-19 brief*. Available at: https://www.worldbank.org/en/topic/agriculture/brief/food-security-and-covid-19 (Accessed: 15 March 2022).

Worley, B. and Powers, R. (2016) 'PCA as a practical indicator of OPLS-DA model reliability', *Current Metabolomics*. NIH Public Access, 4(2), p. 97. doi: 10.2174/2213235X04666160613122429.

Worrall, D. *et al.* (2012) 'Treating seeds with activators of plant defence generates long-lasting priming of resistance to pests and pathogens', *New Phytologist*. New Phytol, 193(3), pp. 770–778. doi: 10.1111/j.1469-8137.2011.03987.x.

Wu, C.-C. *et al.* (2010) 'L-Glutamine inhibits beta-aminobutyric acid-induced stress resistance and priming in Arabidopsis.', *Journal of experimental botany*. Oxford University Press, 61(4), pp. 995–1002. doi: 10.1093/jxb/erp363.

Wu, C. *et al.* (2008) 'Estimating chlorophyll content from hyperspectral vegetation indices: Modeling and validation', *Agricultural and Forest Meteorology*. Elsevier, 148(8–9), pp. 1230–1241. doi: 10.1016/J.AGRFORMET.2008.03.005.

Wu, W. (2014) 'The Generalized Difference Vegetation Index (GDVI) for Dryland Characterization', *Remote Sensing 2014, Vol. 6, Pages 1211-1233*. Multidisciplinary Digital Publishing Institute, 6(2), pp. 1211–1233. doi: 10.3390/RS6021211.

Xie, C., Yang, C. and He, Y. (2017) 'Hyperspectral imaging for classification of healthy and gray mold diseased tomato leaves with different infection severities', *Computers and Electronics in Agriculture*. Elsevier, 135, pp. 154–162. doi: 10.1016/J.COMPAG.2016.12.015.

Xue, J. and Su, B. (2017) 'Significant remote sensing vegetation indices: A review of developments and applications', *Journal of Sensors*. doi: 10.1155/2017/1353691.

Yassin, M. *et al.* (2021) 'The rise, fall and resurrection of chemical-induced resistance agents', *Pest Management Science*. doi: 10.1002/ps.6370.

Younes, I. *et al.* (2014) 'Chitin extraction from shrimp shell using enzymatic treatment. Antitumor, antioxidant and antimicrobial activities of chitosan', *International journal of biological macromolecules*. Int J Biol Macromol, 69, pp. 489–498. doi: 10.1016/J.IJBIOMAC.2014.06.013.

Zarco-Tejada, P. J. *et al.* (2001) 'Scaling-up and model inversion methods with narrowband optical indices for chlorophyll content estimation in closed forest canopies with hyperspectral data', *IEEE Transactions on Geoscience and Remote Sensing*, 39(7), pp. 1491–1507. doi: 10.1109/36.934080.

Zarco-Tejada, P. J. *et al.* (2003) 'Steady-state chlorophyll a fluorescence detection from canopy derivative reflectance and double-peak red-edge effects', *Remote Sensing of Environment*. Elsevier, 84(2), pp. 283–294. doi: 10.1016/S0034-4257(02)00113-X.

Zarco-Tejada, P. J. *et al.* (2005) 'Assessing vineyard condition with hyperspectral indices: Leaf and canopy reflectance simulation in a row-structured discontinuous canopy', *Remote Sensing of Environment*. Elsevier, 99(3), pp. 271–287. doi: 10.1016/J.RSE.2005.09.002.

Zarco-Tejada, P. J. *et al.* (2013) 'A PRI-based water stress index combining structural and chlorophyll effects: Assessment using diurnal narrow-band airborne imagery and the CWSI thermal index', *Remote Sensing of Environment*. Elsevier, 138, pp. 38–50. doi: 10.1016/J.RSE.2013.07.024.

Zarco-Tejada, P. J. and Miller, J. R. (1999) 'Land cover mapping at BOREAS using red edge spectral parameters from CASI imagery', *Journal of Geophysical Research: Atmospheres*. John Wiley & Sons, Ltd, 104(D22), pp. 27921–27933. doi: 10.1029/1999JD900161.

Zehra, A. *et al.* (2017) 'Activation of defense response in tomato against Fusarium wilt disease triggered by Trichoderma harzianum supplemented with exogenous chemical inducers (SA and MeJA)', *Revista Brasileira de Botanica*. Springer International Publishing, 40(3), pp. 651–664. doi: 10.1007/s40415-017-0382-3.

Zhang, D. *et al.* (2015) 'Chitosan Controls Postharvest Decay on Cherry Tomato Fruit Possibly via the Mitogen-Activated Protein Kinase Signaling Pathway', *Journal of Agricultural and Food Chemistry*. American Chemical Society, 63(33), pp. 7399–7404. doi: 10.1021/ACS.JAFC.5B01566.

Zhang, J. R., Liu, S. S. and Pan, L. L. (2021) 'Enhanced Age-Related Resistance to Tomato Yellow Leaf Curl Virus in Tomato Is Associated With Higher Basal Resistance', *Frontiers in Plant Science*. Frontiers Media S.A., 12, p. 1594. doi: 10.3389/FPLS.2021.685382/BIBTEX.

Zhong, Y. *et al.* (2014) 'DL-β-aminobutyric acid-induced resistance in soybean against Aphis glycinesmatsumura (Hemiptera: Aphididae)', *PLoS ONE*, 9(1). doi: 10.1371/journal.pone.0085142.

Zhou, J. *et al.* (2016) 'Triazole fungicide tebuconazole disrupts human placental trophoblast cell functions', *Journal of Hazardous Materials*, 308, pp. 294–302. doi: 10.1016/j.jhazmat.2016.01.055.

Zhu, H. *et al.* (2017) 'Hyperspectral Imaging for Presymptomatic Detection of Tobacco Disease with Successive Projections Algorithm and Machine-learning Classifiers', *Scientific Reports 2017 7:1*. Nature Publishing Group, 7(1), pp. 1–12. doi: 10.1038/s41598-017-04501-2.

Zimmerli, L. *et al.* (2000) 'Potentiation of pathogen-specific defense mechanisms in Arabidopsis by β-aminobutyric acid', *Proceedings of the National Academy of Sciences of the United States of America*. National Academy of Sciences, 97(23), pp. 12920–12925. doi: 10.1073/pnas.230416897.

Zimmerli, L., Métraux, J. P. and Mauch-Mani, B. (2001) 'beta-Aminobutyric acid-induced protection of Arabidopsis against the necrotrophic fungus Botrytis cinerea', *Plant physiology*. Plant Physiol, 126(2), pp. 517–523. doi: 10.1104/PP.126.2.517.

Zubrod, J. P. *et al.* (2019) 'Fungicides: An Overlooked Pesticide Class?', *Environmental Science and Technology*. American Chemical Society, 53(7), pp. 3347–3365. doi: 10.1021/ACS.EST.8B04392/SUPPL_FILE/ES8B04392_SI_001.PDF.